Synthesis and Characterization of Multiple Controlled Polymers by Living Radical Polymerization

リビングラジカル重合による
多重制御構造ポリマーの合成と解析

Yu MIURA

三浦　悠

2007

dedicated to my loving
parents, Takashi & Misako
sister, Mami
and
to all my friends
for their continuous encouragement

this thesis in token of gratitude and affection

CONTENTS

General Introduction

Background

Control of Polymer Primary Structure. Natural polymers or macromolecules exhibit distinctive properties and functions mainly due to the regularity of their highly ordered structures, in which multiple primary components such as polymer chain lengths, stereochemistry of the polymers, and the sequence of the repeating units are regulated. In contrast, general synthetic polymers have distributions in their structures, which are inherent to the industrial or conventional synthetic methods that cannot rival the natural polymer biosynthesis in terms of the precision control. However, owing to the tremendous precedent researches for controlling the primary structures of synthetic polymers, the chain length and stereoregularity have now been controlled by living polymerizations and stereospecific or stereoregular polymerizations, respectively, both of which have had a great impact on the developments of polymeric materials based on their controlled primary structures.

Living and Stereospecific Radical Polymerizations. Living polymerization, defined as a chain polymerization without chain transfer and chain termination, is often used for the synthesis of polymer with controlled chain length and controlled architectures such as block copolymers. Since the groundbreaking discovery of living anionic polymerization by Szwarc half a century ago,[1] there have been noticeable progresses in living ionic polymerizations in terms of initiators, monomers, and various well-defined polymers such as block, tapered block or gradient, graft, and star or star-shaped copolymers.[2] However, living ionic polymerization always requires cumbersome handling and rigorous purification of solvents and monomers due to the susceptible nature of the ionic propagating species to polar compounds such as water.

On the other hand, radical polymerization is one of the most widespread methods in polymer synthesis because of many advantages, such as wide variety of monomers, mild reaction conditions, and tolerance to polar groups. However, it had been difficult to control the molecular weights and molecular weight distributions of the resulting polymers due to the recombination and disproportionation reactions inherent to the neutral radical-growing species.[3]

The first report for realizing living radical polymerization dates back to 1980s while the control of the molecular weights was still far from that by living ionic polymerization at that time.[4] In 1990s, a great progress in the control was achieved by using nitroxide as a reversible capping agent for the growing carbon radical species, and the polymerization was termed as nitroxide-mediated polymerization (NMP), in which the highly active carbon radical species is transiently stabilized as the covalent carbon-oxygen bond while the covalent terminal can reversibly generate the growing carbon radical species on the heat stimulus (Scheme 1).[5–7] Further developments in living radical polymerizations were achieved in the subsequent years by the emergence of metal-catalyzed living radical polymerization[8–12] or atom transfer radical polymerization (ATRP) and reversible addition-fragmentation chain transfer (RAFT) polymerization,[13,14] which have been used for not only the control of the molecular weights but also the synthesis of various polymers with controlled structures. The general concept for all these living radical polymerizations lies in the introduction of the covalent dormant species that can reversibly generate the growing radical species on some stimuli such as heat, catalysts, and another radical species. Among them, the metal-catalyzed living radical polymerization is one of the most widely employed methods mainly because of the high controllability, a wide variety of available monomers involving methacrylates, acrylates, styrene, acrylamides, and vinyl esters, and the stability and easy accessibility of the carbon-halogen bonds as the initiating sites. This polymerization can be catalyzed by various transition metal complexes such as ruthenium, iron, and copper complexes, which reversibly activate the dormant carbon–halogen terminals via the one-electron redox reaction to generate the growing radical species (Scheme 1).

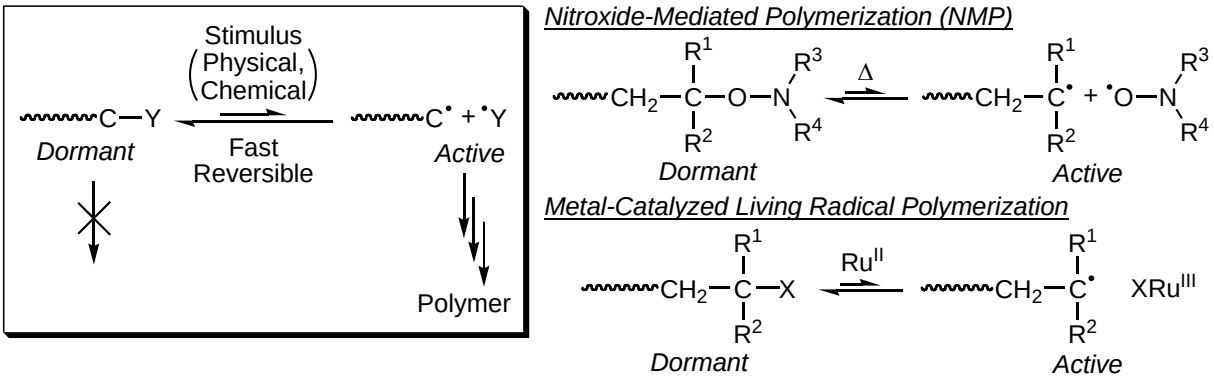

Scheme 1. Representative Living Radical Polymerizations.

Stereoregularity of polymers is another important factor of the polymer structures because it significantly influences their properties such as glass transition temperatures (T_gs) and strengths. Stereoregularity had been also difficult to control by radical polymerization due to the non-stereospecific propagation of neutral radical-growing species with an sp^2-like planar structure. However, recent developments in stereospecific radical polymerization[15] have allowed the control of the stereoregularity by several methods, in which vinyl monomers with bulky substituents,[16] fluoroalcohols as solvents,[17] or Lewis acids as additives are employed.[18,19] Quite recently, a combination of the living and stereospecific radical polymerizations has enabled not only the simultaneous control of both molecular weights and stereoregularity but also the synthesis of stereoblock polymers consisting segments with different tacticities.[20]

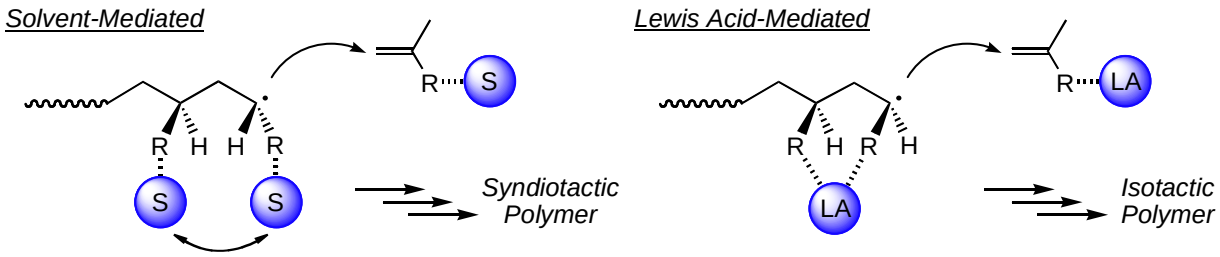

Scheme 2. Solvent- and Lewis Acid-Mediated Stereospecific Radical Polymerizations.

Recent progresses in living and stereospecific radical polymerizations have thus widened their potentials for preparing a variety of polymers with multiple controlled architectures, which have not been synthesized.

Graft Polymers. Graft polymer is a class of branched polymers and is defined as a copolymer with one or more graft chains which is different from the backbone chains in chemical nature or composition.[21] Graft copolymer is used in industry for several applications, such as compatibilizer, polymer modifier, and adhesive, because the two chemically different components connected through covalent bonds solve the interfacial problems between the different materials. These industrially used graft copolymers are generally synthesized by generating radicals randomly on the backbone chain to initiate the graft polymerization. However, this method suffers from side reactions such as coupling reaction of two graft chains and chain transfer accompanying the homopolymers to result in ill-controlled products in terms of the numbers, lengths, and positions of the graft chains.

However, progresses in living polymerization have now enabled the synthesis of well-defined graft copolymers, which may exhibit their distinctive properties and functions.

Well-Defined Graft Copolymers by Living Polymerization There are three general synthetic methods for well-defined graft copolymers with controlled backbone and graft chain lengths, i.e., "grafting-from", "grafting-onto", and "grafting-through" methods (Scheme 3).[22] For all three methods, the dual use of living polymerizations is required in

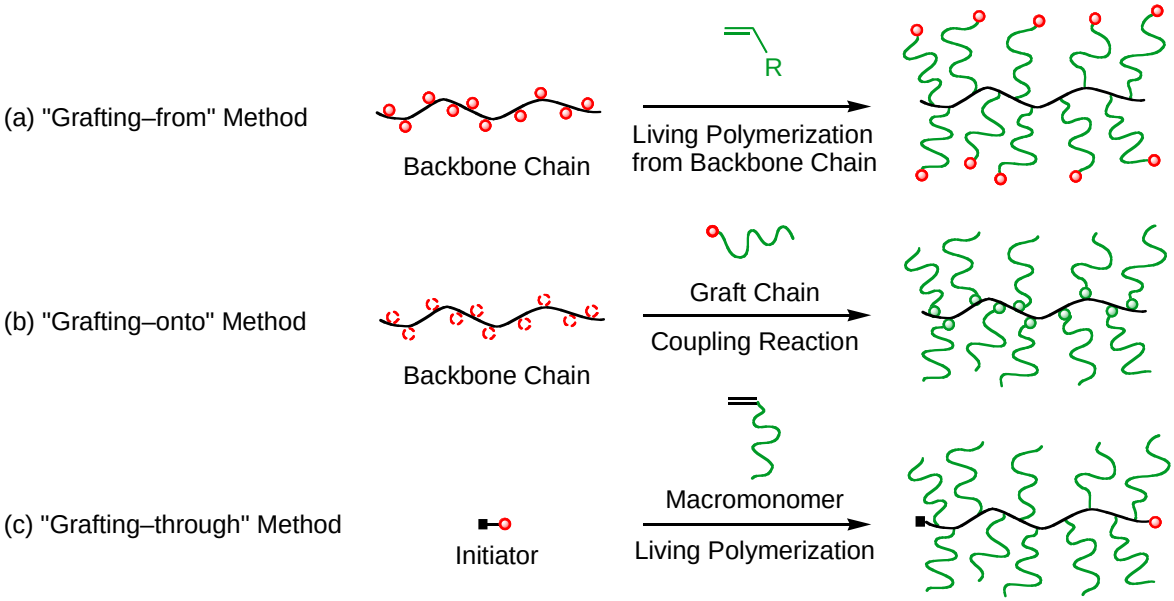

Scheme 3. Synthetic Methods for Well-Defined Graft Copolymers by Living Polymerization.

the synthesis of both backbone and graft chains. (a) The "grafting-from" method involves living graft polymerization from the backbone chains with multifunctional initiating sites, which were also prepared by living polymerization. (b) The "grafting-onto" method is based on the covalent attachment of living polymers to backbone chains with controlled lengths and reactive groups, which are synthesized by living polymerization. (c) The "grafting-through" method relies on living polymerization of macromonomers bearing a polymerizable end group prepared by living polymerization. Although each method has its respective feature, the method (b) and (c) should often require cumbersome purification or fractionation of the products to separate the residual unattached chain polymers or unreacted macromonomers from the graft copolymers. In contrast, the method (a) only needs simple separation of the graft copolymers from the unreacted low molecular-weight monomers in most cases. Thus, the method (a) seems to be the most suitable for the

synthesis of multiple controlled graft copolymers.

Objectives

The studies presented in this thesis thus aim to establish the synthetic methods of polymers with multiple controlled primary structures by living radical polymerization and stereospecific radical polymerization.

The first objective of this study was to design well-defined graft polymers with the controlled lengths of backbones and graft chains and the controlled grafting positions. The author thus used living radical polymerizations for the "grafting-from" method [(a) in Scheme 3] to construct multiple controlled graft polymers [(I) in Scheme 4]. The backbone polymers with multiple initiating sites for the living radical polymerizations were prepared by free or living radical polymerizations, in which the control of the backbone lengths can be possible only for the latter [(I)-(1) and (I)-(2), respectively]. The important

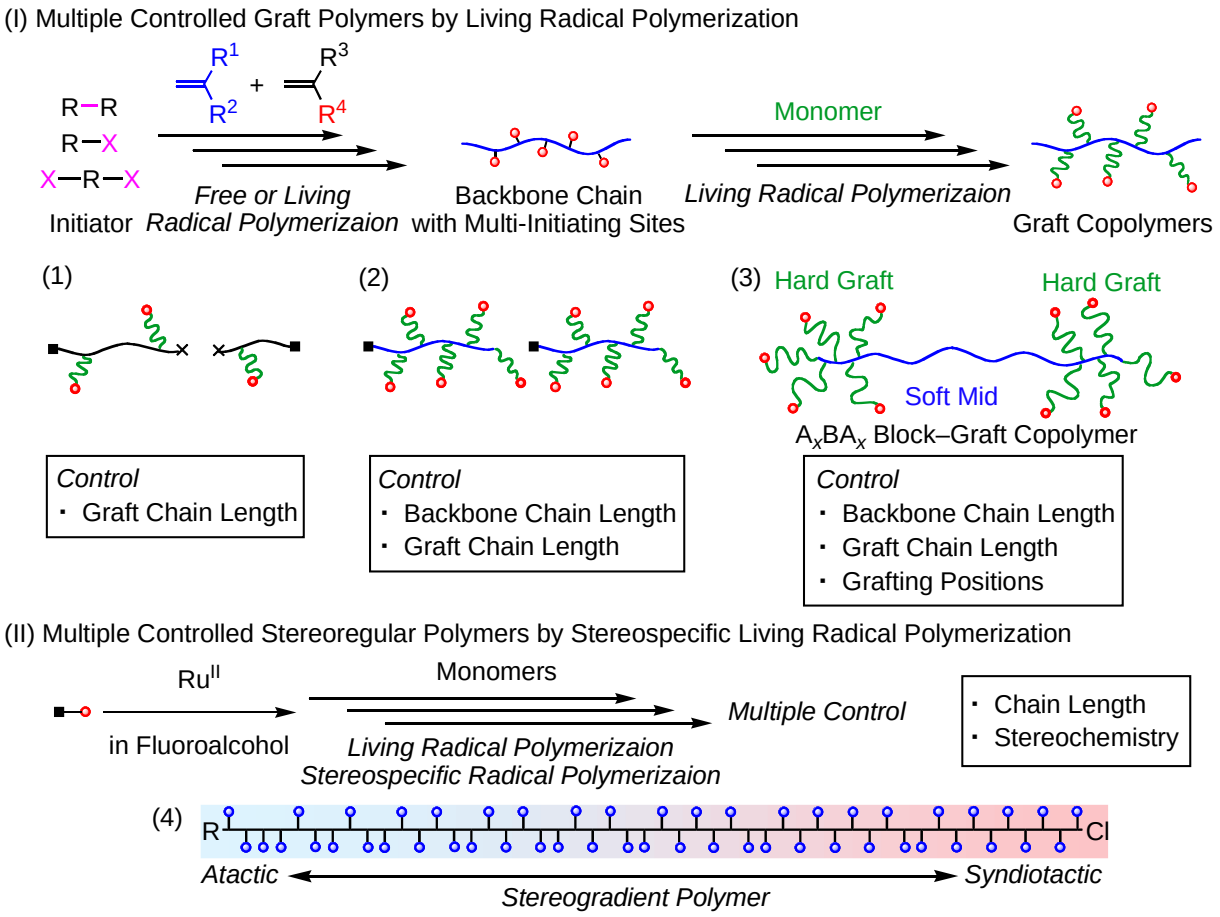

Scheme 4. Synthesis of Multiple Controlled Polymers by Living Radical Polymerization.

point in the synthesis of the backbone polymers is efficient and easy introduction of the multiple initiating sites for the living radical graft polymerizations. The comonomers for the backbone chain should possess suitable groups such as dormant covalent bond that is intact during the first polymerization or the potentially reactive substituent that can be easily transformed into the dormant covalent bond after the first polymerization. To this end, the author used two types of monomers for the grafting points, i.e., a monomer with C–ON pendant for the nitroxide-mediated graft polymerizations and another one with O-Si group, which can be changed into an ester moiety with C–halogen bond for the metal-catalyzed living radical polymerizations. The living radical "grafting-from" polymerizations of various monomers were then examined under optimized conditions for the formation of the uniform lengths of the graft chains. Further studies were directed to additional control of the grafting positions, for which A_xBA_x-type block–graft copolymers were synthesized by using metal-catalyzed living radical block and graft polymerization thus established [(I)-(3)]. Especially, hard segments were introduced as the outer graft chains (B) while soft segments as the middle parts (A) for a new thermoplastic material.

The second objective of this study was to construct a fundamentally new type of polymers with multiple controlled structures in terms of chain length and stereochemistry of the polymers by a combination of living and stereospecific radical polymerizations. For this, stereogradient polymer, in which the tacticity continuously varies along the chain, was prepared by metal-catalyzed stereospecific living radical polymerizations [(II)-(4)]. The synthetic strategy was explored for this new type of polymers because of few precedent examples.

Outline of This Study

With the aforementioned objectives in mind, the author carried out a series of studies that are described in the present thesis. **Part I** (Chapters 1–4) deals with the multiple controlled graft polymers with controlled backbone and graft chain lengths and controlled grafting positions by living radical polymerization. **Part II** (Chapter 5) discusses stereogradient polymers with controlled chain length and stereoregularity by stereospecific living radical polymerization.

In Part I, ***Chapter 1*** focuses on the control of graft chain length by nitroxide-mediated polymerization (Scheme 5). A backbone chain was prepared at a lower temperature by free radical copolymerization of methyl methacrylate (MMA) and a monomer with a nitroxyl group on the side chain (**1**), and was subsequently employed as a multifunctional macroinitiator for the nitroxide-mediated graft polymerizations of styrene (St) or *n*-butyl acrylate (BA) at a higher temperature to form the graft chains with the controlled length.

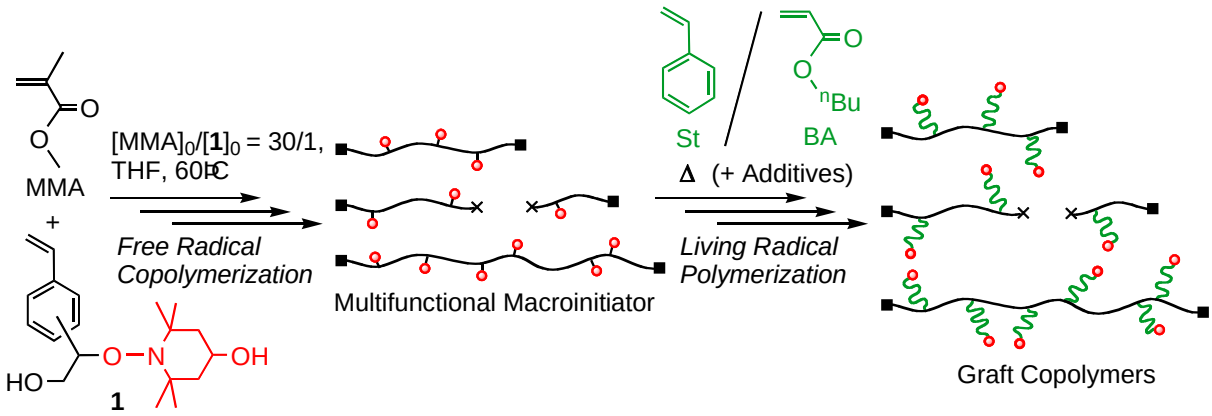

Scheme 5. Graft Polymers of Styrene and Acrylate: Control of Graft Chain Lengths.

Chapter 2 describes the control of both backbone and graft chain lengths by ruthenium-catalyzed living radical polymerization (Scheme 6). The backbone chain with the controlled chain lengths was first synthesized by ruthenium-catalyzed living radical random copolymerization of MMA and 2-(trimethylsilyloxy)ethyl methacrylate (TMSHEMA). The obtained polymer was allowed to react in situ with an acid bromide with another C–Br bond and was efficiently changed into the multifunctional initiator with C–Br bonds via the direct transformation of the silyl group into the ester without isolation and deprotection procedures. The obtained multifunctional macroinitiator was then employed for the ruthenium-catalyzed "grafting-from" radical polymerization of methacrylates, acrylates, and styrene to form the graft copolymers with controlled molecular weights ($M_w/M_n \sim 1.1$) by optimization of the conditions. The detachment of PSt graft chains from the backbone chains showed the uniform length of the graft chains ($M_w/M_n \sim 1.3$) to prove the control of both backbone and graft chains.

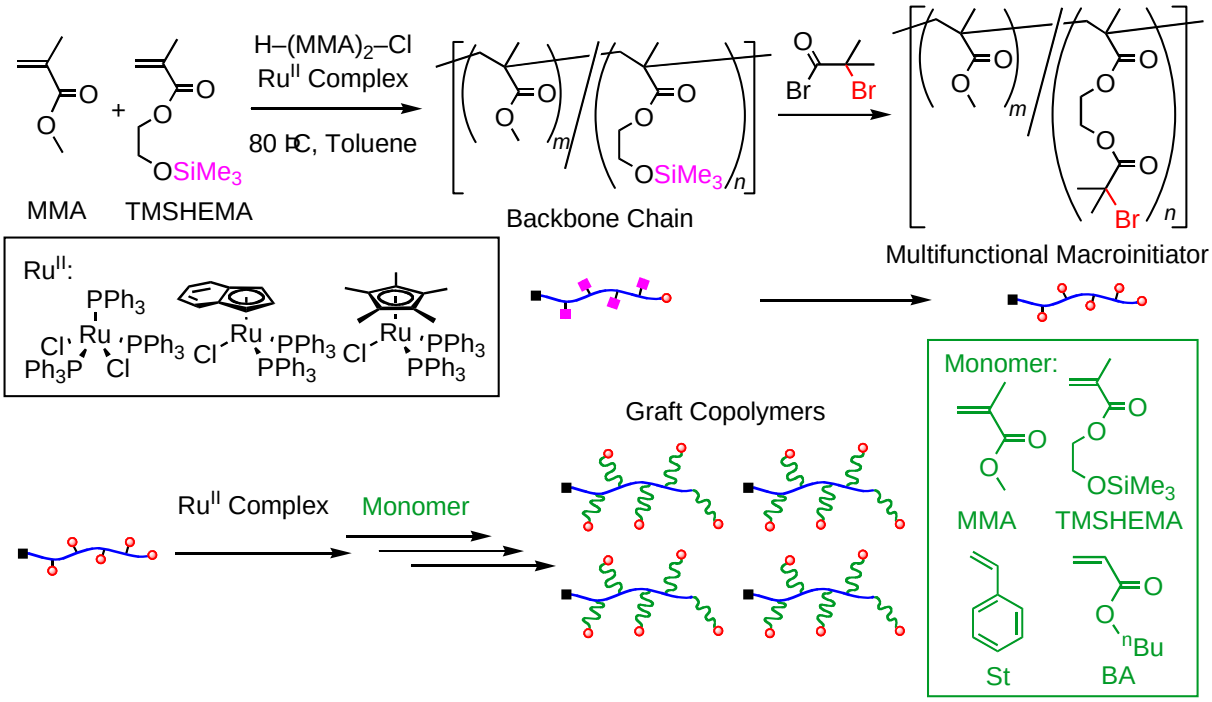

Scheme 6. Graft Polymers of Methacrylate, Acrylate, and Styrene: Control of Backbone and Graft Chain Lengths.

Chapter 3 and ***4*** deal with the synthesis of A_xBA_x-type block and graft copolymers with the controlled grafting positions in addition to the controlled backbone and graft chain lengths (Scheme 7). Especially, the A_xBA_x-type block–graft copolymers were designed to have the outer hard grafts and middle soft segments for a new type of thermoplastic elastomers.[23] On the basis of the molecular design, MMA (Chapter 3) or St (Chapter 4) was employed as the hard outer graft segments while dodecyl methacrylate (DMA) with a long alkyl chain ($C_{12}H_{25}$) as the middle soft segment.

A multifunctional macroinitiator (I_xBI_x) was first prepared in one pot by the ruthenium-catalyzed living radical block copolymerization of DMA (B segment) and TMSHEMA initiated by a bifunctional initiator followed by direct transformation of the silyloxyl group into the ester with a C–Br bond. The I_xBI_x multifunctional initiator, isolated only by precipitation, was then employed for the ruthenium-catalyzed "grafting-from" living radical polymerization of MMA or St as A segments to afford the A_xBA_x copolymers with the controlled backbone and graft chain lengths. A series of A_xBA_x copolymers were prepared by varying the numbers and/or lengths of the graft

chains.

The resultant A_xBA_x copolymers were characterized by a variety of measurements, i.e., NMR, size-exclusion chromatography (SEC), multiangle laser light scattering (MALLS), differential scanning calorimetry (DSC), dynamic viscoelasticity, tensile test, transmission electron microscopy (TEM), transmission electron microtomography (TEMT), and atomic force microscopy (AFM). Especially, a single molecule visualization by AFM revealed the dumbbell-like structure of the A_xBA_x copolymers for the first time. The morphologies of styrene–methacrylate-based A_xBA_x copolymers were analyzed by TEM and TEMT to show different features from the corresponding ABA triblock copolymers, as well as the differences in their mechanical properties. Thus, the author developed and

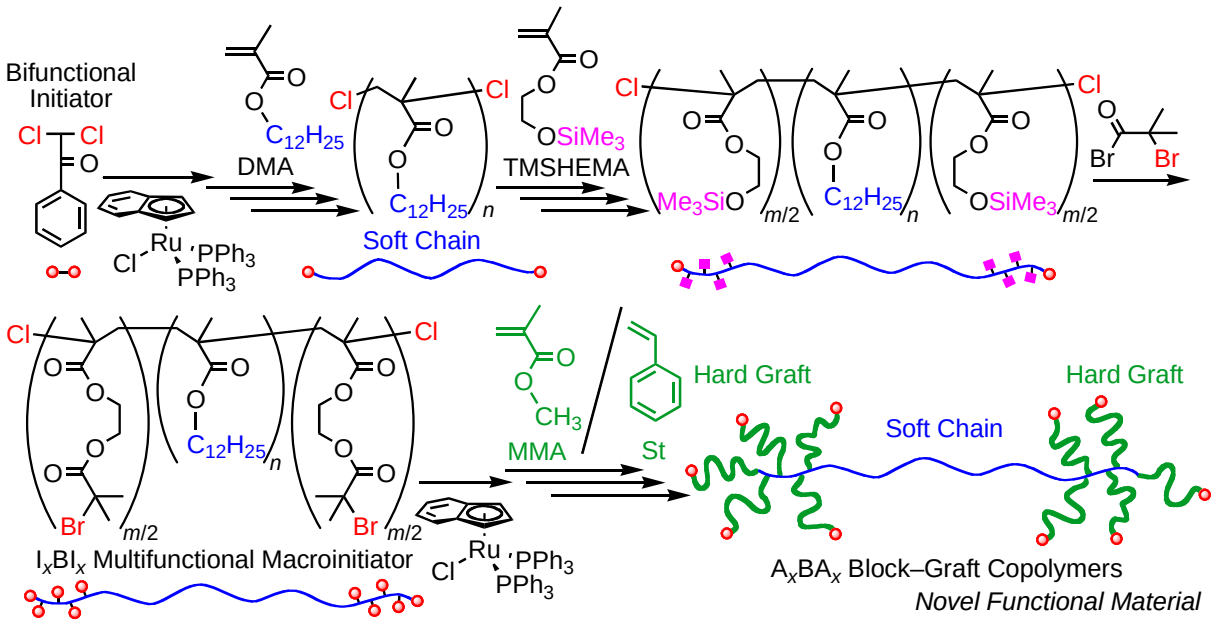

Scheme 7. A_xBA_x-Type Block–Graft Copolymers: Control of Backbone and Graft Chain Lengths and Grafting Positions.

evaluated the A_xBA_x copolymers as new thermoplastic materials.

In **Part II**, the author decided to design a fundamentally new type of multiple controlled polymers in terms of chain length and stereochemistry by a combination of living and stereospecific radical polymerization.

Chapter 5 is therefore directed to the synthesis of stereogradient polymers by stereospecific living radical copolymerization of two monomers that have different

stereospecificities and reactivities (Scheme 8). The strategy is based on ruthenium-catalyzed living radical copolymerizations of 2-hydroxyethyl methacrylate (HEMA) and the silyl-capped HEMA [(*tert*-butyldimethylsilyl)-HEMA] in bulky fluoroalcohols, in which the former was polymerized faster than the latter while the syndiotacticity was higher for the latter.

This resulted in the stereogradient poly(HEMA) with controlled molecular weights ($M_w/M_n \sim 1.2$), of which the *rr* content gradually increased along the chain from one end to the other, after the removal of the silyl groups. The author thus established the new synthetic strategy for stereogradient polymers by stereospecific living radical

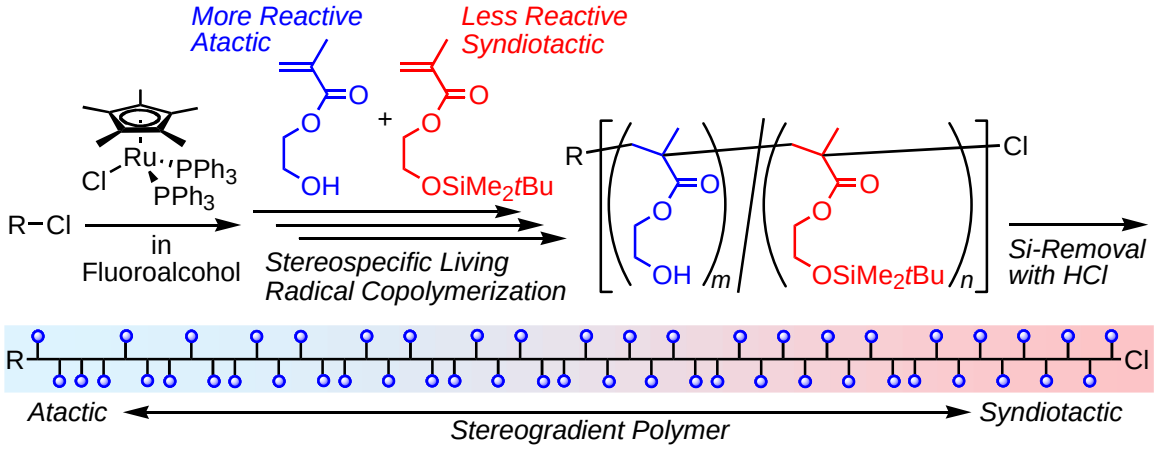

Scheme 8. Stereogradient Polymers by Stereospecific Living Radical Polymerization.

polymerizations.

REFERENCES

(1) (a) Szwarc, M.; Levy, M; Milkovich, R. *J. Am. Chem. Soc.* **1956**, *78*, 2656–2657. (b) Szwarc, M.; *Nature* **1956**, *17*, 1168–1169.

(2) (a) Morton, M. *Anionic Polymerization: Principles and Practice;* Academic Press: New York, 1983; pp 221–232. (b) Kennedy, J. P.; Ivan, B.; *Designed Polymers by Carbocationic Macromolecular Engineering*: *Theory and Practice*; Hanser Publishers: Munich, 1992; p 96. (c) Sawamoto, M.; Kamigaito, M. In *New Methods of Polymer Synthesis*; Ebdon, J. R., Eastmond, G. C., Eds.; Blackie: Glasgow, U.K., 1995; Vol. 2, pp 37–68.

(3) For a review on radical polymerization, see: Moad, G.; Solomon, D. H. *The Chemistry of Radical Polymerization*: *Second fully revised edition*; Elsevier: Oxford, U.K., 2006.

(4) Otsu, T.; Yoshida, M. *Makromol. Chem. Rapid Commun.* **1982**, *3*, 127–132.

(5) Solomon, D. H.; Rizzardo, E.; Cacioli, P. US 4581429, 1986 (*Chem. Abstr.* **1985**, *102*, 221335q).

(6) (a) Georges, M. K.; Veregin, R. P. N.; Kazmaier, P. M.; Hamer, G. K. *Macromolecules* **1993**, *26*, 2987–2988. (b) Georges, M. K.; Veregin, R. P. N.; Kazmaier, P. M.; Hamer, G. K. *Trends. Polym. Sci.* **1994**, *2*, 66–72.

(7) (a) Hawker, C. J. *J. Am. Chem. Soc.* **1994**, *116*, 11185–11186. (b) Hawker, C. J.; Bosman, A. W.; Harth, E. *Chem. Rev.* **2001**, *101*, 3661–3688.

(8) (a) Kato, M.; Kamigaito, M.; Sawamoto, M.; Higashimura, T. *Macromolecules* **1995**, *28*, 1721–1723. (b) Kamigaito, M.; Ando, T.; Sawamoto, M. *Chem. Rev.* **2001**, *101*, 3689–3745. (c) Kamigaito, M.; Ando, T.; Sawamoto, M. *Chem. Rec.* **2004**, *4*, 159–175.

(9) (a) Wang, J.-S.; Matyjaszewski, K. *J. Am. Chem. Soc.* **1995**, *117*, 5614–5615. (b) Matyjaszewski, K.; Xia, J. *Chem. Rev.* **2001**, *101*, 2921–2990.

(10) Percec, V.; Barboiu, B. *Macromolecules* **1995**, *28*, 7970–7972.

(11) Granel, C.; Dubois, P.; Jérôme, R.; Teyssié, P. *Macromolecules* **1996**, *29*, 8576–8582.

(12) Haddleton, D. M.; Jasieczek, C. B.; Hannon, M. J.; Shooter, A. J. *Macromolecules* **1997**, *30*, 2190–2193.

(13) (a) Chiefari, J.; Chong, Y. K.; Ercole, F.; Krstina, J. Jeffery, K.; Tam, P. T. Le.; Mayadunne, R. T. A.; Meijs, G. F.; Moad, C. L.; Moad, G.; Rizzardo, E.; Thang, S. H. *Macromolecules* **1998**, *31*, 5559–5562. (b) Chong, Y. K.; Kristina, J.; Tam, P. T. Le.; Moad, G.; Postma, A.; Rizzardo, E.; Thang, S. H. *Macromolecules* **2003**, *36*, 2256–2272.

(c) Chiefari, J.; Mayadunne, R. T. A.; Moad, C. L.; Moad, G.; Rizzardo, E.; Postma, A.; Skidmoe, M. A.; Thang, S. H. *Macromolecules* **2003**, *36*, 2273–2283.

(14) Destarac, M.; Bzducha, W.; Taton, D.; Gauthier-Gillaizeau, I.; Zard, S. Z. *Macromol. Rapid Commun*. **2002**, *23*, 1049–1054.

(15) For a review, see: Habaue, S.; Okamoto, Y. *Chem. Rec*. **2001**, *1*, 46–52.

(16) (a) Nakano, T.; Mori, M.; Okamoto, Y. *Macromolecules* **1993**, *26*, 867–868. (b) Nakano, T.; Makita, K.; Okamoto, Y. *Polym. J*. **1998**, *30*, 681–683. (c) Hoshikawa, N.; Hotta, Y. Okamoto, Y. *J. Am. Chem. Soc*. **2003**, *125*, 12380–12381.

(17) (a) Yamada, K.; Nakano, T.; Okamoto, Y. *Macromolecules* **1998**, *31*, 7598–7605. (b) Isobe, Y.; Yamada, K.; Nakano, T. Okamoto, Y. *Macromolecules* **1999**, *32*, 5979–5981. (c) Isobe, Y.; Yamada, K.; Nakano, T.; Okamoto, Y. *J. Polym. Sci., Part A*: *Polym. Chem.* **2000**, *38*, 4693–4703.

(18) Matsumoto, A.; Nakamura, S. *J. Appl. Polym. Sci*. **1999**, *74*, 290–296.

(19) (a) Isobe, Y.; Nakano, T.; Okamoto, Y. *J. Polym. Sci., Part A*: *Polym. Chem*. **2001**, *39*, 1463–1471. (b) Isobe, Y.; Fujioka, D.; Habaue, S.; Okamoto, Y. *J. Am. Chem. Soc*. **2001**, *123*, 7180–7181. (c) Suito, Y.; Isobe, Y.;Habaue, S.; Okamoto, Y. *J. Polym. Sci., Part A*: *Polym. Chem*. **2002**, *40*, 2496–2500. (d) Isobe, Y.; Suito, Y.; Habaue, S.; Okamoto, Y. *J. Polym. Sci., Part A*: *Polym. Chem*. **2003**, *41*, 1027–1033.

(20) For reviews, see: (a) Kamigaito, M.; Satoh, K.; Wan, D.; Sugiyama, Y.; Koumura, K.; Shibata, T.; Okamoto, Y. *ACS Symp. Ser*. **2006**, *944*, 26–39. (b) Kamigaito, M.; Satoh, K. *J. Polym. Sci., Part A*: *Polym. Chem*. **2006**, *44*, 6147–6158.

(21) IUPAC, 'Basic Definitions of Terms Relating to Polymers', *Pure Appl. Chem*., **1974**, *40*, 479–491.

(22) For reviews, see: (a) Davis, K. A.; Matyjaszewski, K. *Adv. Polym. Sci*. **2002**, *159*, 107–152. (b) Börner, H.; Matyjaszewski, K. *Macromol. Symp*. **2002**, *177*, 1–15. (c) Bhattacharya, A.; Misra, B. N. *Prog. Polym. Sci*. **2004**, *29*, 767–814. (d) Hadjichristidis, N.; Iatrou, H.; Pitsikalis, M.; Mays, J. *Prog. Polym. Sci*. **2006**, *31*, 1068–1132.

(23) Holden, G.; Kricheldorf, H. R.; Quirk, R. P. *Thermoplastic Elastomers,* 3rd ed.; Hanser Publishers: Munich, 2004.

CHAPTER 1

GRAFT POLYMERS OF STYRENE AND ACRYLATE: CONTROL OF GRAFT CHAIN LENGTHS

ABSTRACT

A simple two-step synthetic method of a graft polymer using a radical process is reported. Using living radical polymerization, graft polymers consisting of a poly(methyl methacrylate) main chain and side chains composed of various monomers, such as styrene and *n*-butyl acrylate, were synthesized. The polymers had a narrow polydispersity. Especially, for the graft polymerization of acrylates, the addition of a small amount of TEMPOL to the polymerization system on the side chain improved the livingness of the polymerization. The effect of added free TEMPOL was also studied on the homopolymerization of *n*-butyl acrylate using an initiator bearing a TEMPOL residue.

INTRODUCTION

The addition of a graft polymer having different monomer sequences as the main and side chains to a mixture of their homopolymers facilitates the formation of a homogenous blend. The polymer alloy thus obtained is expected to have excellent physical properties, which are valuable when used as products. The control of the side chain length of a graft polymer can produce a graft copolymer with a well-defined structure, which is expected to improve the physical properties of the surface and interface of a material.[1–3] The living radical polymerization with a broad applicability[4–13] seems to be suitable to produce the graft copolymers of various monomers.

Living radical polymerizations have been achieved by several procedures including nitroxide-mediated polymerization (NMP),[4–6] metal-catalyzed polymerization,[7–9] reversible addition-fragmentation chain transfer (RAFT) polymerization,[10–12] and organotellurium-mediated living radical polymerization (TERP).[13] In the present study, the author used the NMP process because of its simple procedure that can be performed without the preparation of a specific agent and the very careful precautions required for the precedure.

The nitroxides used in the NMP method are commercially available, stable in air, and easy to apply to a large-scale production. Therefore, several examples of the graft polymerization using the NMP method have been reported.[14–17] Here, the author used **1**[18] bearing a 4-hydroxy-(2,2,6,6-tetramethylpiperydine-1-oxyl) (TEMPOL) residue as the monomer to obtain the prepolymer with methyl methacrylate (MMA) and subsequently employed the prepolymer for the nitroxide mediated graft polymerization of styrene (St) and *n*-butyl acrylate (*n*-BuA) (Scheme 1).

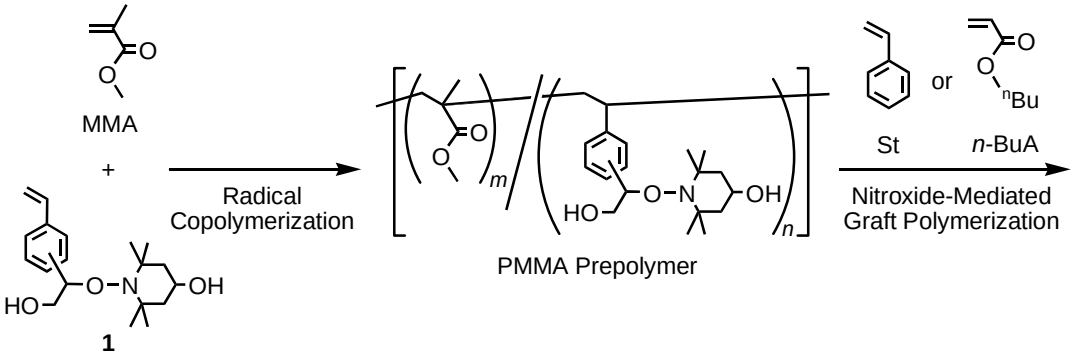

Scheme 1. Overview of graft polymerization using nitroxide-mediated polymerization.

EXPERIMENTAL

Materials

MMA (Tokyo Kasei, purity >99%) was washed with aq. NaOH (5%) and water, dried over magnesium sulfate, and distilled over calcium hydride under reduced pressure before use. St and *n*-BuA (both Tokyo Kasei, purity >99%) were distilled under reduced pressure before use. Cyclohexanone, *N*,*N*-dimethylformamide (DMF), and tetrahydrofuran (THF) (both Wako, purity >99%) were distilled under a reduced pressure before use. An initiator, *tert*-butylperoxypivalate, were used as received from the NOF Corporation. 4-Hydroxy-(2,2,6,6-tetramethylpiperydine-1-oxyl) (TEMPOL) (Aldrich) was also used as received.

Synthesis of the Monomer Bearing a TEMPOL Residue

m-/*p*-[2-Hydroxy-1-(4'-hydroxy-2',2',6',6'-tetramethylpiperidine-1'-oxy)ethyl]- styrene

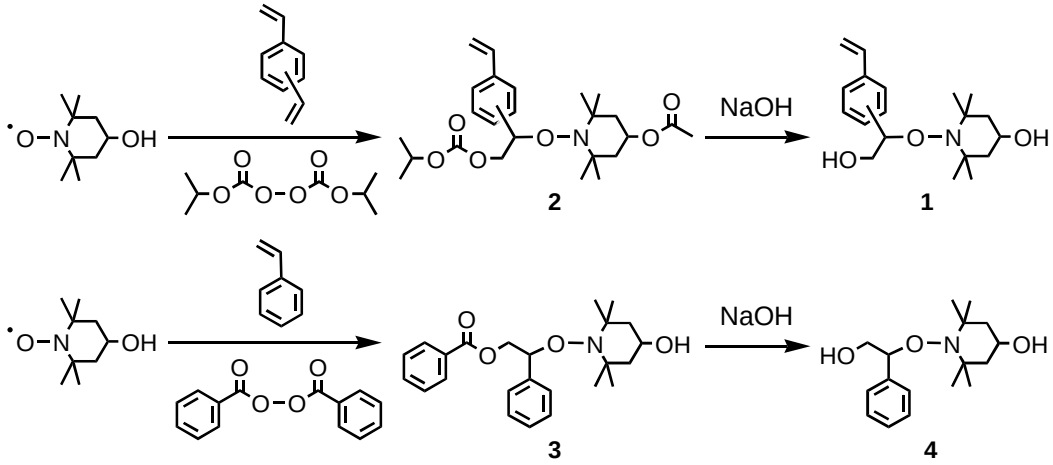

Scheme 2. Syntheses of **1**–**4**.

(**1**) (Scheme 2) was synthesized as follows.[18] 4-Acetoxy-2,2,6,6-tetramethylpiperidine-1-oxyl (2.14 g, 10.0 mmol) was dissolved in a mixture of 1,3- and 1,4-divinylbenzene (DVB-960, Nippon Steel Chemical Group, 15.0 g) and cooled to 0 ˚C. To the solution was added diisopropylperoxydicarbonate (2.08 g, 10.0 mmol) under dry nitrogen, and the mixture was heated to 55 ˚C for 5 h. After cooling, the reaction mixture was evaporated to dryness. The crude product was purified by column chromatography eluting with dichloromethane/hexane = 1/1 to give the purified

m-/*p*-[2-isopropyloxycarbonyloxy-1-(4'-acetoxy-2',2',6',6'-tetramethylpiperidine-1'-oxy)ethyl]styrene (**2**) (3.16 g, 70.5%). To a solution of **2** (2.24 g, 5.0 mmol) in ethanol (50 mL) was added aq. 10% NaOH solution (8.0 g) and refluxed for 2 h. The reaction mixture was concentrated under reduced pressure and diluted with diethyl ether (140 mL). The solution was washed with water (50 mL × 3). The organic layer was dried with sodium sulfate and evaporated to dryness. The crude product was purified by recrystallization from a mixed solvent of ethyl acetate/hexane to afford **1** as a white solid (1.13 g, 71.0%). ^{1}H NMR spectrum was shown in Figure 1. MS (FAB) *m*/*z* (%): 320 $[M+H]^+$; EA calcd (%) for $C_{19}H_{29}NO_3$ (319.21) C, 71.44; H, 9.15; N, 4.38. Found: C, 71.40; H, 9.19; N, 4.45.

Synthesis of Prepolymer

The preparation of the prepolymer was carried out under dry nitrogen in a glass tube equipped with a 3-way stopcock. In a typical polymerization, MMA (2.1 mL, 20 mmol), **1** (0.20 g, 0.65 mmol), THF (10 mL), and *tert*-butylperoxypivalate (1.4 mmol in 0.36 mL) were placed in the glass tube under dry nitrogen, which was left in a thermostated bath at 60 ˚C for 5 h. The reaction was terminated by cooling them at –78 ˚C. The reaction mixture was precipitated in a large excess of methanol and isolated by centrifugation. The molar ratio of MMA to **1** in the obtained polymer was determined by ^{1}H NMR. Each prepolymer was yielded around 48% after centrifugation.

Graft Polymerization on the Prepolymer

Graft polymerization was carried out in sealed glass vials. In a typical example, the prepolymer (0.3 g, M_n = 40,800 and M_w/M_n = 1.53), styrene (1.7 mL), and DMF (1.9 mL) were mixed in a glass flask. The feed weight ratio of the prepolymer and each monomer (St, *n*-BuA) was 1/5. The solution was then divided into glass vials. The vials were cooled with liquid nitrogen, evacuated, and purged with dry nitrogen. The polymerization was initiated by immersing them in a thermostated bath at 125 ˚C. The reaction was terminated by cooling them at –78 ˚C. Homopolymerization of *n*-BuA was carried out in the same method.

Separation of the Styrene Homopolymer from the Graft Polymer

The graft polymer sample (conversion = 79.4%, M_n = 113,800, M_w/M_n = 2.06) was ground with a pestle in a mortar. The sample (100 mg) was then added to cyclohexane (10

mL), which dissolves only the styrene homopolymer, and stirred for 1 h. The mixture was divided into cyclohexane-insoluble and -soluble parts by filtration, and each part was dried under reduced pressure. The insoluble part (50 mg) was added to cyclohexane (5 mL) and stirred for 1 h. The mixture was again separated as insoluble and soluble parts by filtration.

Synthesis of the Initiator Bearing TEMPOL

The initiator (**4**) bearing TEMPOL was synthesized according to the synthetic method for a similar compound.[19] The preparation of 1-benzyloxy-2-phenyl-2-(4'-hydroxy-2',2',6',6'-tetramethylpiperidine-1'-oxy)ethane (**3**), a precursor of **4**, was first carried out. To a solution of benzoyl peroxide (3.00 g, 12.4 mmol) in distilled styrene (128 mL, 1.11 mol) was added TEMPOL (4.80 g, 27.9 mmol) under dry nitrogen, which was heated at 80 ˚C for 25 h. After cooling, the reaction mixture was evaporated to dryness and the resulting yellow viscous liquid was purified by column chromatography eluting with chloroform/hexane = 8/2 followed by chloroform to give the purified initiator as a pale yellow solid (0.626 g, 6.4 %). To a solution of **3** (0.382 g, 0.962 mmol) in ethanol (12.0 mL) was added aq. 1N NaOH (1.20 mL, 1.20 mmol) under dry nitrogen, which was refluxed for 2 h. After cooling, the reaction mixture was evaporated to dryness and dissolved in a mixture of water (20 mL) and chloroform (20 mL). The aqueous layer was further extracted with chloroform (10 mL × 2), and the combined organic layers were evaporated to dryness. The crude product was purified by column chromatography eluting with chloroform followed by chloroform/2-propanol = 1/1 to give the purified initiator (**4**) as a white solid (0.230 g, 81.5%).

Measurements

The number average molecular weights (M_n) and polydispersities (M_w/M_n) of the polymers were measured by size exclusion chromatography (SEC) using THF at a flow rate 1.0 mL/min. at 40 ˚C on two polystyrene gel columns; TSKgel G3000H_{HR} and TSKgel GMH_{HR}-H, that were connected to a JASCO PU-980 precision pump and a JASCO RI-930 detector. The molecular weight was calibrated against eight standard polystyrene samples (M_n = 526–900,000). The monomer conversions were determined from the concentration of the residual monomer measured by gas chromatography using methyl benzoate as the internal standard, which was added after the reaction was terminated.

RESULTS AND DISCUSSION

Synthesis of the Prepolymer

First, the copolymerization of MMA with **1** (Scheme 2) at a molar ratio of 30/1 was carried out to obtain the linear prepolymer with TEMPOL residues as the side chains. The obtained copolymer contained less MMA (22/1) compared with the feed molar ratio (30/1). This indicates that **1** is more reactive than MMA. This result agrees with that of the copolymerization of a large excess MMA and styrene (St) under the same condition. Figure 1 shows the ^{1}H NMR spectra of the prepolymer and **1**. After the copolymerization, the peaks

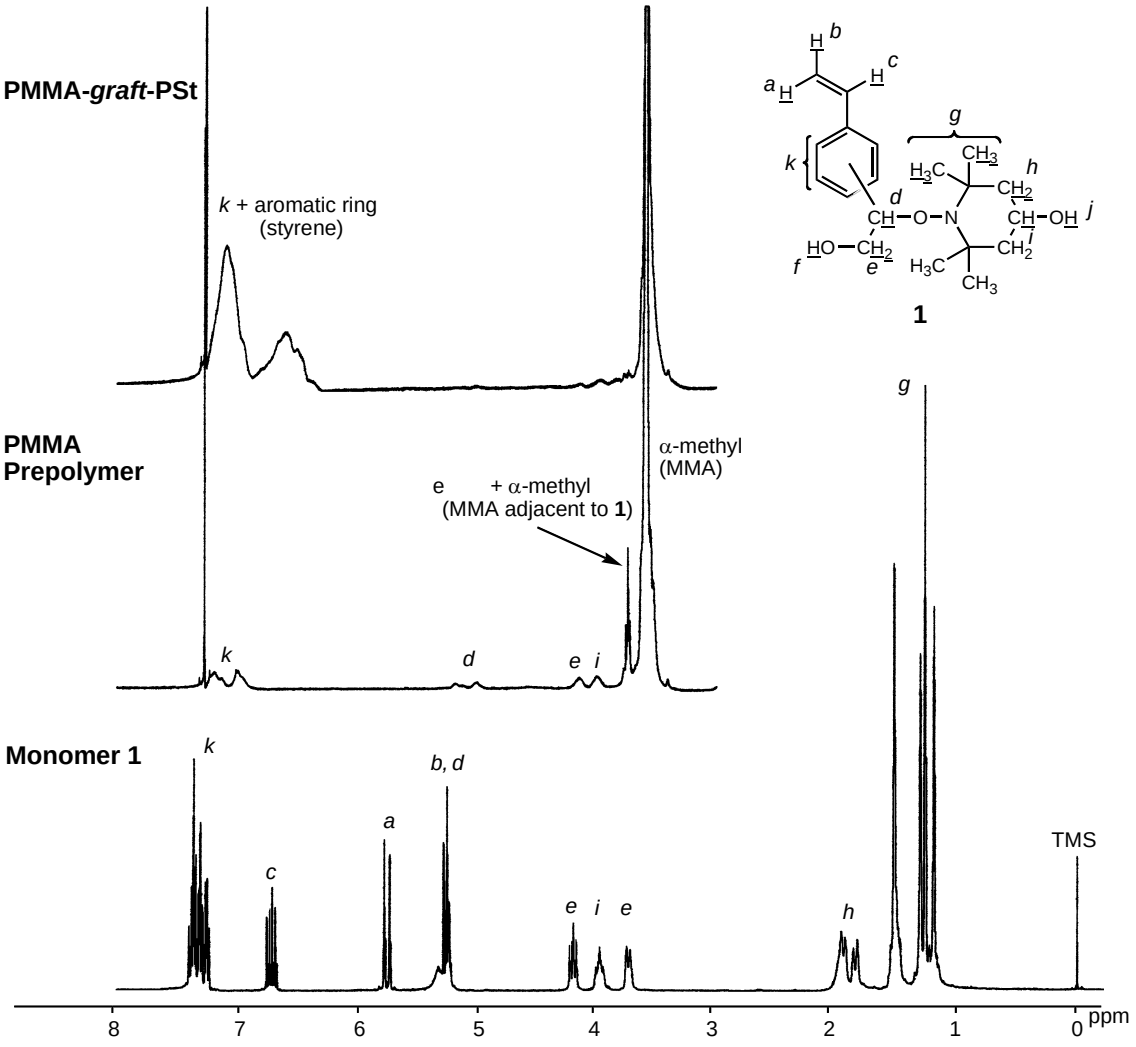

Figure 1. ^{1}H NMR analysis of intermediary products generated during the synthesis of PMMA-*graft*-PSt.

due to a vinyl group (a–c) disappeared and the peaks of the TEMPOL residues (i, j) were observed in the prepolymer.

Graft Polymerization of Styrene on the Prepolymer

To the prepolymer (M_n = 40,800 and M_w/M_n = 1.53, MMA/**1** = 22/1, yield = 48%), the St monomer was added and heated at 125 ˚C in DMF to prepare graft copolymers via dissociation of the TEMPOL residues in the prepolymer. Figure 2 shows the SEC curves of the graft polymers obtained at various conversions and Figure 3 shows the plots of the St conversion versus M_n or M_w/M_n in the graft polymerization of St on the prepolymer at the weight ratio of prepolymer/St = 1/5. As the conversion increased, M_n increased without a

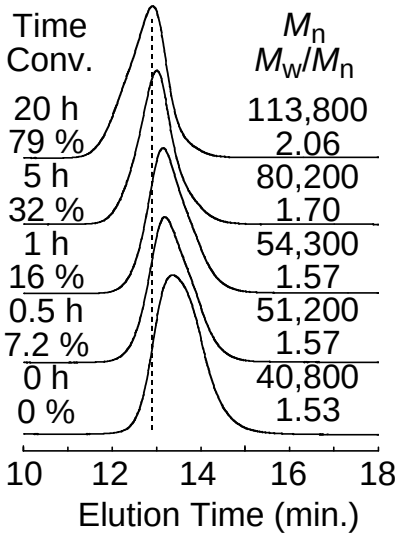

Figure 2. SEC curves in the graft polymers obtained from the prepolymer and St in DMF at 125 ˚C: Prepolymer/St/DMF = 0.3/1.5/1.8 (g); conv. was determined by GC.

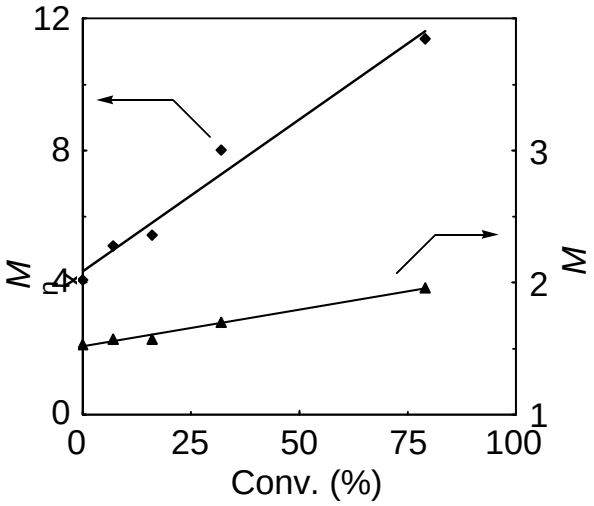

Figure 3. Conversion vs. M_n (◆) and M_w/M_n (▲) in the graft polymerization of St.

significant increase in the polydispersity. These results support the fact that the graft polymerization proceeded in a living manner.

The graft polymerization system may also produce a styrene homopolymer. This was

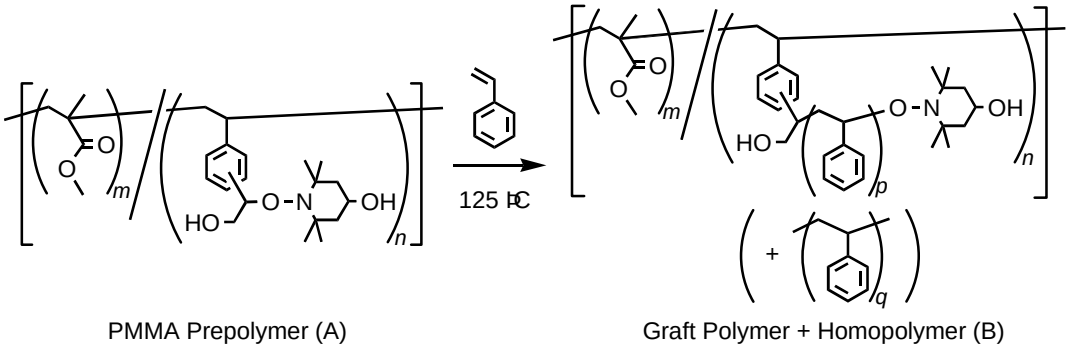

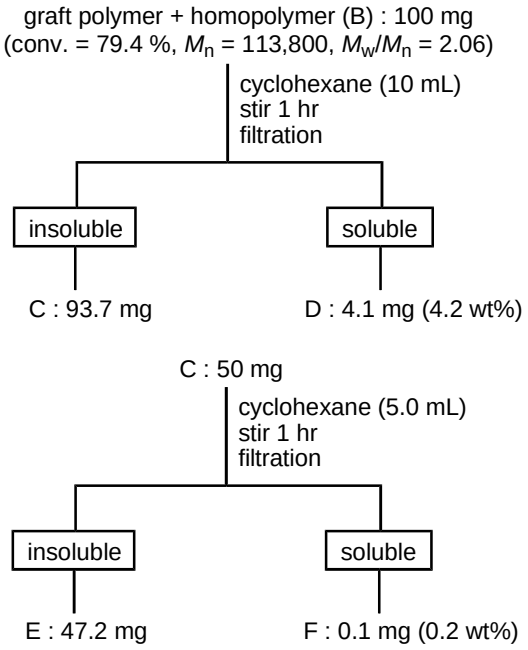

Scheme 3. Separation of the styrene homopolymer from the graft polymer.

confirmed according to the method described in the experimental section and the results are shown in Scheme 3. From the first filtration, a cyclohexane-insoluble part (93.7 mg) and soluble part (4.1 mg) were obtained. The second filtration afforded a cyclohexane-insoluble part (47.2 mg) and soluble part (0.1 mg). The molar ratios, **1**/MMA and St/MMA, of each part calculated by ^{1}H NMR are summarized in Table I. The calculation was performed according to the following equations.

$$\frac{\mathbf{1}}{\mathrm{MMA}} = \frac{\mathrm{n}}{\mathrm{m}} = \frac{4\mathrm{n}/4}{3\mathrm{m}/3} = \frac{\text{area (aromatic ring)} / 4}{\text{area } (\alpha\text{-methyl}) / 3} \ (= \mathrm{Y})$$

$$\frac{St}{MMA} = \frac{n(p+q)}{m} = \frac{\{4n + 5n(p+q) - 4n\} / 5}{3m / 3} = \frac{\text{area (aromatic ring)} / 5}{\text{area } (\alpha\text{-methyl}) / 3} - \frac{4}{5} Y$$

Table I. Molar Ratios in Fractions A–F Obtained by ^{1}H NMR

Fraction	**1** / MMA molar ratio	St / MMA molar ratio
A	0.0461	-
B	0.0461	5.51
C	0.0461	5.28
D	~ 0	>> 1
E	0.0461	5.18
F	-	-

The ^{1}H NMR of the cyclohexane-soluble part separated during the second filtration (Fraction F in Table I) indicated the absence of a polymer, suggesting that the St homopolymer was completely separated by the first filtration. Therefore, the efficiency of the graft polymerization was calculated to be 94% by the following equation.

$$X = \frac{\frac{St\ (\text{graft polymer})}{MMA}}{\frac{St\ (\text{graft polymer}) + St\ (\text{homopolymer})}{MMA}} = \frac{5.18}{5.51} = 94.0\ (\%)$$

The graft polymerization of styrene on the prepolymer efficiently proceeded almost without forming styrene homopolymers.

Graft Polymerization of *n*-Butyl Acrylate on the Prepolymer

As described above, the graft polymerization of styrene on the prepolymer proceeded in a living fashion and the graft polymers with a controlled side chain were obtained. Although the living polymerization of styrene effectively proceeded using the nitroxide, the living radical polymerization of an acrylate such as *n*-butyl acrylate (*n*-BuA) may be difficult because this has been realized only using the designed nitroxide.[20–24] The living radical polymerization of acrylates using other initiator or catalyst systems has been reported.[10, 13, 25–29]

The graft polymerization of *n*-BuA on the prepolymer (M_n = 32,400 and M_w/M_n = 1.46, MMA/**1** = 23/1, yield = 43%) was carried out in DMF at 125 °C. The polymerization did not proceed in a living manner, but reached a 94 % conversion after 4 h. The polymerization

proceeded by forming both the graft polymer and the *n*-BuA homopolymer. The polymerization may start in a short time mainly by the radicals produced via the dissociation

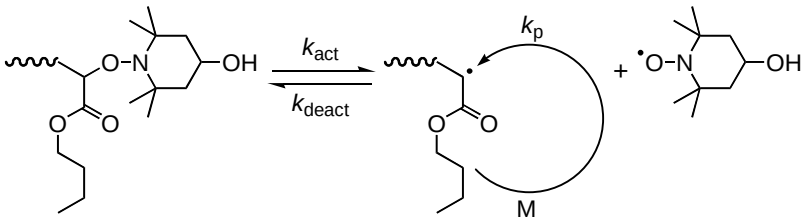

Scheme 4. Mechanism of NMP process.

of the TEMPOL residues. However, rapid equilibrium between the TEMPOL residues and the dissociated species (Scheme 4) cannot take place due to the existence of negligible amounts of the TEMPOL radical.

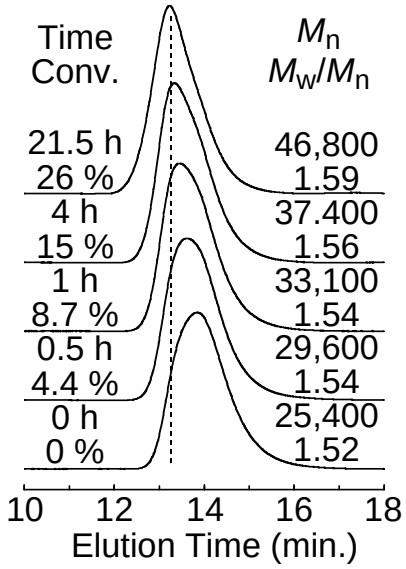

Figure 4. SEC curves of the graft polymers obtained from prepolymer and *n*-BuA in the presence of TEMPOL in DMF at 125 ˚C: Prepolymer/*n*-BuA/DMF = 0.3/1.5/1.8 (g); $[TEMPOL]_0$ = 0.15 mmol/L.

To shift this equilibrium to the dormant species, small amounts of TEMPOL were added to the polymerization system. Figure 4 shows the SEC curves of the obtained polymers via the graft polymerization of *n*-BuA in the presence of TEMPOL. As the reaction proceeded, the peak tops of the obtained polymers moved to a higher molecular weight as well as in the graft polymerization of styrene. Figure 5 shows the plots of the *n*-BuA conversion versus M_n or M_w/M_n for the graft polymerization. In the absence of

TEMPOL, the polymerization rapidly proceeded and the molecular weights were almost constant regardless of the conversion. As the polymerization proceeded, the polydispersities increased and finally reached 5.0 after 4 h. On the other hand, in the presence of TEMPOL, the graft polymerization of *n*-BuA on the prepolymer (M_n = 25,400 and M_w/M_n = 1.52, MMA/**1** = 22/1, yield = 46 %) was also carried out in DMF at 125 °C. The reaction was depressed, and the molecular weights increased with an increase in the conversion, keeping the polydispersities around 1.5.

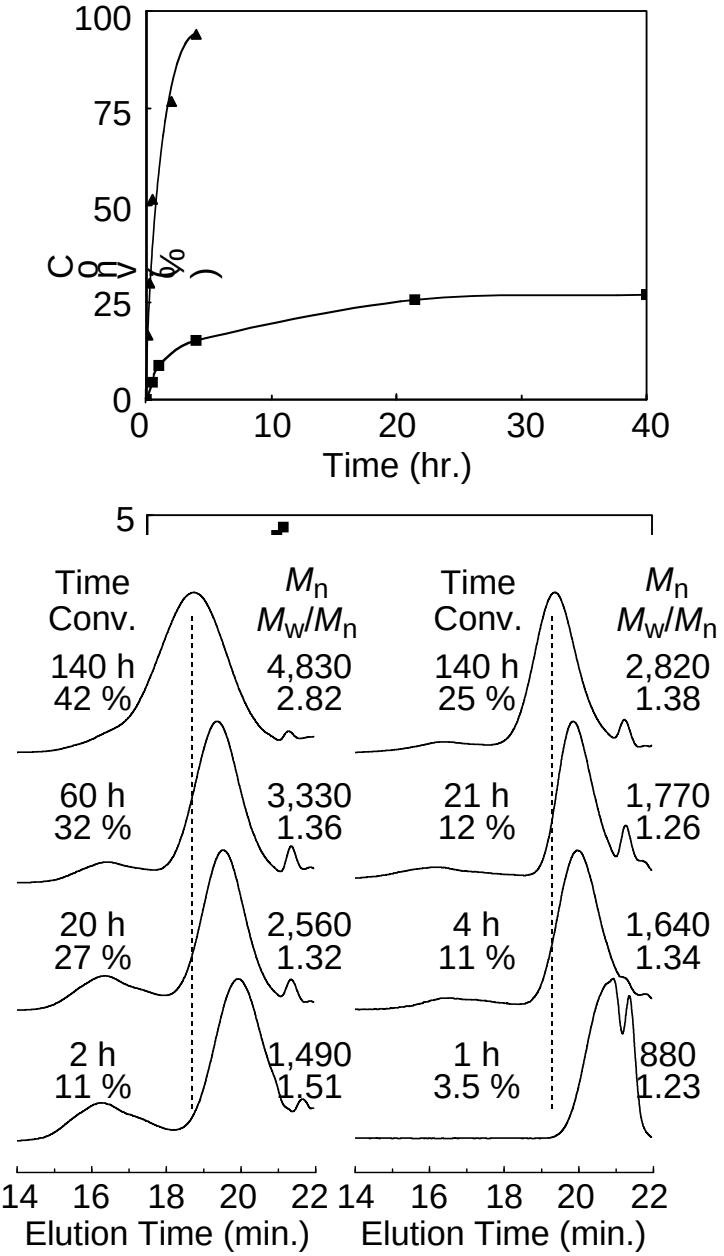

Figure 6. SEC curves of polymers of *n*-BuA in the absence (left) and presence (right) of TEMPOL in DMF at 125 ˚C: **4**/*n*-BuA/DMF = 0.035/1.5/1.8 (g); $[TEMPOL]_0$ = 0.15 mmol/L (right).

The graft polymerization system may also produce a *n*-BuA homopolymer by undesirable thermal initiation similar to the graft polymerization of styrene. The separation of the *n*-BuA homopolymer from the graft polymer was attempted by the same method as the separation of styrene homopolymer but failed.

To confirm the effect of added free TEMPOL on the polymerization of *n*-BuA, the homopolymerization of *n*-BuA was carried out in the presence and absence of TEMPOL using the initiator **4** (Scheme 2) that has the same structure as that in the prepolymer. The polymerization proceeded in both the cases, while a faster polymerization occurred in the absence of TEMPOL (42% and 25% conversion in 140 h). Figure 6 shows the SEC curves

of the homopolymers of *n*-BuA and the M_n and M_w/M_n values for the main peaks of the curves. Although the main peaks of the SEC curves moved to higher molecular weight with an increase in conversion and showed narrow polydispersities in both polymerizations, narrower ones were obtained for the polymers obtained in the presence of TEMPOL. In addition, higher molecular weight fraction, which was probably formed by uncontrolled radical polymerization, was larger in the absence of TEMPOL. Furthermore, the main peaks became finally broader (M_w/M_n = 2.82), for the polymers obtained without TEMPOL in 42% conversion. These results suggest that addition of TEMPOL reduces the concentration of the radical species and makes the polymerization more controllable.

Influence of TEMPOL Concentration

Since TEMPOL exhibited a clear effect on the polymerization, its effect on the graft polymerization of the prepolymer (M_n = 34,300 and M_w/M_n = 1.50, MMA/**1** = 22/1, yield = 49%) was further studied. The results are summarized in Table II and Figure 7. The effect on the polydispersity was clearly observed at $[\text{TEMPOL}]_0/[\textbf{1} \text{ in Prepolymer}]_0 = 5 \times 10^{-6}$ and the conversions decreased with an increase in the TEMPOL content.

Table II. Graft Polymerization of *n*-BuA on the Prepolymer in Cyclohexanone at 125 ˚C[a]

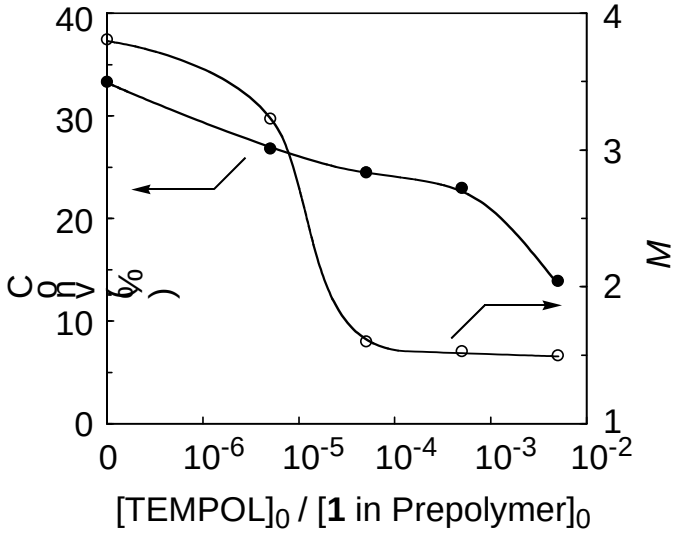

Figure 7. Effect of $[TEMPOL]_0/[\mathbf{1}$ in Prepolymer$]_0$ on conversion (●) and M_w/M_n (○).

15		3	24.8	3.08	1.81
16		5	26.8	2.11	3.23
17	0	0	0	3.39	1.48
18		1	25.7	2.28	2.73
19		3	32.7	2.30	2.91
20		5	33.3	2.03	3.81

[a]Prepolymer / *n*-BuA / Cyclohexanone = 0.1 / 0.5 / 1.2 (g).
[b]Determined by GC. [c]Determined by SEC in THF (PS standard).

CONCLUSIONS

The syntheses of the graft polymers with various side chains were carried out using the monomer **1** having a TEMPOL residue. The prepolymer was first prepared by the copolymerization of MMA and **1**. The graft polymers were obtained through the dissociation of the TEMPOL residue of **1**. The graft polymerization of St on the prepolymer proceeded in a living manner. The addition of a small amount of TEMPOL made the graft polymerization of *n*-BuA on the prepolymer more controllable.

REFERENCES

(1) Thomas, H. R.; O'Malley, J. J. *Macromolecules*, **1979**, *12*, 323.

(2) Yamashita, Y.; Tsukahara, Y.; Ito, K.; Okada, K.; Tajima, Y. *Polym. Bull.*, **1981**, *5*, 335 .

(3) Petel, N. M.; Dwight, D. W.; Hedrick, J. L.; Webster, D. C.; McGrath, J. E. *Macromolecules*, **1988**, *21*, 2689.

(4) Georges, M. K.; Veregin, R. P. N.; Kazmaier, P. M.; Hamer, G. K. *Macromolecules* **1993**, *26*, 2987.

(5) Hawker, C. J. *J. Am. Chem. Soc.* **1994**, *116*, 11185.

(6) Hawker, C. J.; Bosman, A. W.; Harth, E. *Chem. Rev.* **2001**, *101*, 3661 and references cited therein.

(7) Kato, M.; Kamigaito, M.; Sawamoto, M.; Higashimura, T. *Macromolecules* **1995**, *28*, 1721.

(8) Wang, J.-S.; Matyjaszewski, K. *J. Am. Chem. Soc.* **1995**, *117*, 5614.

(9) Kamigaito, M.; Ando, T.; Sawamoto, M. *Chem. Rev.* **2001**, *101*, 3689 and references cited therein.

(10) Chiefari, J.; Chong, Y. K.; Ercole, F.; Krstina, J. Jeffery, K.; Tam, P. T. Le.; Mayadunne, R. T. A.; Meijs, G. F.; Moad, C. L.; Moad, G.; Rizzardo, E.; Thang, S. H. *Macromolecules* **1998**, *31*, 5559.

(11) Quinn, J. F.; Rizzardo, E.; Davis, T. P. *Chem. Commun.*, **2001**, *11*, 1044.

(12) Kirci, B.; Lutz, J.-F.; Matyjaszewski, K. *Macromolecules*, **2002**, *35*, 2448.

(13) Yamago, S.; Iida, K.; Yoshida, J.-i. *J. Am. Chem. Soc.*, **2002**, *124*, 2874.

(14) Grubbs, R. B.; Hawker, C. J.; Dao, J.; Frechet, J. M. J. *Angew. Chem., Int. Ed.*, **1997**, *36*, 270.

(15) Russell, K. E. *Prog. Polym. Sci.*, **2002**, *27*, 1007 and references cited therein.

(16) Bowden, N. B.; Dankova, M.; Wiyatno, W.; Hawker, C. J.; Waymouth, R. M. *Macromolecules*, **2002**, *35*, 9246.

(17) Ejaz, M.; Ohno, K.; Tsujii, Y.; Fukuda, T. *ACS Polymer Preprints*, **2003**, *44*, 532.

(18) Hayashi, M.; Nakamura, T. *Jpn Kokai Tokkyo Koho (Patent)*, **2000**, 2000–95744 .

(19) Hawker, C. J.; Barcley, G. G.; Orellana, A.; Dao, J.; Devonport, W. *Macromolecules*, **1996**, *29*, 5245.

(20) Listigovers, N. A.; Georges, M. K.; Odell, P. G.; Keoshkerian, B. *Macromolecules*,

1996, *29*, 8992.

(21) Keoshkerian, B.; Szkurhan, A. R.; Georges, M. K. *Macromolecules*, **2001**, *34*, 6531.

(22) Benoit, D.; Chaplinski, V.; Braslau, R.; Hawker, C. J. *J. Am. Chem. Soc.*, **1999**, *121*, 3904.

(23) Farcet, C.; Charleux, B.; Pirri, R. *Macromolecules*, **2001**, *34*, 3823.

(24) Cameron, N. R.; Reid, A. J. *Macromolecules*, **2002**, *35*, 9890.

(25) Wang, J.-S.; Matyjaszewski, K. *Macromolecules*, **1995**, *28*, 7901.

(26) Percec, V.; Barboiu, B.; Kim, H.-J. *J. Am. Chem. Soc.*, **1998**, *120*, 305.

(27) Moineau, G.; Minet, M.; Dubois, Ph.; Teyssie, Ph.; Senninger, T.; Jerome, R. *Macromolecules*, **1999**, *32*, 27.

(28) Uegaki, H.; Kotani, Y.; Kamigaito, M.; Sawamoto, M. *Macromolecules*, **1998**, *31*, 6756.

(29) Ohishi, I.; Baek, K.-Y.; Kotani, Y.; Kamigaito, M.; Sawamoto, M. *J. Polym. Sci., Part A: Polym. Chem.*, **2002**, *40*, 2033.

CHAPTER 2

GRAFT POLYMERS OF METHACRYLATE, ACRYLATE, AND STYRENE: CONTROL OF BACKBONE AND GRAFT CHAIN LENGTHS

ABSTRACT

The ruthenium-catalyzed living radical polymerization was first applied to the synthesis of a series of well-defined graft polymers with the controlled lengths of both the backbone and graft chains. The synthetic method was based on the ruthenium-catalyzed "grafting-from" polymerization of various monomers, such as methacrylate, acrylate, and styrene, from the backbone polymers also obtained via the ruthenium-catalyzed living radical polymerization. The backbone polymer was first synthesized by the ruthenium-catalyzed living radical random copolymerization of methyl methacrylate (MMA) and 2-(trimethylsilyloxy)ethyl methacrylate (TMSHEMA) followed by the in-situ transformation of the silyloxyl group into the ester with a C–Br bond via direct reaction with the acid bromide (2-bromoisobutyryl bromide). The obtained multifunctional macroinitiator was employed for the ruthenium-catalyzed "grafting-from" radical polymerization of MMA, *n*-butyl acrylate, styrene, and TMSHEMA to afford a series of the graft polymers ($M_w/M_n \sim 1.1$) with controlled lengths of the backbone and graft chains.

INTRODUCTION

Radical polymerization is one of the most widely employed methods in industrial polymer synthesis, but usually results in poorly-controlled polymers in terms of the primary structures such as molecular weights, molecular weight distributions (MWDs), and their architectures. However, in recent years, living/controlled radical polymerizations have been significantly developed to allow the syntheses of various well-defined polymers not only with controlled molecular weights and with defined end-groups, but also with controlled architectures, such as block, graft, and star polymers. These rapidly spreading polymerizations can be mainly categorized into the following three processes: the nitroxide-mediated polymerization (NMP),[1–4] the metal-catalyzed living radical polymerization or atom transfer radical polymerization (ATRP),[5–9] and the reversible addition-fragmentation chain transfer (RAFT) polymerization.[10]

Graft copolymers, defined as comb-shaped branched polymers with a number of attached graft chains on the backbone chain, can be generally obtained by three methods, i.e.; "grafting-onto", "grafting-from", and "grafting-through" methods. The last two methods are effective for synthesizing well-defined graft polymers when combined with living polymerization. The various living radical polymerizations mentioned above have also been used for the graft copolymer synthesis.[11–13] The "grafting-through" method,[14–21] which involves the polymerizations of macromonomers, produced controlled graft copolymers, but often resulted in an incomplete monomer consumption due to the poor reactivity of the macromonomers at higher conversions.[21] On the other hand, "grafting-from" by living radical polymerizations[22–34] has been applied as an efficient method to synthesize graft copolymers having various grafting chains. In this method, relatively high molecular weight polymers with multifunctional initiating sites can be used as the backbone chain to produce the high molecular weight graft copolymers.[24–30] More recently, graft copolymers with controlled molecular weights both in the graft and backbone chains have also been attained by the combination of the living radical polymerizations.[32–34] Another excellent application of the Cu-mediated ATRP to the "grafting-from" method is the growth of densely grafted chains on a material surface.[35–42]

In this chapter, the author reports the synthesis of the graft copolymers with controlled lengths of both the backbone and graft chains via the repeated

ruthenium-catalyzed living radical polymerizations (Scheme 1). The ruthenium-catalyzed living radical polymerization is one of the most versatile and controllable systems that can be employed for a wide variety of monomers such as methacrylates, acrylates, and styrenes. The controllability in terms of molecular weights, MWDs, and end-functionality of the halogen group is the most reliable and excellent among the other metal-catalyzed living radical polymerizations. Although the ruthenium-catalyzed polymerization has been used for the synthesis of various end-functionalized,[43,44] block,[45] and star polymers,[46–49] no applications of the systems to the graft polymer synthesis have been reported.

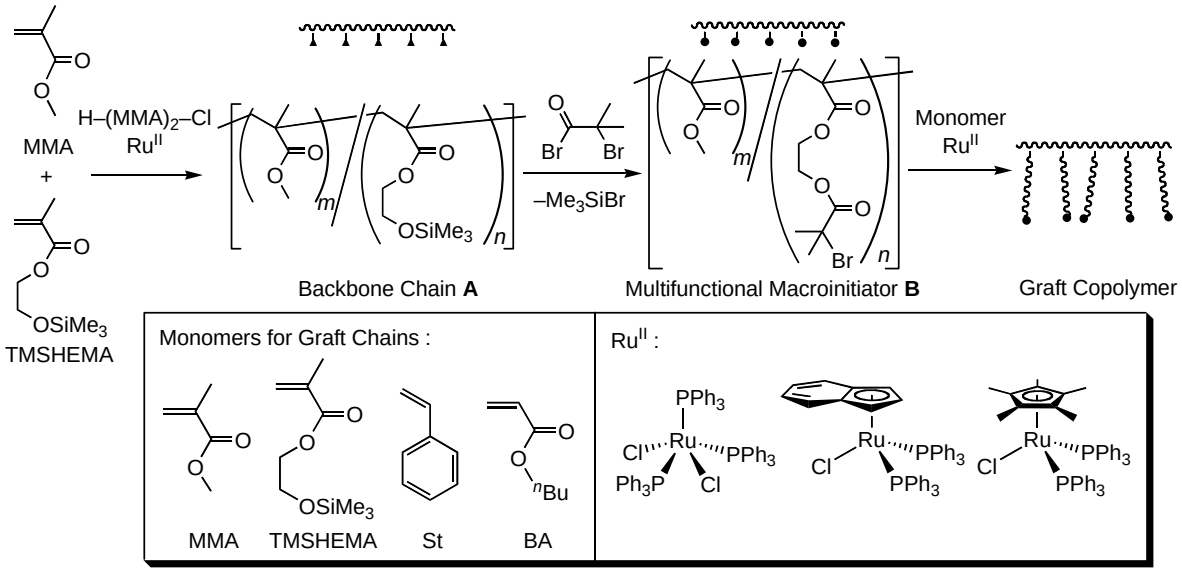

Scheme 1. Graft copolymerization via ruthenium-catalyzed living radical polymerization.

Thus, the author first synthesized poly(methacrylate)s with multifunctional initiating sites and controlled molecular weights via the ruthenium-catalyzed living radical random copolymerization of methyl methacrylate (MMA) and 2-(trimethylsilyloxy)ethyl methacrylate (TMSHEMA), followed by the in-situ transformation of the Si-group into the ester with a C–Br bond via direct reaction with the acid bromide (2-bromoisobutyryl bromide). The author then employed the ruthenium-catalyzed "grafting-from" living radical polymerization of various monomers, such as MMA, TMSHEMA, *n*-butyl acrylate (BA), and styrene (St), for the synthesis of a series of graft copolymers with different types of monomers and controlled chain lengths.

EXPERIMENTAL

Materials

MMA (Tokyo Kasei; >99%) was washed with aq. NaOH (5%) and water, dried over magnesium sulfate, and distilled from calcium hydride under reduced pressure before use. St, BA (both Tokyo Kasei; >99%) and TMSHEMA (Aldrich; >96%) were distilled over calcium hydride under reduced pressure before use. $Me_2C(CO_2Me)CH_2C(CO_2Me)(Me)Cl$ [H–$(MMA)_2$–Cl] as an initiator, was prepared and purified by distillation as reported.[50] $RuCl_2(PPh_3)_3$, (STREM; >99%) $Ru(Ind)Cl(PPh_3)_2$, $Ru(Cp^*)Cl(PPh_3)_2$ (both were donated from Wako Chemicals), $Al(acac)_3$ (acac: acetylacetonate), Al(O*t*-Bu)$_3$ (both Wako Chemicals; >98%) were used as received. All metal compounds were handled in a glove box (VAC) under a moisture- and oxygen-free argon atmosphere (H_2O, <1 ppm; O_2, <1 ppm). Toluene was distilled from sodium and benzophenone and bubbled with dry nitrogen over 15 minutes right before use. *n*-Bu_3N (as an additive), *n*-hexane, and tetralin (as an internal standards for gas chromatographic analysis of the monomers) were distilled from calcium hydride before use. 2-Bromoisobutyryl bromide (BIBB, Aldrich; >98%) was distilled before use.

Synthesis of the Backbone Chain

All polymerizations were carried out by syringe technique under dry nitrogen in glass tubes equipped with a three-way stopcock or in baked and sealed glass vials. A typical example for the copolymerization of MMA and TMSHEMA with H–$(MMA)_2$–Cl/$Ru(Ind)Cl(PPh_3)_2$/*n*-Bu_3N is given below. In a 50 mL round-bottomed flask was placed $Ru(Ind)Cl(PPh_3)_2$ (10 mg, 0.013 mmol), hexane (0.30 mL), MMA (1.01 mL, 9.38 mmol), TMSHEMA (0.68 mL, 3.12 mmol), H–$(MMA)_2$–Cl (0.25 mL of 509 mM solution in toluene, 0.13 mmol) and *n*-Bu_3N (0.16 mL of 400 mM solution in toluene, 0.064 mmol) at room temperature. The total volume of reaction mixture was 6.40 mL. Immediately after mixing, nine aliquots (0.70 mL each) of the solutions were injected into backed glass tubes. The reaction vials were sealed and placed in an oil bath kept at 80 ˚C under vigorous stirring. In predetermined intervals, the polymerization was terminated by cooling the reaction mixtures to –78 ˚C. Monomer conversion was determined by gas chromatography with hexane as an internal standard. The quenched reaction solution was precipitated into hexane and isolated by centrifugation. After three times of the precipitation, the precipitate was

evaporated to dryness to yield the product, which was subsequently dried overnight *in vacuo* at room temperature.

In-situ Transformation of the Backbone Chain into the Multifunctional Initiator

An in-situ synthetic method of multifunctional macroinitiator **B** via direct reaction with the acid bromide is given below. In a 50 mL round-bottomed flask was synthesized the backbone chain **A** as shown above. Directly to the quenched reaction solution was then added 2-bromoisobutyryl bromide (2.0 mL, 16.2 mmol, 6.0 equiv to the trimethylsilyl unit) at room temperature under stirring for 36 h. The reaction mixture was precipitated into hexane and isolated by centrifugation. After three times of the precipitation, the precipitate was diluted with acetone and precipitated into hexane. The precipitate was then evaporated to dryness to yield the product, which was subsequently dried overnight *in vacuo* at room temperature.

Ruthenium-Catalyzed "Grafting-from" Copolymerization of Various Monomers

A typical example for the graft copolymerization of MMA on the multifunctional macroinitiator **B** with $Ru(Ind)Cl(PPh_3)_2/Al(acac)_3$ is given below. In a 50 mL round-bottomed flask was placed polymer **B** (75 mg, 0.13 mmol C–Br bonds), $Ru(Ind)Cl(PPh_3)_2$ (10 mg, 0.013 mmol), $Al(acac)_3$ (0.163 g, 0.50 mmol), hexane (0.32 mL), and MMA (0.68 mL, 6.30 mmol) at room temperature. The total volume of reaction mixture was 12.60 mL. Immediately after mixing, ten aliquots (1.00 mL each) of the solutions were injected into backed glass tubes. The reaction vials were sealed and placed in an oil bath kept at 80 ˚C under vigorous stirring. In predetermined intervals, the polymerization was terminated by cooling the reaction mixtures to –78 ˚C. Monomer conversion was determined by gas chromatography with hexane as an internal standard. The quenched reaction solution was precipitated into methanol and isolated by centrifugation. After three times of the precipitation, the precipitate was evaporated to dryness to yield the product, which was subsequently dried overnight *in vacuo* at room temperature.

Detachment of Polystyrene Graft Chains from the Backbone

Prior to the hydrolysis, the graft copolymers were fractionated by preparative SEC to remove a small amount of the higher molecular weight fraction. The fractionated graft

copolymer with PSt graft chains (60 mg) was then placed in a 25 mL round-bottom flask and dissolved in THF (9.0 mL). After adding KOH solution (0.3 g dissolved in 3.0 mL of methanol), the mixture was heated to 80 ˚C for 24 h. The solvent was removed by evaporation, and 6.0 mL of $CHCl_3$ was added to the remaining solid. The solution was washed with water (6.0 mL × 3). The organic layer was evaporated to dryness to yield the product, which was subsequently dried overnight *in vacuo* at room temperature to give 50 mg of the detached polystyrene.

Measurements

The ^{1}H NMR spectra were recorded on a Varian Gemini 2000 spectrometer (400 MHz) in $CDCl_3$ at 50 ˚C. The number average molecular weights (M_n) and molecular weight distributions (MWDs: M_w/M_n) of the polymers were measured by size exclusion chromatography (SEC) using THF at a flow rate 1.0 mL/min. at 40 ˚C on two polystyrene gel columns; both Shodex KF-805L, that were connected to a JASCO PU-980 precision pump and a JASCO RI-930 detector. The molecular weight was calibrated against seven standard poly(methyl methacrylate) samples (M_n = 1,990–6,590,000) or eight standard polystyrene samples (M_n = 526–900,000). The monomer conversions were determined from the concentration of the residual monomer measured by gas chromatography using hexane or tetralin as the internal standard. The absolute weight-average molecular weight (M_w) of the polymers was determined by multiangle laser light scattering (MALLS) in tetrahydrofuran (THF) at 40 ˚C on Wyatt Technology DAWN DSP photometer (λ = 633 nm). The refractive index increment (dn/dc) was measured in THF at 25 ˚C on Wyatt Optilab rEX refractmeter (λ = 633 nm). For example, the dn/dc value was 0.103 mL/g for the graft polymer of PMMA graft chains.

RESULTS AND DISCUSSION

Synthesis of Well-Defined Backbone Polymer by Ruthenium-Catalyzed Living Radical Random Copolymerization of MMA and TMSHEMA

The ruthenium-catalyzed living radical polymerization was first employed for the synthesis of the well-defined backbone polymers. For this, the author copolymerized MMA

and TMSHEMA using two representative ruthenium complexes [$RuCl_2(PPh_3)_3$ and $Ru(Ind)Cl(PPh_3)_2$], both of which are effective for the living radical polymerization of methacrylates,[5,51] to obtain copolymers with the silyloxy-groups in the pendants. The mixture of MMA and TMSHEMA (3:1 molar ratio) was thus polymerized with the two ruthenium complexes in conjunction with H–$(MMA)_2$–Cl [$Me_2C(CO_2Me)CH_2C(CO_2Me)(Me)Cl$] as the initiator in the presence of *n*-Bu_3N in toluene at 80 ˚C.

Both monomers were smoothly copolymerized at almost the same rate, which shows the random or statistical copolymerization of MMA and TMSHEMA. Figure 1 shows the dependence of the number-average molecular weights (M_n) of the obtained copolymers on the polymer yield calculated from the conversions of each monomer. With both $RuCl_2(PPh_3)_3$ and $Ru(Ind)Cl(PPh_3)_2$, the M_n increased in direct proportion to the copolymer yield and agreed well with the calculated values assuming that one molecule of the initiator [H–$(MMA)_2$–Cl] generates one living polymer chain. Both series of the SEC curves shifted to a higher molecular weight with the increasing yields. The MWDs were narrow throughout the reaction while they were narrower with $Ru(Ind)Cl(PPh_3)_2$ than with $RuCl_2(PPh_3)_3$. These results indicated that $Ru(Ind)Cl(PPh_3)_2$ is more suitable for the synthesis of the well-controlled copolymers of MMA and TMSHEMA similar to the homopolymer of MMA.[51] Thus, the random copolymer of MMA/TMSHEMA with fairly

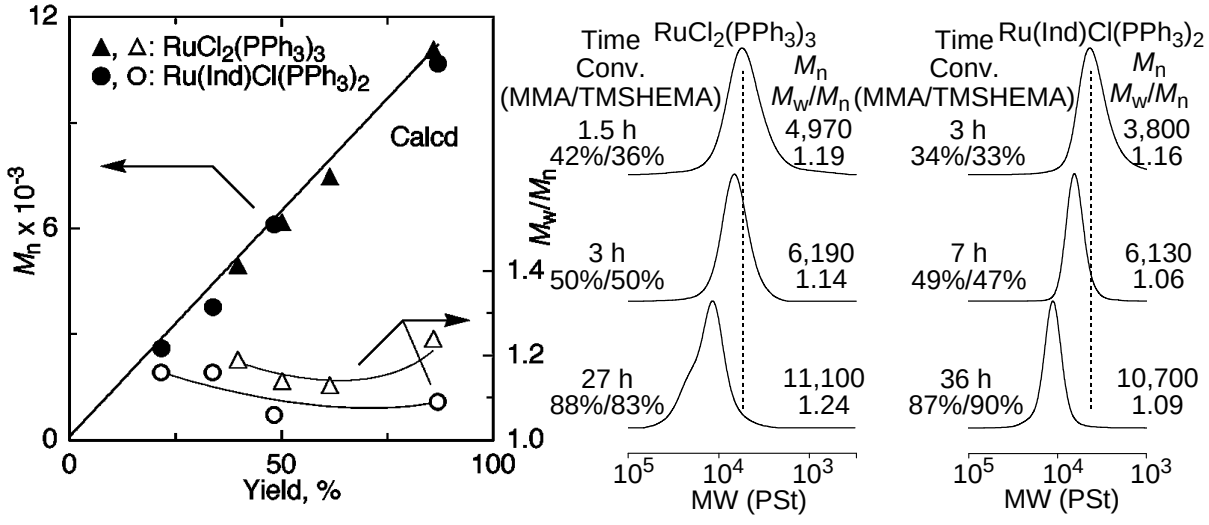

Figure 1. Random copolymerization of MMA and TMSHEMA with $RuCl_2(PPh_3)_3$ or $Ru(Ind)Cl(PPh_3)_2$ in toluene at 80 ˚C: $[MMA]_0$ = 1.5 M; $[TMSHEMA]_0$ = 0.5 M; $[H–(MMA)_2–Cl]_0$ = 20 mM, $[RuCl_2(PPh_3)_3]_0$ = 10 mM and $[n\text{-}Bu_2NH]_0$ = 40 mM (▲, △), $[Ru(Ind)Cl(PPh_3)_2]_0$ = 2.0 mM and $[n\text{-}Bu_3N]_0$ = 10 mM (●, ○).

narrow MWDs (M_n = 10,500, M_w/M_n = 1.08) was obtained as a precursor of the multifunctional macroinitiator (copolymer **A** in Scheme 1).

In-situ Transformation of the Silyloxy-Groups into the Ester with C–Br Bond via Direct Reaction with the Acid Bromide

The well-defined copolymer **A** obtained with $Ru(Ind)Cl(PPh_3)_2$ was then converted into the multifunctional macroinitiator **B**. The already reported transformation method mainly for the copper-mediated ATRP included two steps: first, the trimethylsilyl groups were deprotected into the hydroxyl form by KF and *n*-Bu_4NF, and then the esterification by an acid bromide with a C–Br bond.[16–19] Considering that the trimethylsilyl halide is a good leaving group, the author investigated the direct transformation of the trimethylsilyl groups into the brominated esters just by adding the carboxylic acid bromide [$Me_2C(Br)COBr$] in situ into the polymerization mixture without using the deprotection process (see the experimental section).

Figure 2 shows the ^1H NMR spectra of the backbone copolymers before and after the transformation with 2-bromoisobutyryl bromide (A and B, respectively). In the spectrum of copolymer **A** (Figure 2A), there were characteristic signals derived from the MMA and TMSHEMA units; i.e., the α-methyl (*f*) and main-chain methylene protons (*e*) for both units, the methoxy groups (*g*) for the MMA units, the methylene (*a* and *b*) and trimethylsilyl groups (*c*) for the TMSHEMA units. The MMA/TMSHEMA composition (75/25), obtained from the peak intensity ratio (*g* vs. *a*+*b*), was in good agreement with the calculated values from the monomer feed ratios and the gas chromatographic conversions of each monomer (73/27).

The transformation was carried out with an excess amount of 2-bromoisobutyryl bromide at r.t. for 24 h. After the transformation, the ^1H NMR spectrum of the copolymers exhibited typical changes (Figure 2B). The signal of the trimethylsilyl groups completely disappeared (*c* in Figure 2A). The *a* and *b* peaks shifted toward a lower magnetic field (peaks *a'* and *b'*, respectively) along with the appearance of an additional peak attributed to the methyl groups adjacent to the C–Br bonds (*d*). The unit ratio of MMA and the introduced brominated ester groups (75/25) agreed well with the ratio of MMA/TMSHEMA in copolymer **A** before the transformation. This indicates that the macroinitiator **B** with

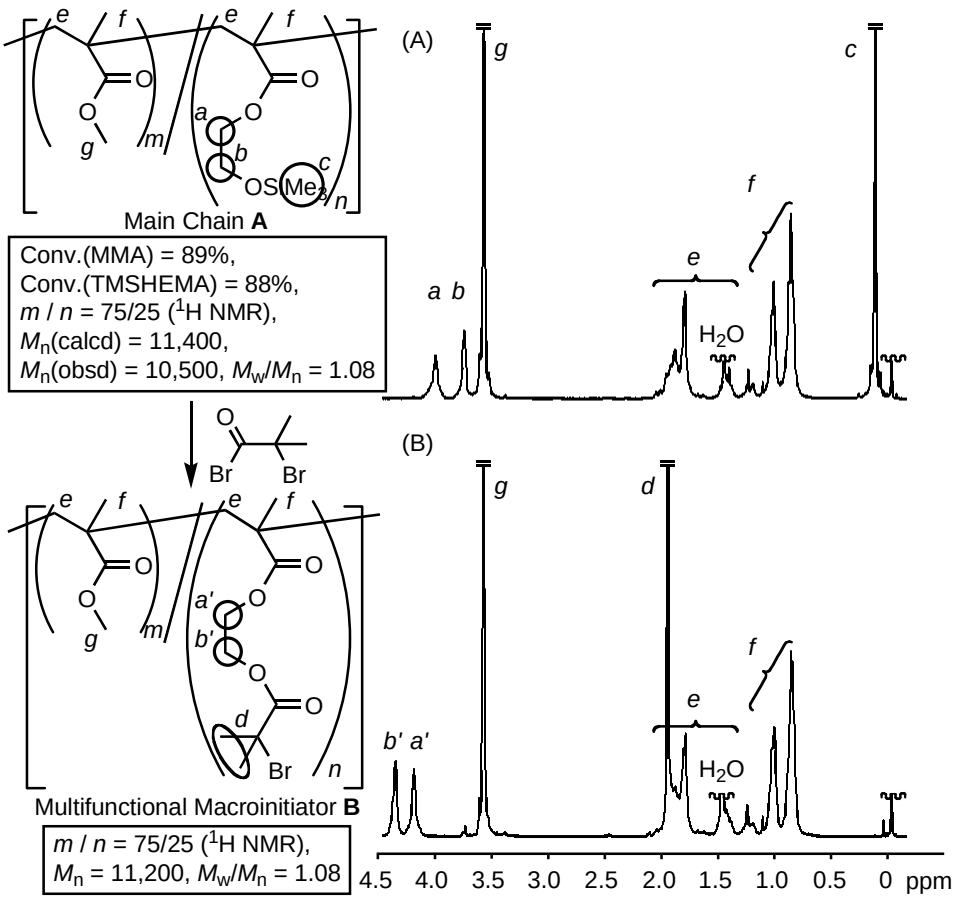

Figure 2. ^{1}H NMR spectra (in $CDCl_3$ at 50 ˚C) of before (A) and after (B) transformation of trimethylsilyloxyl groups in the backbone **A**.

multi-initiating sites on the side groups was successfully derived by the direct in-situ transformation of the trimethylsilyl groups. This method is simpler than the reported one because the two steps, i.e., the isolation of the polymer from the polymerization mixture and the deprotection of the silyl groups, can be omitted.

Ruthenium-Catalyzed Grafting-from Copolymerization of Various Monomers

The multifunctional macroinitiator **B** was then employed for the graft polymerization of MMA in conjunction with $Ru(Ind)Cl(PPh_3)_2$ in toluene at 80 ˚C in the presence of a series of additives, such as *n*-Bu_3N, $Al(O$*t*-$Bu)_3$, and $Al(acac)_3$, which are effective for enhancing the rate and the controllability of the Ru-catalyzed living radical polymerization.[46,51]

The graft polymerization of MMA smoothly proceeded with the macroinitiator **B**/Ru-system in the presence of these additives, while the graft polymerization did not reach

quantitative monomer conversion (< 50%). With all the additives, the SEC curves of the obtained polymers shifted to higher molecular weights (Figure 3). However, the polymers obtained with *n*-Bu_3N showed a broader MWD (M_w/M_n = 1.53) and a shoulder in the high molecular region, indicating some intermolecular recombination between the graft chains in the highly active Ru(Ind)Cl$(PPh_3)_2$/*n*-Bu_3N system.[52] As for the aluminum additives, Al$(acac)_3$ produced polymers with unimodal and narrow MWDs (M_n = 82,500, M_w/M_n = 1.16). In contrast, the polymers obtained with Al(O*t*-Bu)$_3$ resulted in a bimodal distribution at the later stage of the polymerization though the main peaks were relatively narrow (M_n = 61,600, M_w/M_n = 1.12). This is due to the detachment of the graft chain via transesterification between the ester-linkage of the initiating site and Al(O*t*-Bu)$_3$.[46] Thus, the graft polymerization of MMA from the multifunctional macroinitiator **B** was successfully induced by the combination of Ru(Ind)Cl$(PPh_3)_2$ and Al$(acac)_3$.

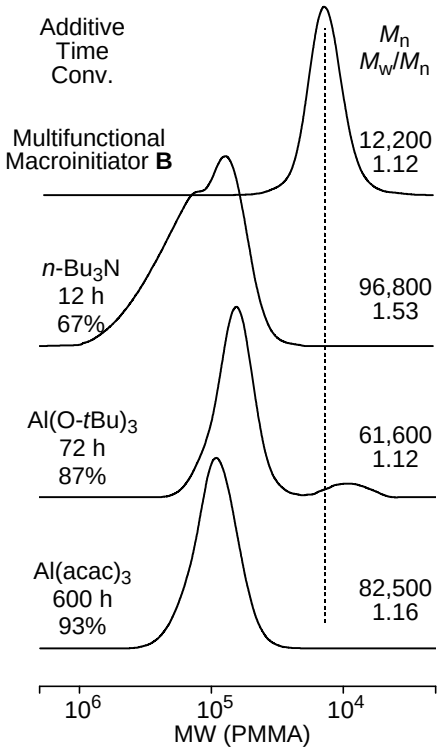

Figure 3. Graft polymerization of MMA from the multifunctional macroinitiator **B** in toluene at 80 ˚C. $[MMA]_0$ = 2.0 M; [C–Br bonds in the macroinitiator **B**]$_0$ = 10 mM; [Ru(Ind)Cl$(PPh_3)_2]_0$ = 1.0 mM; [additive]$_0$ = 40 mM.

Figure 4 shows typical examples of the Ru-catalyzed graft polymerization of MMA with the multifunctional macroinitiator **B** in the presence of Al$(acac)_3$ in toluene at 80 ˚C,

where the monomer concentration was varied ($[MMA]_0$ = 0.5 or 2.0 M). Both the graft polymerizations proceeded smoothly. The first-order kinetic plots were almost linear, indicating almost no significant irreversible termination during the polymerization.

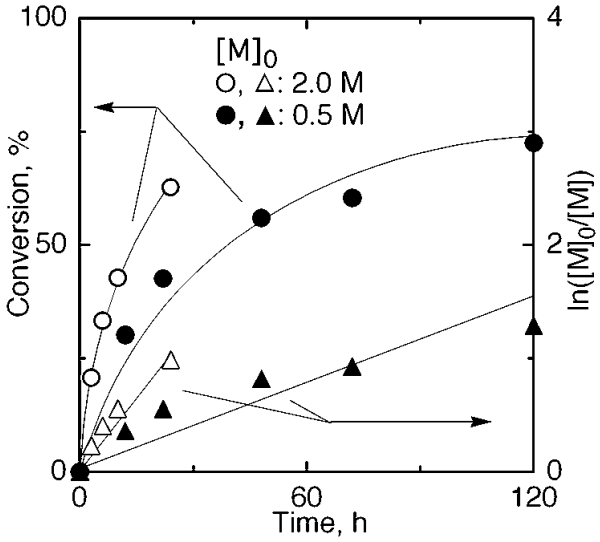

Figure 4. Graft polymerization of MMA from the multifunctional macroinitiator **B** in toluene at 80 ˚C. $[MMA]_0$ = 2.0 M (○: conversion, △: first-order plot) or 0.5 M (●: conversion, ▲: first-order plot); [C–Br bonds in the macroinitiator **B**]$_0$ = 10 mM; $[Ru(Ind)Cl(PPh_3)_2]_0$ = 1.0 mM; $[Al(acac)_3]_0$ = 40 mM.

Figure 5 shows the M_n and the SEC curves of the graft polymers of MMA obtained using the $Ru(Ind)Cl(PPh_3)_2/Al(acac)_3$ initiating system for various initial monomer concentrations ($[MMA]_0$ = 2.0 or 0.5 M). During the early stage of the polymerizations, the M_n values (filled circles and triangles), based on a PMMA standard calibration, increased in direct proportion to the monomer conversion and were close to the calculated values assuming that one molecule of **B** generates one molecule of the graft polymer. The MWDs were also unimodal and relatively narrow ($M_w/M_n < 1.2$). As the polymerization proceeded, however, the increase in the M_n leveled off in both cases. Especially, at a higher monomer concentration, the M_n of the polymer became lower than the calculated values.

The molecular weight and the mean radius of gyration (R_z) of the graft polymer was then measured by SEC equipped with multiangle laser light-scattering (MALLS) and a refractive index as a dual detector. The M_n (open circles) calculated from the absolute molecular weights (M_w) by MALLS agreed well with the calculated values throughout the reactions. These results indicated that the hydrodynamic volumes of the graft polymers are

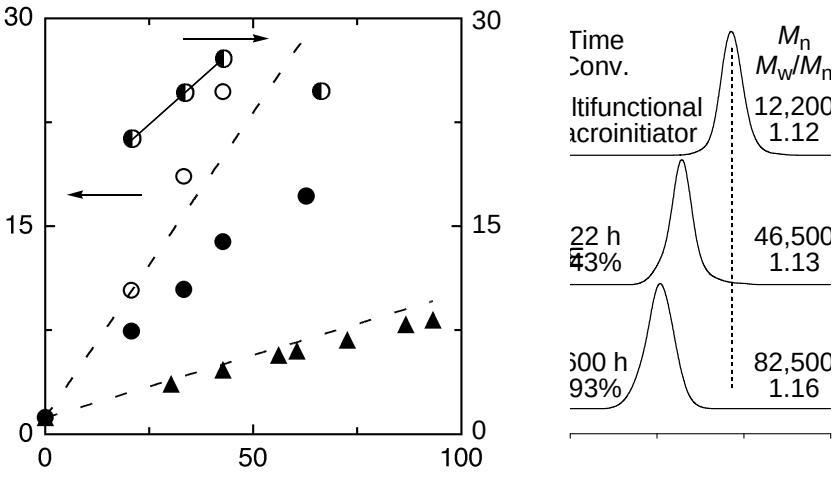

Figure 5. M_n, M_w/M_n, and MWD curves of graft polymer obtained with macroinitiator **B**/Ru(Ind)Cl(PPh_3)$_2$/Al(acac)$_3$ in toluene at 80 ˚C. [MMA]$_0$ = 2.0 M (●: M_n(SEC–RI), ○: M_n(SEC–MALLS), ◐: R_z) or 0.5 M (▲: M_n(SEC-RI)); [C–Br bonds in the macroinitiator **B**]$_0$ = 10 mM; [Ru(Ind)Cl(PPh_3)$_2$]$_0$ = 1.0 mM; [Al(acac)$_3$]$_0$ = 40 mM.

quite different from those of the linear polymers due to their branched structures and that the graft chains efficiently grew from the multi-initiating site of **B**. The R_z values (half-filled circles) slightly increased with the monomer conversion. Furthermore, it is also notable that the controlled graft copolymerization reached a high monomer conversion (>90%) without any remarkable recombination.

To further demonstrate the wide feasibility of the ruthenium-catalyzed "grafting-from" radical polymerization, other monomers, such as TMSHEMA, St, and BA, were employed with the multifunctional macroinitiator **B** in the presence of the ruthenium complexes (Figure 6). A functional methacrylate, TMSHEMA, was polymerized with the Ru(Ind)Cl(PPh_3)$_2$/Al(acac)$_3$ initiating system to give the copolymers with narrow MWDs (M_w/M_n <1.2) even at a very high conversion (~90%) (Figure 6B). The trimethylsilyloxyl groups in the graft chains can be converted into the hydroxyl functions that produce the hydrophilic grafts.

The graft copolymerization of BA was successfully done with Ru(Cp*)Cl(PPh_3)$_2$ in place of Ru(Ind)Cl(PPh_3)$_2$ to provide narrow MWDs (M_n = 113,000 M_w/M_n = 1.09) (Figure 6C) because the former has proven more effective for acrylate polymerization with narrow MWDs.[53,54] The M_n of the obtained PMMA-*g*-PBA determined by SEC-MALLS (M_n =182,000) was also close to the calculated M_n value from the gas chromatographic

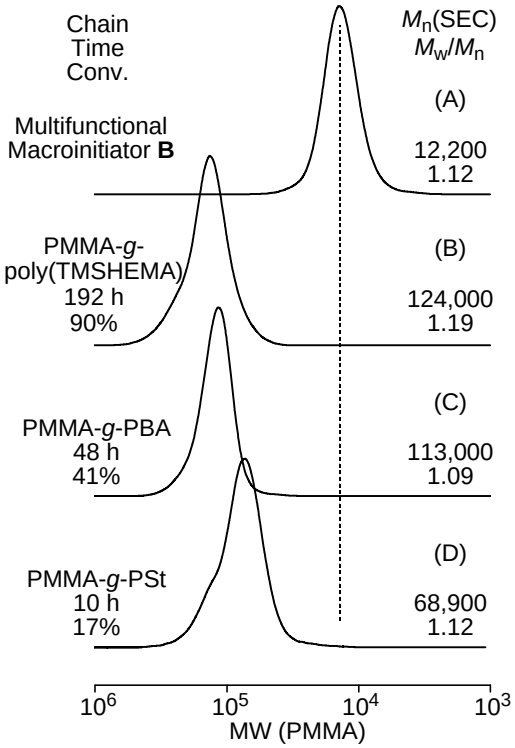

Figure 6. Graft copolymerization of (B) TMSHEMA, (C) BA, and (D) St from (A) the multifunctional macroinitiator **B** in toluene at 80 ˚C. Conditions; TMSHEMA: $[TMSHEMA]_0$ = 0.5 M; [C–Br bonds in the macroinitiator **B**]$_0$ = 10 mM; $[Ru(Ind)Cl(PPh_3)_2]_0$ = 1.0 mM; $[Al(acac)_3]_0$ = 40 mM. BA: $[BA]_0$ = 4.0 M; [C–Br bonds in the macroinitiator **B**]$_0$ = 20 mM; $[Ru(Cp^*)Cl(PPh_3)_2]_0$ = 2.0 mM; $[n\text{-}Bu_3N]_0$ = 10 mM. St: $[St]_0$ = 2.0 M; [C–Br bonds in the macroinitiator **B**]$_0$ = 10 mM; $[Ru(Ind)Cl(PPh_3)_2]_0$ = 0.5 mM; $[Al(O\textit{t}\text{-}Bu)_3]_0$ = 20 mM.

conversions [M_n(calcd) = 202,000]. The graft copolymerization of another type of vinyl monomer, St, with $Ru(Ind)Cl(PPh_3)_2/Al(O\textit{t}\text{-}Bu)_3$ resulted in narrow MWDs (M_n = 68,900, M_w/M_n = 1.12) (Figure 6D) though a small fraction of higher molecular weight products was observed as a shoulder of the main peak due to some intermolecular coupling reactions. Thus, the ruthenium-catalyzed "grafting-from" living radical polymerization was effective in producing well-controlled graft copolymers consisting of various grafts derived from methacrylate, acrylate, styrene, and functionalized monomers by the judicious combination of ruthenium complexes and additives depending on the monomer.

To confirm the graft copolymerization of these monomers, the obtained graft copolymers were analyzed by ^{1}H NMR spectroscopy. Figure 7 shows the ^{1}H NMR spectra of the original multifunctional macroinitiator **B** (A), a graft polymer with the MMA-grafts

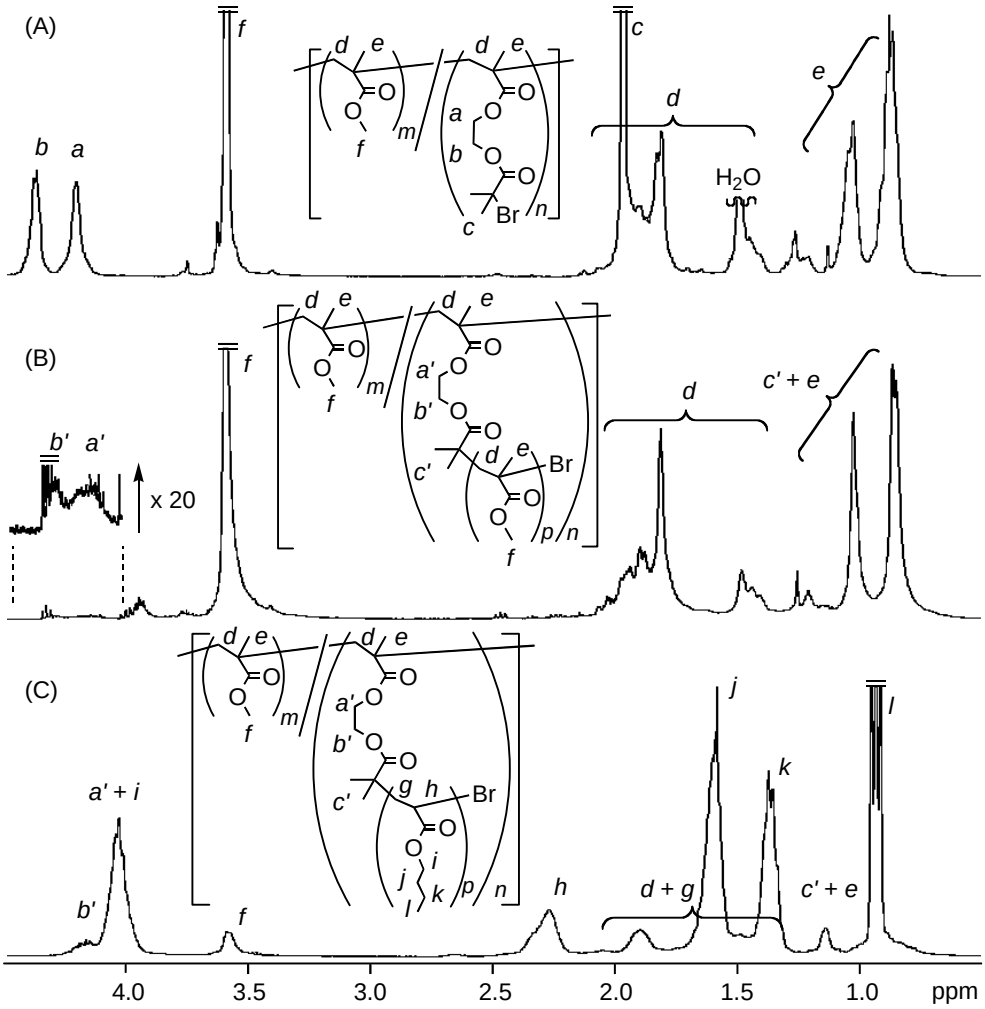

Figure 7. ^{1}H NMR spectra (in $CDCl_3$ at 50 ˚C) of (A) original multifunctional macroinitiator **B**, (B) graft copolymer of MMA, and (C) BA as the side chains.

(B) and the BA-grafts (C). After the graft polymerizations, the ^{1}H NMR spectra of the copolymers exhibited typical absorptions of these monomers in addition to the original base polymers (Figures 7B and 7C vs. 7A). The signals of the methyl (*c*) and methylene (*a* and *b*) peaks of the original bromoester groups shifted toward a higher magnetic field, which indicates the initiation of the graft copolymerization from these groups. In Figure 7C, the additional peaks were assignable to the *n*-butyl ester protons (*g*–*l*), and the unit ratio of MMA on the backbone chain and BA on the graft chains (10/90) agreed well with the calculated ratio from the gas chromatographic conversions (10/90). These results support the fact that the obtained graft copolymers contain these monomer units at the expected levels in the graft chains.

Analysis of Graft Chains by Detachment from the Backbone

In the graft copolymers thus far prepared, the graft chains should be connected to the main chain via the ester linkages that can be hydrolyzed into the main and arm chains. To confirm the molecular weights and MWDs of these graft chains, hydrolysis of the ester linkages in the graft copolymer of PMMA-*g*-PSt was carried out using potassium hydroxide in a mixture of methanol and tetrahydrofuran (1/3 v/v) at 80 ˚C (Scheme 2).[47]

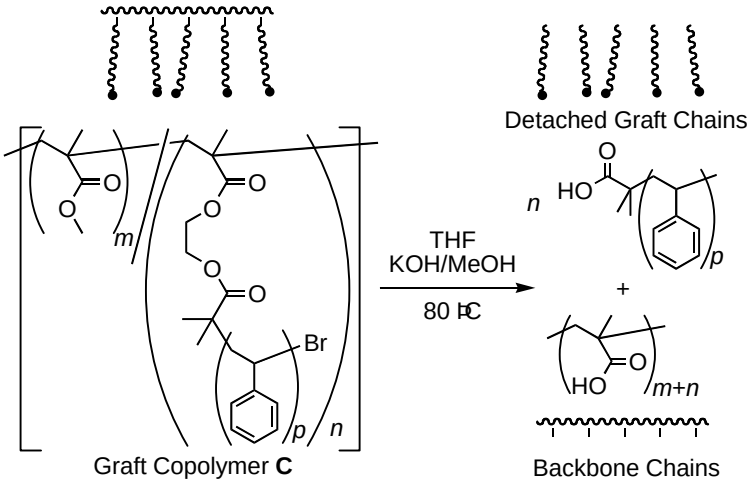

Scheme 2. Detachment of PSt graft chains from the PMMA backbone chains.

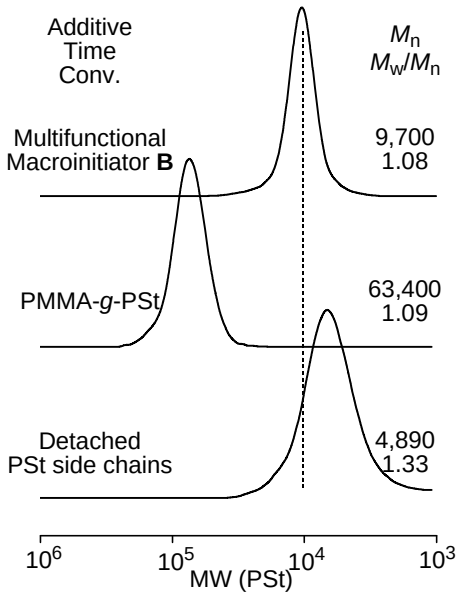

Figure 8. SEC curves of original multifunctional macroinitiator **B** (top), graft copolymer of St on the macroinitiator **B** in toluene at 80 ˚C after fractionation; $[St]_0$ = 2.0 M; [C–Br bonds in the macroinitiator **B**]$_0$ = 10 mM; $[Ru(Ind)Cl(PPh_3)_2]_0$ = 0.5 mM; $[Al(O\textit{t}\text{-}Bu)_3]_0$ = 20 mM (middle), and hydrolyzed PSt graft chains (bottom).

Figure 8 shows the SEC curves of the polymers obtained before and after the hydrolysis along with the macroinitiator **B**. After the hydrolysis, the SEC curves shifted toward lower molecular weights (M_n = 4,890) with relatively narrow MWDs (M_w/M_n = 1.33), indicating that the grafted PSt chains were detached from the backbone PMMA chains and that the PSt grafts had the controlled molecular weights.[47] The higher polydispersity index of the detached polymers than that of the graft polymers is due to that the molecular weight is lower for the former and that the differences in the molecular weights are statistically diminished in the graft polymers that are schematically obtained by connecting the graft chains together on the backbone polymers. The initiation efficiency (*f*) in the graft copolymerization was calculated from the ratio of the M_n(SEC) of the detached chain to the calculated value assuming that each initiating site forms one graft chain. The high initiation efficiency, f = 85%, supports the rapid initiation in comparison to the propagation in the graft polymerization.

Figure 9 shows the ^{1}H NMR spectra of the polymers obtained after the hydrolysis. After the hydrolysis, the polymers exhibited the typical signals of PSt; i.e., main-chain aliphatic protons (*b* and *c*) and aromatic protons (*d*). In addition to these large absorptions, small signals due to the end groups appeared at 1.0 ppm, which were assignable to the α-methyl groups at the terminal derived from the brominated esters of the initiating site. The molecular weight calculated by the ratio of the aromatic protons (*d*) to the methyl protons (*a*) at the end group [M_n(NMR) = 4,530] is close to that of the SEC [M_n(SEC) = 4,890]. These results also indicate that the graft copolymerization with the ruthenium-catalyzed system proceeded in a living manner from the initiating sites in the

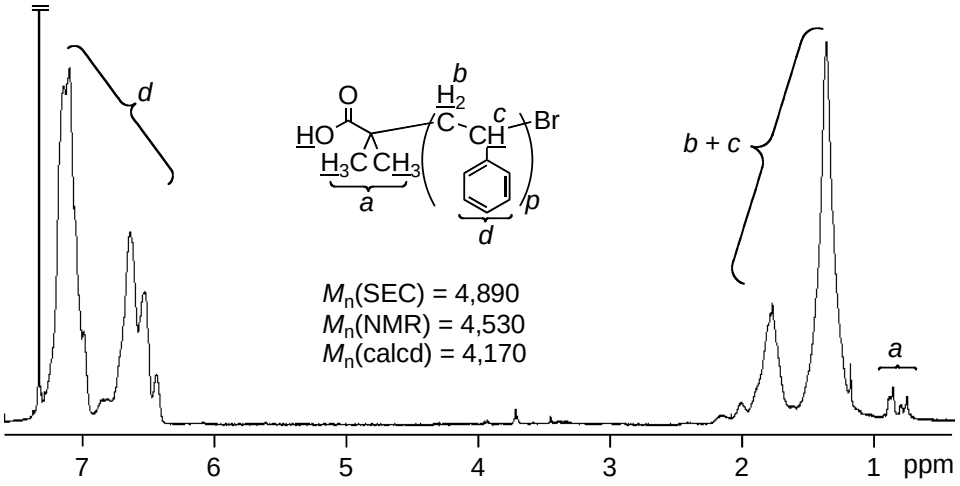

Figure 9. ^{1}H NMR spectrum (in $CDCl_3$ at 50 ˚C) of hydrolyzed PSt graft chains.

backbone chain.

CONCLUSIONS

A series of well-defined graft copolymers with controlled molecular weights in both the backbone and graft chains were prepared via the ruthenium-catalyzed living radical polymerizations. The backbone chain was synthesized by the ruthenium-catalyzed living radical copolymerization of MMA and TMSHEMA and was directly transformed into the macroinitiator with multi-initiating sites of C–Br bonds on the side groups. The macroinitiator was further employed for the ruthenium-catalyzed graft copolymerization of various monomers, such as methacrylate, acrylate, and styrene, resulting in the graft copolymers ($M_w/M_n \sim 1.1$) with controlled graft chain lengths.

REFERENCES

(1) Georges, M. K.; Veregin, R. P. N.; Kazmaier, P. M.; Hamer, G. K. *Macromolecules* **1993**, *26*, 2987–2988.

(2) Georges, M. K.; Veregin, R. P. N.; Kazmaier, P. M.; Hamer, G. K. *Trends. Polym. Sci.* **1994**, *2*, 66–72.

(3) Hawker, C. J. *J. Am. Chem. Soc.* **1994**, *116*, 11185–11186.

(4) Hawker, C. J.; Bosman, A. W.; Harth, E. *Chem. Rev.* **2001**, *101*, 3661–3688.

(5) Kato, M.; Kamigaito, M.; Sawamoto, M.; Higashimura, T. *Macromolecules* **1995**, *28*, 1721–1723.

(6) Kamigaito, M.; Ando, T.; Sawamoto, M. *Chem. Rev.* **2001**, *101*, 3689–3745.

(7) Kamigaito, M.; Ando, T.; Sawamoto, M. *Chem. Rec.* **2004**, *4*, 159–175.

(8) Wang, J.-S.; Matyjaszewski, K. *J. Am. Chem. Soc.* **1995**, *117*, 5614–5615.

(9) Matyjaszewski, K.; Xia, J. *Chem. Rev.* **2001**, *101*, 2921–2990.

(10) Chiefari, J.; Chong, Y. K.; Ercole, F.; Krstina, J. Jeffery, K.; Tam, P. T. Le.; Mayadunne, R. T. A.; Meijs, G. F.; Moad, C. L.; Moad, G.; Rizzardo, E.; Thang, S. H. *Macromolecules* **1998**, *31*, 5559–5562.

(11) For reviews, see: 11–13. Davis, K. A.; Matyjaszewski, K. *Adv. Polym. Sci.* **2002**, *159*, 1–167.

(12) Börner, H. G.; Matyjaszewski, K. *Macromol. Symp.* **2002**, *177*, 1–15.

(13) Bhattacharya, A.; Misra, B. N. *Prog. Polym. Sci.* **2004**, *29*, 767–814.

(14) Mori, H.; Müller, A. H. E. *Prog. Polym. Sci*., **2003**, *28*, 1403–1439.

(15) Cai, Y.; Hartenstein, M.; Müller, A. H. E. *Macromolecules*, **2004**, *37*, 7484–7490.

(16) Roos, S. G.; A. H. E. Müller, A. H. E.; Matyjaszewski, K. *Macromolecules*, **1999**, *32*, 8331–8335.

(17) Shinoda, H.; Matyjaszewski, K.; Okrasa, L.; Mierzwa, M.; Pakula, T. *Macromolecules* **2003**, *36*, 4772–4778.

(18) Neugebauer, D.; Zhang, Y.; Pakula, T.; Sheiko, S. S.; Matyjaszewski, K. *Macromolecules* **2003**, *36*, 6746–6755.

(19) Neugebauer, D.; Theis, M.; Pakula, T.; Wegner, G.; Matyjaszewski, K. *Macromolecules*, **2006**, *39*, 584–593.

(20) Haddleton, D. M.; Perrier, S.; Bon, S. A. F. *Macromolecules*, **2000**, *33*, 8246–8251.

(21) Yamada, K.; Miyazaki, M.; Ohno, K.; Fukuda, T.; Minoda, M. *Macromolecules*, **1999**, *32*, 290–293.

(22) Cheng, G.; Böker, A.; Zhang, M.; Krausch, G.; Müller, A. H. E. *Macromolecules*, **2001**, *34*, 6883–6888.

(23) Li, C.; Gunari, N.; Fischer, K.; Janshoff, A.; Schmidt, M. *Angew. Chem., Int. Ed*., **2004**, *43*,1101–1104.

(24) Beers, K. L.; Gaynor, S. G.; Matyjaszewski, K.; Sheiko, S. S.; Möller, M. *Macromolecules* **1998**, *31*, 9413–9415.

(25) Börner, H. G.; Beers, K. L.; Matyjaszewski, K.; Sheiko, S. S.; Möller, M. *Macromolecules* **2001**, *34*, 4375–4383.

(26) Börner, H. G.; Duran, D.; Matyjaszewski, K.; da Silva, M.; Sheiko, S. S. *Macromolecules* **2002**, *35*, 3387–3394.

(27) Qin, S.; Matyjaszewski, K.; Xu, H.; Sheiko, S. S. *Macromolecules* **2003**, *36*, 605–612.

(28) Lord, S. J.; Sheiko, S. S.; LaRue, I.; Lee, H.-I.; Matyjaszewski, K. *Macromolecules* **2004**, *37*, 4235–4240.

(29) Sumerlin, B. S.; Neugebauer, D.; Matyjaszewski, K. *Macromolecules* **2005**, *38*, 702–708.

(30) Lee, H.; Matyjaszewski, K.; Yu, S.; Sheiko, S. S. *Macromolecules* **2005**, *38*, 8264–8271.

(31) Chapter 1 of this thesis; *Polym. J*. **2005**, *37*, 617–624.

(32) Grubbs, R. B.; Hawker, C. J.; Dao, J.; Fréchet, J. M. J. *Angew. Chem., Int. Ed*., **1997**, *36*, 270–272.

(33) Venkatesh, R.; Yajjou, L.; Koning, C. E.; Klumperman, B. *Macromol. Chem. Phys*., **2004**,

205, 2161–2168.

(34) Khelfallah, N.; Gunari, N.; Fischer, K.; Gkogkas, G.; Hadjichristidis, N.; Schmidt, M. *Macromol. Rapid Commun.*, **2005**, *26*, 1693–1697.

(35) For reviews, see: 35–37. Pyun, J.; Matyjaszewski, K. *Chem. Mater.*, **2001**, *13*, 3436–3448.

(36) Pyun, J.; Kowalewski, T.; Matyjaszewski, K. *Macromol. Rapid Commun.*, **2003**, *24*, 1043–1059.

(37) Edmondson, S.; Osborne, V. L.; Huck, W. T. S. *Chem. Soc. Rev.*, **2004**, *33*, 14–22.

(38) Ejaz, M.; Yamamoto, S.; Ohno, K.; Tsujii, Y.; Fukuda, T. *Macromolecules*, **1998**, *31*, 5934–5936.

(39) Yamamoto, S.; Ejaz, M.; Tsujii, Y.; Matsumoto, M.; Fukuda, T. *Macromolecules*, **2000**, *33*, 5602–5607.

(40) Yamamoto, S.; Ejaz, M.; Tsujii, Y.; Fukuda, T. *Macromolecules*, **2000**, *33*, 5608–5612.

(41) Yamamoto, S.; Tsujii, Y.; Fukuda, T. *Macromolecules*, **2000**, *33*, 5995–5998.

(42) Sakata, H.; Kobayashi, M.; Otsuka, H.; Takahara, A. *Polym. J.*, **2005**, *37*, 767–775.

(43) Baek, K.-Y.; Kamigaito, M.; Sawamoto, M. *J. Polym. Sci., Part A: Polym. Chem.*, **2002**, *40*, 1937–1944.

(44) Ando, T.; Kamigaito, M.; Sawamoto, M. *Macromolecules*, **1998**, *31*, 6708–6711.

(45) Kotani, Y.; Kato, M.; Kamigaito, M.; Sawamoto, M. *Macromolecules*, **1996**, *29*, 6979–6982.

(46) Ueda, J.; Matsuyama, M.; Kamigaito, M.; Sawamoto, M. *Macromolecules*, **1998**, *31*, 557–562.

(47) Ueda, J.; Kamigaito, M.; Sawamoto, M. *Macromolecules*, **1998**, *31*, 6762–6768.

(48) Baek, K.-Y.; Kamigaito, M.; Sawamoto, M. *Macromolecules*, **2001**, *34*, 215–221.

(49) Terashima, T.; Kamigaito, M.; Baek, K.-Y.; Ando, T.; Sawamoto, M. *J. Am. Chem. Soc.*, **2003**, *125*, 5288–5289.

(50) Ando, T.; Kamigaito, M.; Sawamoto, M. *Macromolecules*, **2000**, *33*, 2819–2824.

(51) Takahashi, H.; Ando, T.; Kamigaito, M.; Sawamoto, M. *Macromolecules* **1999**, *32*, 3820–3823.

(52) Hamasaki, S.; Kamigaito, M.; Sawamoto, M. *Macromolecules*, **2002**, *35*, 2934–2940.

(53) Ando, T.; Kamigaito, M.; Sawamoto, M. *Macromolecules*, **2000**, *33*, 5825–5829.

(54) Watanabe, Y.; Ando, T.; Kamigaito, M.; Sawamoto, M. *Macromolecules*, **2001**, *34*,

4370–4374.

CHAPTER 3

A_xBA_x-TYPE BLOCK–GRAFT POLYMERS WITH SOFT MIDDLE SEGMENTS AND HARD OUTER GRAFT CHAINS OF METHACRYLATES: CONTROL OF BACKBONE AND GRAFT CHAIN LENGTHS AND GRAFTING POSITIONS

ABSTRACT

Ruthenium-catalyzed living radical polymerization was applied to the synthesis of a series of all methacrylic well-defined A_xBA_x-type block–graft copolymers consisting of soft middle segments [dodecyl methacrylate (DMA)] and hard outer graft chains [methyl methacrylate (MMA)] with controlled lengths of the backbone and graft chains and controlled graft numbers. This synthetic method was based on the $CHCl_2(COPh)$/ $Ru(Ind)Cl(PPh_3)_2$-initiated sequential living radical block copolymerization of DMA and 2-(trimethylsilyoxy)ethyl methacrylate (TMSHEMA) followed by the direct transformation of the silyloxy groups into the ester with C–Br bond by 2-bromoisobutyroyl bromide and the ruthenium-catalyzed "grafting-from" polymerization of MMA. A series of the block–graft copolymers were then characterized by NMR, size-exclusion chromatography (SEC), multiangle laser light scattering (MALLS), differential scanning calorimetry (DSC), dynamic viscoelasticity, transmission electron microscopy (TEM), and atomic force microscopy (AFM). The NMR and SEC-MALLS indicate the well-defined synthesis of the A_xBA_x block–graft copolymers with graft chains as branched structure. The DSC and viscoelasticity show the presence of two transitions suggesting a microphase separation, which was observed by TEM and proved different from that of the ABA triblock copolymer with the same composition. A visualization of single molecules by AFM was achieved for the first time to show the dumbbell-like structure.

INTRODUCTION

Designed polymers with well-defined architectures have been attracting much interest as new polymeric materials for many applications due to their excellent properties and various functions stemming from their unique structures, such as block–graft, and star copolymers.[1] The steady advances in living radical polymerizations over this past decade now allows the synthesis of new polymeric materials with well-defined and complex architectures,[2–14] most of which relies on either of three processe,; i.e, the nitroxide-mediated polymerization (NMP),[2,3] the metal-catalyzed living radical polymerization or atom transfer radical polymerization (ATRP),[4–9] and the reversible addition–fragmentation chain transfer (RAFT) polymerization.[10,11] The Kyoto group has been developing the metal-catalyzed living radical polymerization of various monomers, including methacrylates, acrylates, acrylamides, styrenes, and vinyl esters, mainly based on a ruthenium or iron complex, which activates the carbon–halogen terminals via the one-electron redox reaction to reversibly generate the radical growing species.[4,5] The ruthenium-based system was then used for the synthesis of various copolymers with precisely defined structures, such as block,[5,15] graft,[16] and star[5,17] copolymers. The author has reported graft copolymers with controlled lengths of both the main and graft chains by the ruthenium-catalyzed living radical "grafting-from" polymerization of methacrylates, acrylates, and styrene.[16]

Block and graft copolymers are generally and widely employed as compatibilizers, polymeric emulsifiers, surface modifiers, thermoplastic elastomers (TPEs), etc. Especially, the ABA-type block copolymers consisting of soft inner and hard outer chains prepared by living anionic polymerizations of dienes and styrenes and their derivatives are employed and commercialized as excellent TPEs.[18] The recently developed metal-catalyzed living radical polymerizations have enabled the straightforward synthesis of fully (meth)acrylic ABA triblock copolymers consisting of a central rubbery poly(alkyl (meth)acrylate) and outer glassy poly(alkyl methacrylate),[4,15,19,20] which can be a highly weatherable material as an alternative for the traditional styrene–diene-based TPEs. Graft copolymers are also industrially important materials, such as acrylonitrile–butadiene–styrene copolymer (ABS) and high-impact polystyrene (HIPS), which are prepared by chain-transfer reactions during conventional radical polymerizations,

while well-defined graft copolymers with controlled main-chain and/or graft-chain lengths have been mostly prepared by living ionic polymerizations.[1] However, recent progresses in living radical polymerizations have also permitted not only the preparation of well-defined graft copolymers but also the modification of surfaces of base materials including films and particles.[21–28] They provide an additional functionality to the base materials by grafting functional monomers such as hydrophilic,[24] hydrophobic,[24,25] and temperature-responsive properties.[26–28]

More complex and well-defined copolymers consisting of both block and graft structures, which are called block–graft, comb graft, or star block copolymers, have been attracting attention in terms of their specific architectural effects on the mechanical properties, microphase-separated morphologies, and micellization behavior.[1] Such well-structured copolymers with controlled main chain, graft chain, and block lengths have been synthesized mainly by living ionic polymerizations, except for several recent examples.[29–42] Among them, the A_xBA_x-type block–graft copolymer, coined as dumbbell[31] or pom–pom[32] copolymers in some references, would become another type of TPE with different properties from those of the ABA triblock copolymers, when a rubbery middle segment (B) and glassy outer grafting segments (A) are employed. Although there are several reports on the synthesis of such A_xBA_x-type block–graft polymers with soft middle and hard outer graft chains, the synthesis relied on living anionic or cationic polymerization that requires cumbersome procedures including highly purifications of the reagents and fractionations of the resultant polymers in addition to the limitations of the monomers.[33,36–39] A few of them used a combination of ionic polymerizations with the Cu-based ATRP grafting from the anionically[37,38] or cationically[39] prepared ABA block copolymers with an uncontrolled number of grafting points generated via chloromethylation or bromination of the polystyrene or the poly(*p*-methylstyrene) segments, respectively. Quite recently, Ohno and Matyjaszewski reported the synthesis of an A_xAA_x-type block–graft poly(*n*-butyl acrylate) [poly(BA)], consisting of BA in the middle and outer graft chains, via Cu-catalyzed block copolymerization of BA and the poly(BA)-macromonomer.[42]

This chapter was thus directed to (1) the first synthesis of a series of all methacrylic A_xBA_x-type block–graft copolymers with soft middle- and hard outer graft-chains via the ruthenium-catalyzed living radical polymerization, (2) the characterization of the

copolymers by NMR, size exclusion chromatography (SEC), multiangle laser light scattering (MALLS), differential scanning calorimetry (DSC), dynamic viscoelasticity, and transmission electron microscopy (TEM), and (3) the direct observation of the single A_xBA_x block–graft copolymer molecule by atomic force microscopy (AFM). For this, a multifunctional macroinitiator (I_xBI_x) was first prepared in one pot by the ruthenium-catalyzed living radical block copolymerization of dodecyl methacrylate (DMA) [soft middle segment (B)] and 2-(trimethylsilyloxy)ethyl methacrylate (TMSHEMA) initiated by a bifunctional initiator, followed by direct transformation of the silyloxyl group into the ester with a C–Br bond upon the reaction with 2-bromoisobutyroyl bromide (I in

Scheme 1). The multifunctional initiator (I_xBI_x), isolated only by precipitation, was then employed for the ruthenium-catalyzed "grafting-from" living radical polymerization of methyl methacrylate (MMA) as hard graft chains (A) to afford the A_xBA_x block–graft copolymers with the controlled length of both the backbone and the graft chains. This "grafting-from" method following the sequential living radical polymerization, and one-pot direct transformation can relatively easily enable the synthesis of a series of A_xBA_x block–graft copolymers with various backbone and graft lengths and graft numbers (*n*, *l*, and *m* in Scheme 1 respectively) to permit the comprehensive studies of the A_xBA_x block–graft copolymers. The author also focused on the effects of graft structures on the

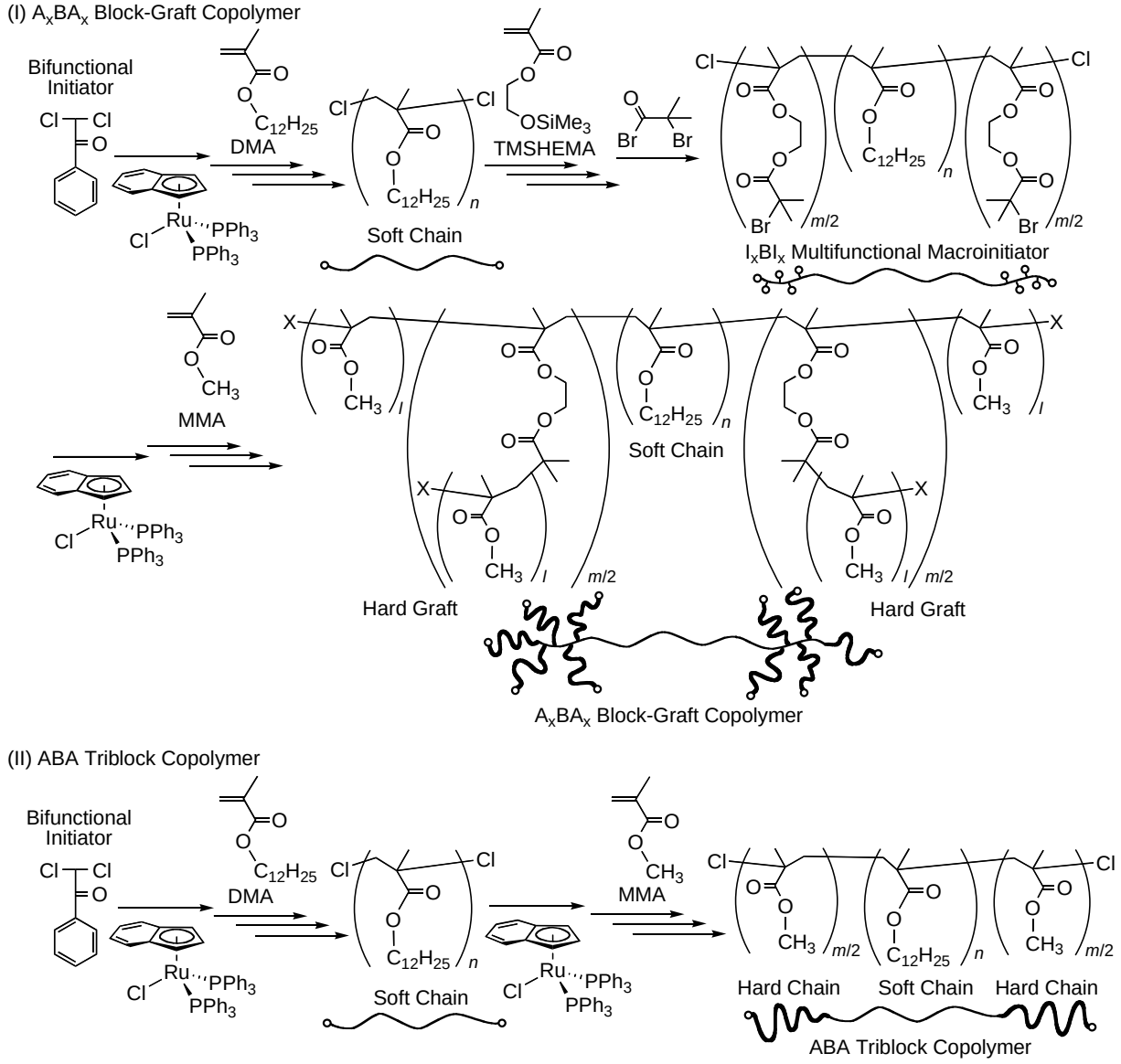

Scheme 1. Synthesis of Well-Defined (I) A_xBA_x Block–Graft Copolymers and (II) ABA Triblock Copolymers via Ruthenium-Catalyzed Living Radical Polymerization.

microphase separation by preparing the ABA triblock copolymers of MMA and DMA (II in Scheme 1) and comparing these results. Another special note is that the dumbbell-like single molecular structure of the A_xBA_x block–graft copolymer was observed for the first time by AFM.

RESULTS AND DISCUSSION

1. Synthesis of Multifunctional Macroinitiator: Ruthenium-Catalyzed Sequential Living Radical Block Copolymerization of DMA and TMSHEMA and One-Pot Transformation to Macroinitiator.

The multifunctional macroinitiator (I_xBI_x) with soft middle poly(DMA) segments and outer multiple initiating sites was first prepared by the ruthenium-catalyzed living radical polymerization of DMA and TMSHEMA, followed by the one-pot transformation of the trimethylsilyloxy groups into the ester with a C–Br bond via direct reaction with 2-bromoisobutyroyl bromide. Herein, TMSHEMA was employed as the precursor of the ester because the Ru(Ind)Cl(PPh_3)$_2$-catalyzed living radical polymerization gave narrower molecular weight distributions (MWDs) (M_w/M_n ~ 1.2) for the homopolymerization of TMSHEMA than for 2-hydroxyethyl methacrylate (HEMA).[16,43] The use of TMSHEMA would also solve the problems in the heterogeneity of the reaction mixture during the block copolymerizations with alkyl methacrylates and HEMA. Furthermore, quantitative one-pot esterification of the TMS group with the ester bromide was possible as reported by us.[16]

For this, DMA was first polymerized with $Ru(Ind)Cl(PPh_3)_2$, which is one of most effective catalysts for the living radical polymerization of methacrylates,[44] in conjunction with 2,2-dichloroacetophenone [$CHCl_2(COPh)$] as the bifunctional initiator in the presence of *n*-Bu_3N in toluene at 80 ˚C.[4] The ruthenium-based system was also quite effective for the methacrylate with a long alkyl chain to induce a relatively fast polymerization and to produce polymers with MWDs (M_w/M_n ~ 1.2), as shown in the size-exclusion chromatograms (SEC) of the produced polymers (Figure 1). After the nearly complete consumption of DMA, a feed of TMSHEMA, 10 mol % of the first DMA feed, was added to the living poly(DMA). The polymerization smoothly proceeded even after the addition of the second monomer. Figure 1 also shows the number-average molecular weights (M_n) and SEC curves of the obtained copolymer of DMA and TMSHEMA. The SEC curve shifted toward higher molecular weights retaining fairly narrow MWDs to result in the block copolymers (M_n = 93,000, M_w/M_n = 1.18) with pendent silyloxy groups on both chain ends. Although the prepared prepolymers were not completely block of DMA and TMSHEMA due to the addition of the second monomer before the complete consumption

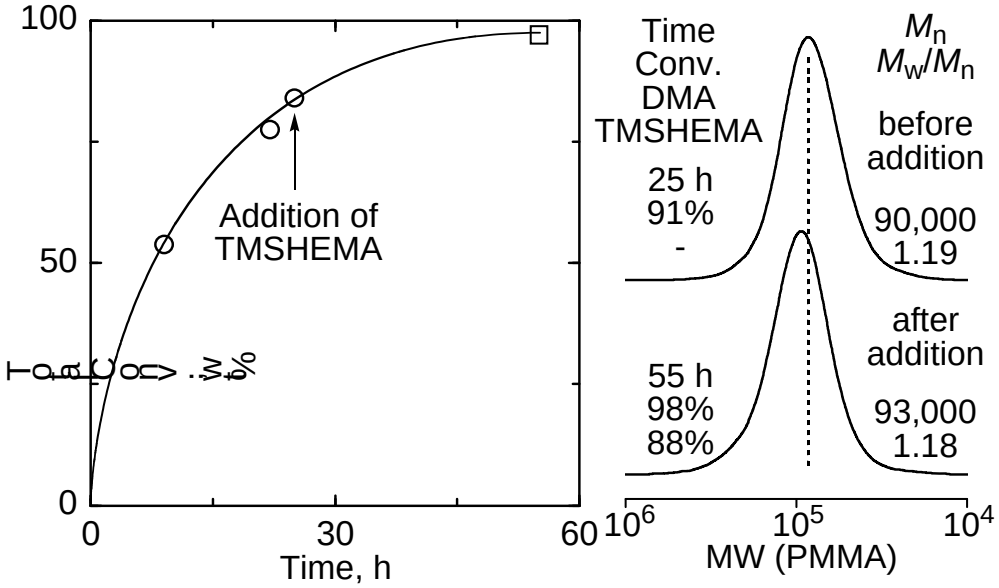

Figure 1. Ruthenium-catalyzed sequential living radical block copolymerization of dodecyl methacrylate (DMA) and 2-(trimethylsilyoxy)ethyl methacrylate (TMSHEMA) with $Ru(Ind)Cl(PPh_3)_2$/*n*-Bu_3N in toluene at 80 ˚C: before addition, $[DMA]_0$ = 2.5 M; $[CHCl_2(COPh)]_0$ = 5.0 mM; $[Ru(Ind)Cl(PPh_3)_2]_0$ = 0.5 mM; $[n\text{-}Bu_3N]_0$ = 10 mM (●); after addition, $[TMSHEMA]_{add}$ = 250 mM in toluene solution (□).

of the first monomer, this method relatively easily enabled the introduction of the grafting points in the both outer blocks without purification of the first polymer.

The ^{1}H NMR spectrum (Figure 2A) of the produced polymers showed the characteristic signals derived from DMA and TMSHEMA, i.e., the ester methylene protons (*g*) with the other alkyl protons (*h–j*) of the DMA units and the ester and silyloxy–ether methylene protons (*a* and *b*) with the trimethylsilyl groups (c) of the TMSHEMA units in addition to the α-methyl (*f*) and main-chain methylene protons (*e*) of both units. The unit ratio of DMA to TMSHEMA calculated from the peak intensity ratio (*a* + *g* vs *b*) was 490/44.1, which was in good agreement with the calculated value of 490/44.4 obtained from the feed ratio and the monomer conversions by gas chromatography. A more detailed analysis of the polymers revealed very small peaks of the aromatic protons derived from the bifunctional initiator [$CHCl_2(COPh)$]. The integration of the small peaks and their ratios to each monomer unit peak gave the number-average degree of polymerization

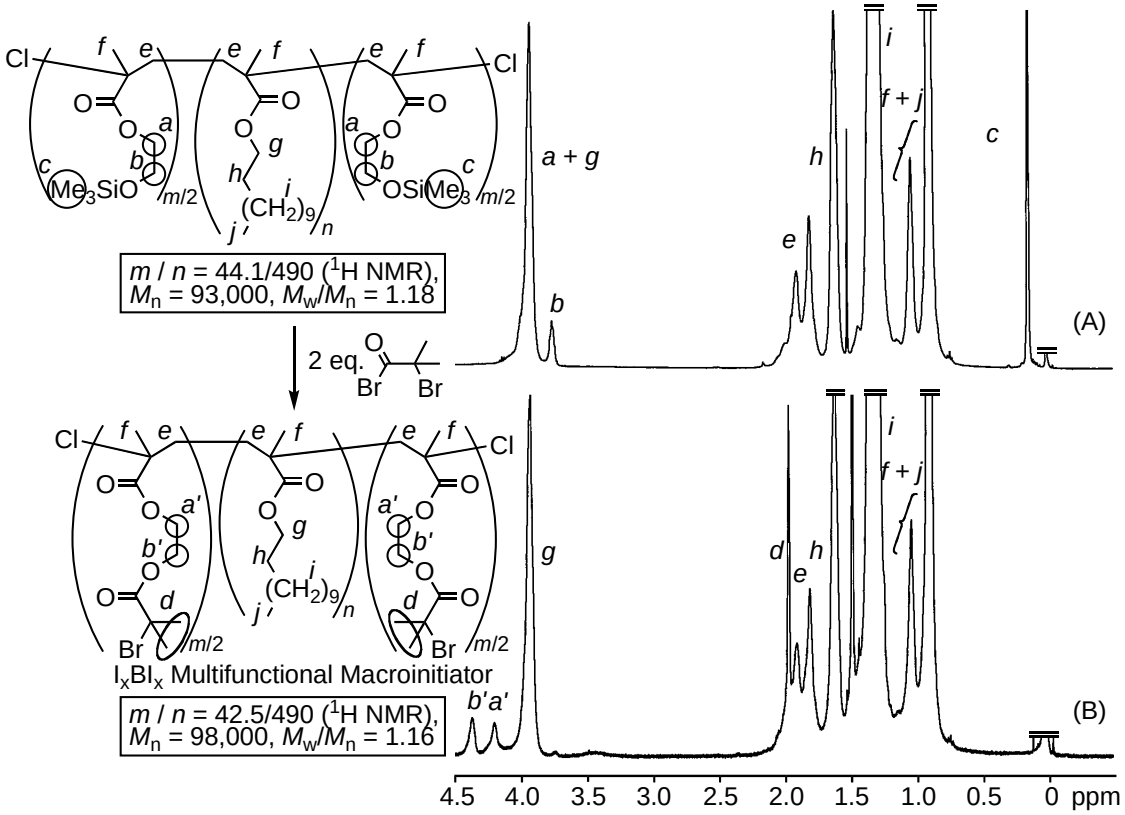

Figure 2. ^{1}H NMR spectra ($CDCl_3$, 50 °C) of the triblock copolymer of dodecyl methacrylate (DMA) and 2-(trimethylsilyoxy)ethyl methacrylate (TMSHEMA) (A; M_n = 93,000, M_w/M_n = 1.18) and the I_xBI_x multifunctional macroinitiator obtained after the direct transformation with 2-bromoisobutyryl bromide (B; M_n = 98,000, M_w/M_n = 1.16).

of the monomer units; DP_n(DMA) = 477 and DP_n(TMSHEMA) = 46.6, which were close to the calculated values, although they may contain some experimental error originating from the very small peaks of the initiator moiety in such a high molecular weight polymer.

These results indicate that the ruthenium-based bifunctional initiating system induced the sequential living radical block copolymerization of DMA and TMSHEMA to give the triblock copolymers with controlled lengths of the soft-middle chains and the outer functional groups.

The trimethylsilyloxy-groups in the triblock copolymers were then converted into the ester with a C–Br bond for the multiple "grafting-from" points via the direct reaction between the silyloxy group and the acid bromide. The author has demonstrated that the direct transformation of the trimethylsilyl group into the ester was achievable for the random copolymers of MMA and TMSHEMA.[16] Thus, 2-bromoisobutyroyl bromide [$Me_2C(Br)COBr$] was directly added to the polymerization solution of the triblock copolymers without isolation for the one-pot transformation. The transformation was carried out with an excess amount of 2-bromoisobutyroyl bromide (2.0 mol equiv to the trimethylsilyl groups) at room temperature for 24 h.

The ^{1}H NMR spectrum of the copolymers obtained after the reaction with $Me_2C(Br)COBr$ exhibited typical changes (Figure 2B), in which the signal of the trimethylsilyl groups completely disappeared (*c* in Figure 2A) and peaks *a* and *b* shifted toward a lower magnetic field and changed into peaks *a'* and *b'*, respectively, along with an appearance of an additional peak attributed to the methyl groups (*d*) adjacent to the C–Br bonds. The unit ratio of DMA and the ester units (490/42.5), calculated from the peak intensity ratio (*g* vs *a'* + *b'*), agreed well with the ratio of DMA/TMSHEMA in the triblock prepolymer (490/44.1). The transformation efficiency based on these peak area ratios was 0.96, which also indicated the quantitative esterfication. The SEC curve of the polymers also showed unimodal and narrow MWDs (M_n = 98,000, M_w/M_n = 1.16).

These results indicate that the I_xBI_x macroinitiator was obtained by a simple one-pot reaction, i.e., the sequential living radical copolymerization of DMA and TMSHEMA followed by the in-situ transformation of the trimethylsilyl groups into the ester with the C–Br bond.

2. Synthesis of A_xBA_x Block–Graft Copolymers: Ruthenium-Catalyzed

Grafting-From Polymerization of MMA.

For the synthesis of the A_xBA_x block–graft copolymers with different graft numbers, macroinitiators with different numbers of initiating sites (f = 47.5 and 10.9), but with the same lengths of the middle soft segments (**1** and **2**, respectively), were prepared and then employed as the multifunctional macroinitiators (Figure 3). Herein, the number of the initiating sites (f) is the sum of the number of the ester units with a C–Br bond (m in

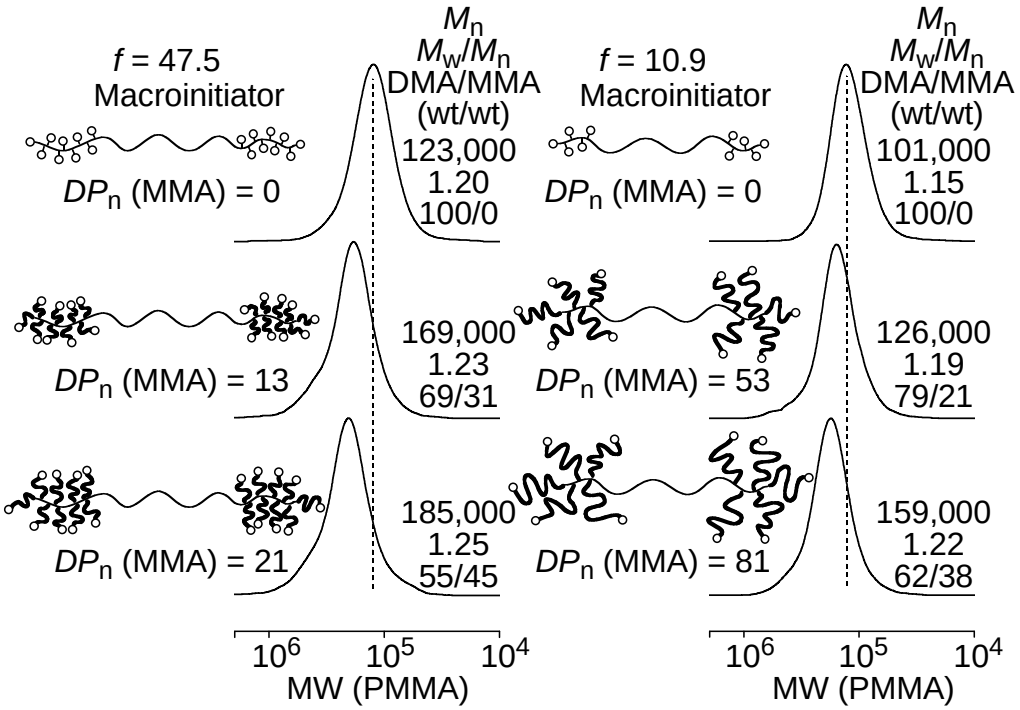

Figure 3. Graft copolymerization of methyl methacrylate (MMA) from the I_xBI_x multifunctional macroinitiator with $Ru(Ind)Cl(PPh_3)_2$/aluminum acetylacetonate [$Al(acac)_3$] in toluene at 80 ˚C. $[MMA]_0$ = 0.7 (left) or 3.0 (right) M; [C–X bonds in the macroinitiator]$_0$ = 9.0 (left) or 9.6 (right) mM; $[Ru(Ind)Cl(PPh_3)_2]_0$ = 1.0 mM; $[Al(acac)_3]_0$ = 40 mM.

Scheme 1) and both terminal units with C–Cl bonds, i.e., m + 2.

The grafting polymerization of MMA from the macroinitiators was carried out with $Ru(Ind)Cl(PPh_3)_2$ in toluene at 80 ˚C in conjunction with aluminum acetylacetonate [$Al(acac)_3$] as an effective additive for enhancing the rate and the controllability of the ruthenium-catalyzed living radical "grafting-from" polymerization.[16] The graft polymerizations smoothly proceeded to lead to the shift of the SEC curves to higher molecular weights maintaining unimodal and narrow MWDs (M_w/M_n ~ 1.2) for both

macroinitiators. The DMA/MMA ratios calculated from the ^{1}H NMR spectra agreed well with the calculated values from the feed ratios and the monomer conversions.

Figure 4 is a plot of the MMA contents (wt %) obtained by the ^{1}H NMR spectra of the block–graft copolymers with almost the same lengths of DMA segments ($m \sim 500$) as a function of the number of initiating sites (f or $m + 2$) and the number-average degree of polymerization of the graft PMMA chains [l or DP_n(MMA)]. The MMA contents increased with the increasing f and l values and were controlled between 13% and 46% by the number (m) and the length (l) of the graft chains. This means that a series of A_xBA_x block–graft copolymers with varying MMA contents can be obtained by changing the two functions. The ruthenium-catalyzed living radical polymerization thus proved to be simple and more effective for the synthesis of a series of the A_xBA_x block–graft copolymers

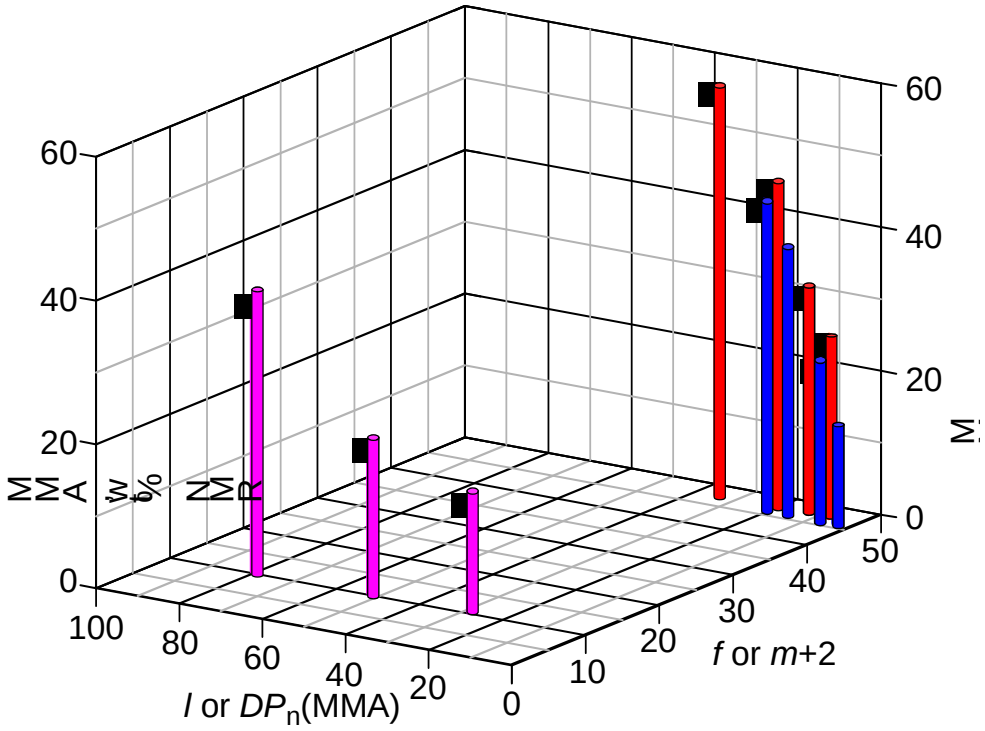

Figure 4. 3D plots of MMA contents (wt %), PMMA graft chain length [l or DP_n(MMA)], and number of initiating sites (f or $m + 2$) in the block–graft copolymers ($n \sim 500$) in the same experiment as for Figure 3.

than the reported methods that relied on the living ionic polymerizations.[33,36–39]

The absolute molecular weights of the A_xBA_x block–graft polymers were then measured by SEC equipped with multiangle laser light scattering (MALLS) and refractive index as a dual detector. Table 1 summarizes these data for a series of the A_xBA_x

block–graft polymers with different graft numbers and graft chain lengths along with those for the ABA triblock copolymers with middle DMA and outer MMA segments.

Table 1. A_xBA_x Block–Graft and ABA Triblock Copolymers Obtained via Ruthenium-Catalyzed Living Radical Polymerization[a]

code	n[b]	f[b] (m+2)	l[b]	M_n		M_w/M_n[d]	M_w		R_z, nm[e]	dn/dc[f]	DMA/MMA, wt/wt		T_g, °C[h]
				calcd[c]	SEC[d]		SEC[d]	MALLS[e]			calcd[g]	obsd[b]	
1	490	46.1	0	137 000	98 000	1.16	114 000	152 000	24.1	0.0827	-	-	n.d.
2	490	46.1	4.1	156 000	116 000	1.21	140 000	168 000	24.4	0.0989	87/13	87/13	–50.5, 54.4
3	490	46.1	8.1	174 000	126 000	1.23	155 000	190 000	24.5	0.1032	77/23	78/22	–51.8, 71.3
4	490	46.1	16	211 000	147 000	1.24	182 000	243 000	26.1	0.1123	63/37	63/37	–51.1, 86.0
5	490	46.1	21	232 000	151 000	1.23	186 000	301 000	26.8	0.1265	57/43	54/46	–52.2, 92.9
6	491	10.9	0	128 000	97 000	1.17	113 000	154 000	22.9	0.0715	-	-	n.d.
7	491	10.9	29	158 000	116 000	1.20	139 000	177 000	24.2	0.0798	80/20	84/16	–50.5, 74.4
8	491	10.9	53	184 000	126 000	1.19	150 000	225 000	28.8	0.0906	69/31	79/21	–48.5, 82.8
9	491	10.9	81	213 000	159 000	1.22	194 000	262 000	32.6	0.1201	59/41	62/38	–52.7, 97.3
10	568	2	0	145 000	116 000	1.21	140 000	178 000	25.7	0.0795	-	-	n.d.
11	568	2	182	181 000	155 000	1.21	188 000	226 000	33.2	0.0906	80/20	82/18	–52.5, 101.2
12	568	2	298	205 000	180 000	1.21	218 000	247 000	37.0	0.1011	71/29	72/28	–48.4, 116.3
13	568	2	438	230 000	199 000	1.22	243 000	273 000	46.5	0.1053	63/37	65/35	–51.2, 116.4

[a]Polymerization conditions: $[MMA]_0/[C–X$ bonds in the macroinitiator$]_0/[Ru(Ind)Cl(PPh_3)_2]_0/[$aluminum acetylacetonate$]_0$ = 700/9.0/1.0/40 mM (codes 2–5), 3000/9.6/1.0/40 mM (codes 7–9), or 4000/2.0/1.0/40 mM (codes 11–13), in toluene at 80 °C. [b]Determined by ^{1}H NMR. [c]M_n(calcd) = M_n(macroinitiator, calcd) + $([M]_0/[C–Br]_0) \times$ conv $\times f \times$ MW(MMA). [d]The number-average molecular weight (M_n), the weight-average molecular weight (M_w), and polydispersity index (M_w/M_n) were determined on size-exclusion chromatography (SEC) by refractive index (RI) detector (PMMA standard). [e]Measured on SEC by multiangle laser light scattering (MALLS) detector (λ = 633 nm). [f]Measured by refractometer (λ = 633 nm). [g]Calculated from feed ratio and monomer conversion. [h]Determined by differential scanning calorimetry (DSC).

As shown in Table 1, the M_w(MALLS) was consistently higher than M_w(SEC) based on the standard PMMA calibration while M_n(SEC) was consistently lower than M_n(calcd). In addition, the differences between M_w(MALLS) and M_w(SEC) or between M_n(SEC) and M_n(calcd) became larger with the increasing number of graft chains (f). This is due to the branched structures of the block–graft copolymers. Furthermore, the M_n that can be calculated from M_w(MALLS) and M_w/M_n agreed well with M_n(calcd), which indicates the well-defined synthesis of the A_xBA_x block–graft polymers without significant coupling and chain-transfer reactions during the living radical polymerizations.

Figure 5 shows double-logarithmic plots of the radius of gyration (R_g) and the molecular weight obtained by MALLS for ABA triblock and A_xBA_x block–graft copolymers with almost the same molecular weights (codes 4 and 13 in Table 1). As studied earlier for linear polymers and branched or graft polymers,[23,45] the slope of the linear plot permits linear and branched polymers to be distinguished. The typical values

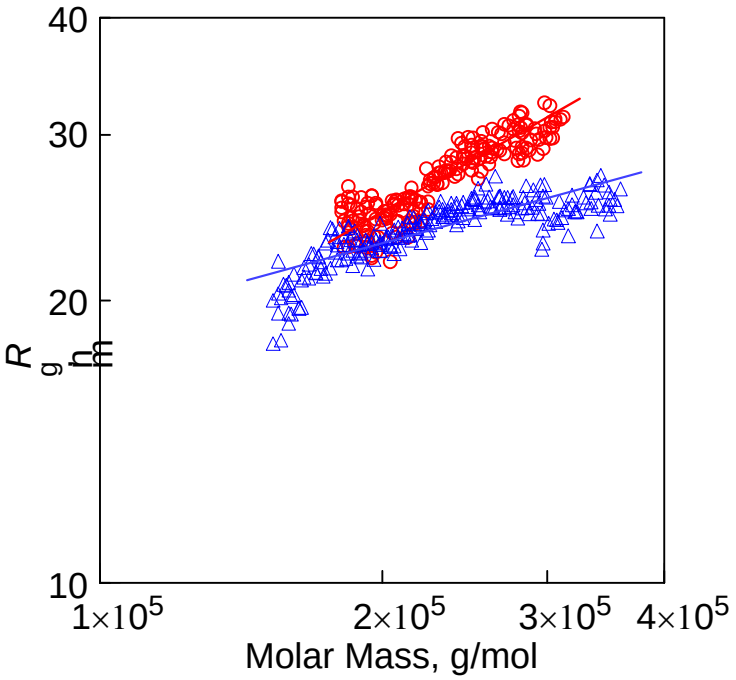

Figure 5. Double logarithmic plots of the radius of gyration (R_g) and the molar mass obtained by MALLS for the ABA triblock copolymer [□; M_n(SEC) = 199,000, M_w(MALLS) = 273,000, M_w/M_n(SEC) = 1.22, A/B = 35/65] and the A_xBA_x block–graft copolymer [△; M_n(SEC) = 147,000, M_w(MALLS) = 243,000, M_w/M_n(SEC) = 1.24, A/B = 37/63, f = 46.1]. The solid lines indicate the fitted lines.

for linear random coils are between 0.5 and 0.6, whereas lower values indicate branching. The slope for the ABA triblock copolymers (code 13) was determined to be 0.53 while that for the A_xBA_x block–graft copolymers (code 4) was 0.23. A less branched A_xBA_x copolymer (code 9) gave a slightly higher value of 0.29. These results also indicate the formation of the branched copolymers.

3. Characterization of A_xBA_x Block–Graft Copolymers.

The properties of the A_xBA_x block–graft copolymers were then characterized by various methods, such as DSC, dynamic viscoelasticity, TEM, and AFM.

Figure 6 shows the DSC curves of various A_xBA_x block–graft copolymers (DMA/MMA = 75/25–43/57, n = 495, f = 47.5, l = 8.1–35). For all four samples, two glass transition temperatures (T_g) around –50 and 75–100 ˚C were observed, corresponding to the transition of the rubbery poly(DMA) and glassy PMMA graft segments, respectively. The homopolymers prepared by conventional radical polymerization at 60 °C showed a T_g at –59 °C for poly(DMA) and at 117 °C for PMMA.[46] The presence of two glass transition temperatures indicates that the A_xBA_x block–graft copolymers have phase-separated structures.

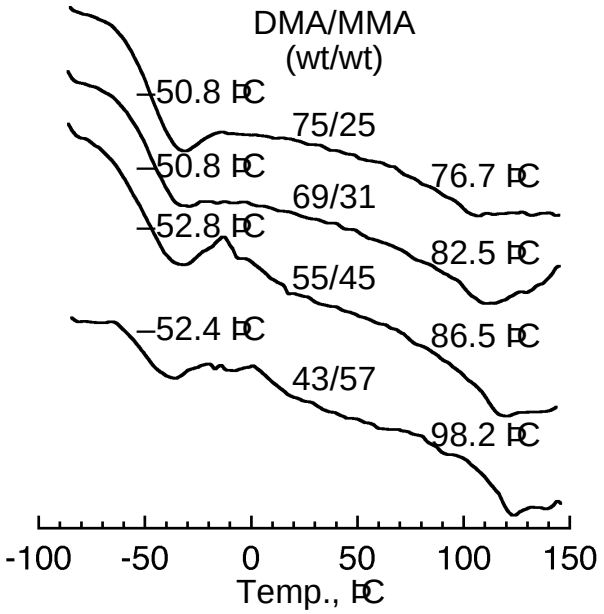

Figure 6. Differential scanning calorimetry (DSC) curves of the A_xBA_x block–graft copolymers (f = 47.5) obtained with the I_xBI_x multifunctional macroinitiator/$Ru(Ind)Cl(PPh_3)_2$/$Al(acac)_3$ in toluene at 80 ˚C.

The author also analyzed all the copolymers in Table 1 by DSC. The higher transition temperature due to the PMMA graft chains increased with the increasing degree of polymerization (l) and reached 116.4 °C, which was almost the same as the T_g reported for PMMA with a similar tacticity.[46] Figure 7 is a plot of the T_g values vs the reciprocal of the M_n of PMMA graft chains. In general, there is a linear relationship between T_g and $1/M_n$ for linear polymers according to Fox–Flory equation[47] while a more detailed analysis showed the presence of two lines which intersect at a critical molecular weight associated with the chain entanglements.[48] In our case, the T_g values for the ABA triblock and the A_xBA_x block–graft copolymers with a lower number ($f \sim 10$) of graft chains are close to those of the linear PMMA with similar molecular weights.[48] However, the T_gs for a higher number of graft chains ($f \sim 45$) were higher than those of the linear PMMA, probably due to the cumulative effects of the graft chains connected together on the main

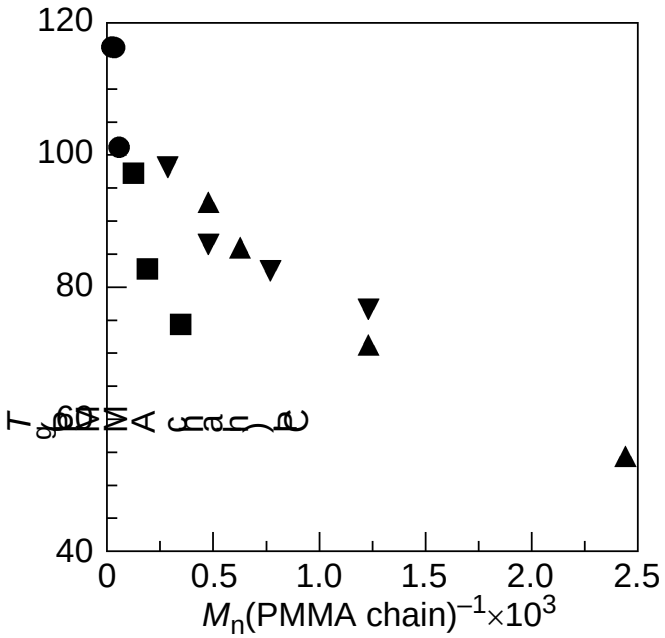

Figure 7. Plots of T_g vs M_n(PMMA chain)$^{-1}$: PMMA chain of the ABA triblock copolymer (●) and A_xBA_x block–graft copolymers: f = 10.9 (■), 46.1 (▲), and 47.5 (▼).

chain.

The dynamic mechanical property of the copolymers was evaluated by the dynamic viscoelasticity. Figure 8 shows the dynamic tensile storage modulus (E') and tan δ (= E''/E') as a function of temperature for the A_xBA_x block–graft copolymer (DMA/MMA = 68/32, n = 487, f = 10.6, l = 65) and the ABA triblock copolymer (DMA/MMA = 65/35, n =

568, l = 438). The two loss peaks in the modulus are associated with the T_g of the rubbery poly(DMA) and that of the glassy PMMA grafting chains. The modulus of the rubbery plateau of the A_xBA_x block–graft copolymer was slightly lower than that of the ABA triblock copolymer, probably due to the differences in the morphologies related to the

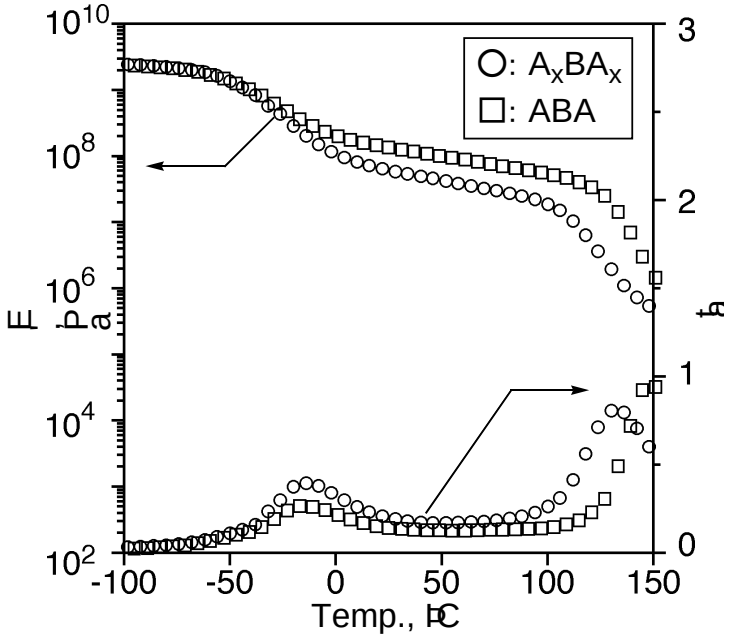

Figure 8. Dynamic tensile storage moduli (E') and tan δ as a function of temperature for the A_xBA_x block–graft copolymer (O; M_n = 141,000, M_w/M_n = 1.20, A/B = 32/68, f = 10.9) and the ABA triblock copolymer (□; M_n = 199,000, M_w/M_n = 1.22, A/B = 35/65). Heating rate: 10 ˚C/min.; frequency: 11 Hz.

molecular structure.

The bulk morphology of the A_xBA_x block–graft copolymers was thus analyzed using TEM and was compared to that of the ABA triblcok copolymer. As shown in Figure 9, the author analyzed three samples with almost the same DMA/MMA contents (~ 65/35), but with different graft numbers and graft lengths [A_xBA_x: DMA/MMA = 63/37, n = 490, f = 46.1, l = 16 (sample a); DMA/MMA = 68/32, n = 487, f = 10.6, l = 65 (sample b); ABA: DMA/MMA = 65/35, n = 568, l = 438 (sample c)]. The microphase morphology of the triblock copolymers that contain ~35 wt % PMMA was expected to be an assembly of cylinders or lamellae of PMMA into the matrix formed by the major component.[49] The ABA triblock copolymer sample showed a complex structure like the co-continuous or disordered cylinders of dark PMMA domains in a brighter cocontinuous poly(DMA) matrix

(Figure 9c). A similar complex image was also obsereved for the (meth)acrylate-based ABA triblock copolymers of MMA and BA prepared by the living anionic block copolymerization,[50] or the difficulty in the selective staining was reported.[19] These are most probably due to the similarity in the structures of these components.[19] In contrast, the morphology of the A_xBA_x block–graft copolymer sample was quite different for both samples. The sample with a lower graft number and longer graft chains showed a lamellae structure with long-range disorders (Figure 9b), while the sample with a higher graft number and shorter graft chains exhibited more complex lamellae-like structures (Figure 9a). Thus, the A_xBA_x block–graft copolymers can form microphase-separated structures, which can be distinguished from that of the ABA triblock copolymers and largely depend on the graft numbers and lengths.

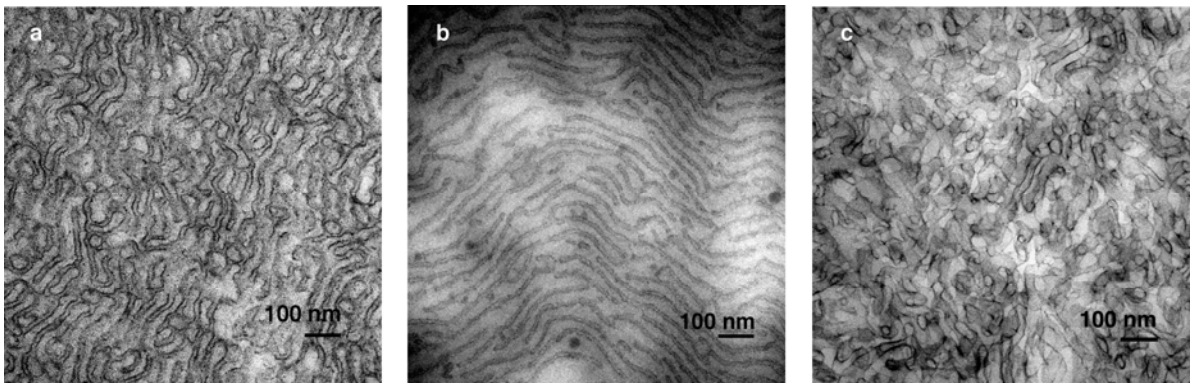

Figure 9. Transmission electron microscope (TEM) images of the A_xBA_x block–graft copolymers [a: M_n(SEC) = 147,000, M_w/M_n = 1.24, A/B = 37/63, f = 46.1; b: M_n(SEC) = 141,000, M_w/M_n = 1.20, A/B = 32/68, f = 10.9] and the ABA triblock copolymer [c: M_n(SEC) = 199,000, M_w/M_n = 1.22, A/B = 35/65]. Stained by aqueous PTA [12-tungsto(VI)phosphoric acid, *n*-hydrate].

For further evaluation of the A_xBA_x block–graft structure, visualization of single molecules was done by AFM for a high molecular weight polymer (n = 495, f = 47.5, l = 247, M_n(SEC) = 791,000, M_w/M_n = 1.27). Figure 10 shows the AFM micrograph of the A_xBA_x block–graft copolymer cast from a 1.0 μg/mL $CHCl_3$ solution on a mica plate. Several images apparently consisting of two spherical objects were observed with more than 0.3 μm distances, which suggests that each image corresponds to a single molecule. An enlarged micrograph in the inset picture shows two round-shaped images with ~90 nm diameters and ~1 nm heights, which were located at an ~50 nm distance. This suggested

to us the dumbbell-like structure of the A_xBA_x block–graft copolymer as expected. This is the first visualization of single molecules of A_xBA_x block–graft copolymers while other graft copolymers with highly dense brushes prepared by Cu ATRP have been reported elsewhere.[22,51]

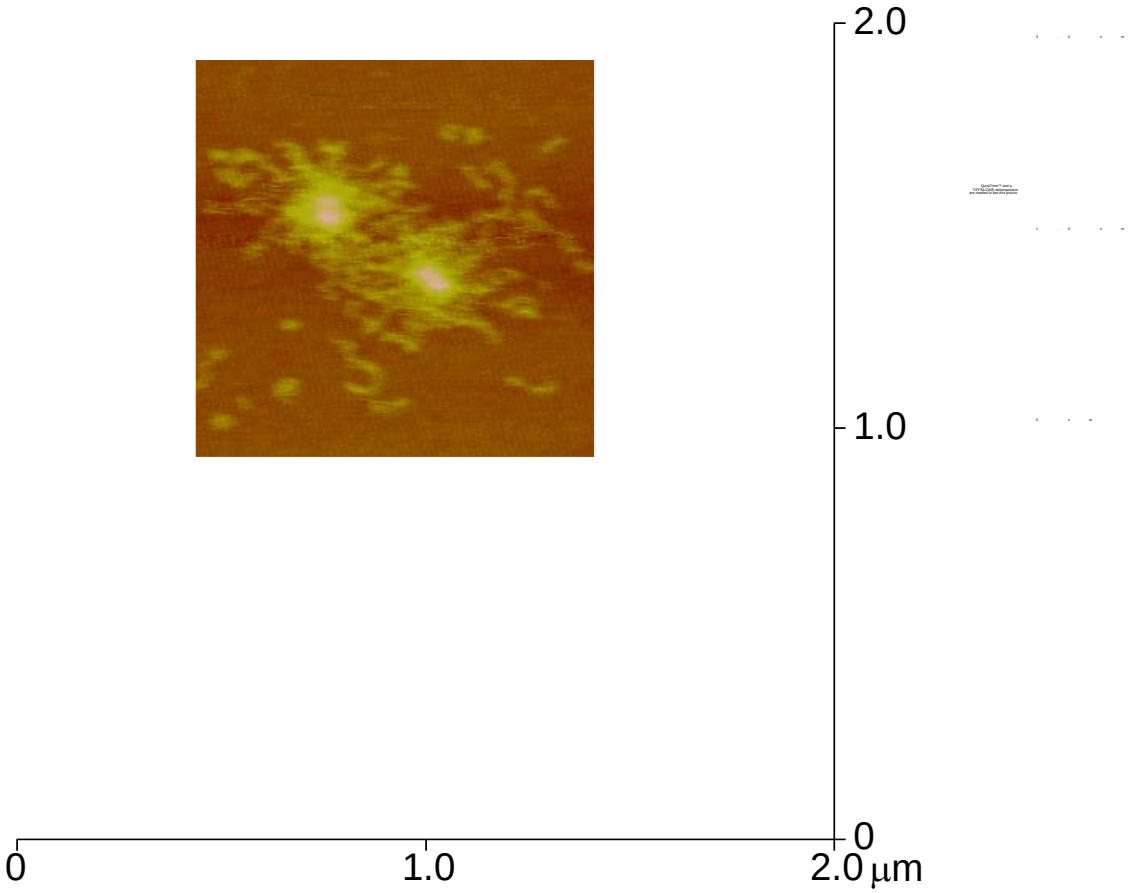

Figure 10. Atomic force microscope (AFM) image of the A_xBA_x block–graft copolymer [M_n(SEC) = 791,000, M_w/M_n = 1.27, A/B = 90/10, f = 47.5] obtained with the I_xBI_x multifunctional macroinitiator/Ru(Ind)Cl(PPh_3)$_2$/Al(acac)$_3$ in toluene at 80 ˚C. [MMA]$_0$ = 8.0 M; [C–X bonds in the macroinitiator]$_0$ = 10 mM; [Ru(Ind)Cl(PPh_3)$_2$]$_0$ = 1.0 mM; [Al(acac)$_3$]$_0$ = 40 mM.

CONCLUSIONS

A series of well-defined A_xBA_x-type block–graft copolymers consisting of soft middle and hard outer graft chains was first prepared by a simple method based on the ruthenium-catalyzed sequential living radical block copolymerization of DMA and TMSHEMA followed by the direct transformation of the silyloxy groups into the ester with

a C–Br bond and the ruthenium-catalyzed grafting-from polymerization of MMA. The DSC and dynamic viscoelastic analysis exhibited two transition points attributed to the T_gs of the poly(DMA) and PMMA segments suggesting a microphase separation, which was observed by TEM and determined to be different from that of the ABA triblcok copolymers. A visualization of single molecules by AFM was achieved for the first time to show the dumbbell-like structure as expected.

EXPERIMENTAL SECTION

Materials

MMA (Tokyo Kasei, >99%) was washed with aqueous NaOH (5%) and water, dried over magnesium sulfate, and distilled from calcium hydride under reduced pressure before use. DMA (Tokyo Kasei, >99%) and TMSHEMA (Aldrich, >96%) were distilled from calcium hydride under reduced pressure before use. $Ru(Ind)Cl(PPh_3)_2$, (provided from Wako Chemicals) and $Al(acac)_3$ (acac = acetylacetonate; Wako Chemicals, >98%) were used as received. All metal compounds were handled in a glovebox (VAC Nexus) under a moisture- and oxygen-free argon atmosphere (O_2, <1 ppm). Toluene was distilled over sodium benzophenone ketyl and bubbled with dry nitrogen over 15 min just before use. *n*-Bu_3N (as an additive), *n*-hexane, and tetralin (as an internal standards for NMR or gas chromatographic analysis of the monomers) were distilled from calcium hydride before use. 2-Bromoisobutyryl bromide (Aldrich, >98%) and 2,2-dichloroacetophenone (Aldrich, >97%) were distilled before use.

Synthesis of Multifunctional Macroinitiator: Ruthenium-Catalyzed Sequential Living Radical Block Copolymerization of DMA and TMSHEMA and One-Pot Transformation to Macroinitiator.

All polymerizations were carried out by the syringe technique under dry nitrogen in glass tubes equipped with a three-way stopcock. A typical example for the polymerization of DMA with $CHCl_2(COPh)$/$Ru(Ind)Cl(PPh_3)_2$/*n*-Bu_3N is given below. In a 50 mL round-bottomed flask was placed $Ru(Ind)Cl(PPh_3)_2$ (10 mg, 0.013 mmol), toluene (5.4 mL), tetralin (0.4 mL), DMA (18.8 mL, 64.1 mmol), $CHCl_2(COPh)$ (0.32 mL of 400

mM solution in toluene, 0.128 mmol) and *n*-Bu_3N (0.64 mL of 400 mM solution in toluene, 0.256 mmol) at room temperature. The total volume of reaction mixture was 25.6 mL. The flask was placed in an oil bath kept at 80 ˚C under vigorous stirring. After the monomer conversion reached 91%, the reaction solution was added TMSHEMA (2.0 mL of 3.23 M solution in toluene, 6.45 mmol). In predetermined intervals, the polymerization was terminated by cooling the reaction mixtures to –78 ˚C. Monomer conversion was determined by ^{1}H NMR with tetralin as an internal standard. To the quenched reaction solution was then added toluene (14 mL) and 2-bromoisobutyryl bromide (1.6 mL, 13.0 mmol, 2.0 equiv to the trimethylsilyoxyl unit) at room temperature under stirring for 24 h. The reaction mixture was precipitated into acetone and isolated by centrifugation. After three times of the precipitation, the precipitate was diluted with toluene and precipitated into methanol. The procedure was repeated three times. The precipitate was then evaporated to dryness to yield the product, which was subsequently dried overnight in vacuo at room temperature (16.6 g, 97% yield; M_n = 98,000, M_w/M_n = 1.16). The polymer was diluted with distilled toluene, and a 2.0 M solution was prepared for the following graft copolymerization.

Synthesis of A_xBA_x Block–Graft Copolymers: Ruthenium-Catalyzed Grafting-From Polymerization of MMA.

Graft copolymerizations were also carried out by the syringe technique under dry nitrogen in glass tubes equipped with a three-way stopcock. A typical example for the graft copolymerization of MMA with the multifunctional macroinitiator I_xBI_x with $Ru(Ind)Cl(PPh_3)_2/Al(acac)_3$ is given below. In a 50 mL round-bottomed flask was placed macroinitiator I_xBI_x (1.2 mL, 0.12 mmol C–Br bonds), toluene (10 mL), hexane (0.5 mL), MMA (0.96 mL, 9.00 mmol), $Ru(Ind)Cl(PPh_3)_2$ (10 mg, 0.013 mmol), and $Al(acac)_3$ (0.166 g, 0.51 mmol) at room temperature. The total volume of reaction mixture was 12.8 mL. The flask was placed in an oil bath kept at 80 ˚C under vigorous stirring. In predetermined intervals, the polymerization was terminated by cooling the reaction mixtures to –78 ˚C. Monomer conversion was determined by gas chromatography with hexane as an internal standard. The quenched reaction solution was precipitated into methanol and isolated by centrifugation. After three times of the precipitation, the precipitate was evaporated to dryness to yield the product, which was subsequently dried

overnight in vacuo at room temperature (0.35 g, 81% yield; M_n = 126,000, M_w/M_n = 1.23).

Synthesis of ABA Triblock Copolymers by Ruthenium-Catalyzed Block Copolymerization of MMA.

Block copolymerizations were carried out from the poly(DMA) bifunctional initiator. A typical example for the synthesis of poly(DMA) bifunctional macroinitiator with $CHCl_2(COPh)$/$Ru(Ind)Cl(PPh_3)_2$/*n*-Bu_3N is given below. In a 50 mL round-bottomed flask were placed $Ru(Ind)Cl(PPh_3)_2$ (12.7 mg, 0.017 mmol), toluene (7.0 mL), tetralin (0.6 mL), DMA (23.4 mL, 79.8 mmol), $CHCl_2(COPh)$ (0.1 mL of 800 mM solution in toluene, 0.080 mmol), and *n*-Bu_3N (0.8 mL of 400 mM solution in toluene, 0.320 mmol) at room temperature. The total volume of reaction mixture was 32.0 mL. The flask was placed in an oil bath kept at 80 ˚C under vigorous stirring. In predetermined intervals, the polymerization was terminated at ~50% conversion by cooling the reaction mixtures to –78 ˚C. Monomer conversion was determined by ^1H NMR with tetralin as an internal standard. The reaction mixture was precipitated into acetone and isolated by centrifugation. After three times of the precipitation, the precipitate was diluted with toluene and precipitated into methanol. The procedure was repeated three times. The precipitate was then evaporated to dryness to yield the product, which was subsequently dried overnight in vacuo at room temperature (12.5 g, 94% yield; M_n = 116,000, M_w/M_n = 1.21). The polymer was diluted with distilled toluene, and a 2.0 M solution was prepared for the following block copolymerization. A typical example for the block copolymerization of MMA on the poly(DMA) bifunctional macroinitiator with $Ru(Ind)Cl(PPh_3)_2$/$Al(acac)_3$ is given below. In a 50 mL round-bottomed flask was placed poly(DMA) bifunctional macroinitiator (7.1 mL, 0.0276 mmol C–Cl bond), *n*-hexane (0.5 mL), MMA (6.0 mL, 55.7 mmol), $Ru(Ind)Cl(PPh_3)_2$ (10.7 mg, 0.014 mmol), and $Al(acac)_3$ (0.179 g, 0.55 mmol) at room temperature. The total volume of reaction mixture was 13.8 mL. The flask was placed in an oil bath kept at 80 ˚C under vigorous stirring. In predetermined intervals, the polymerization was terminated by cooling the reaction mixtures to –78 ˚C. Monomer conversion was determined by gas chromatography with hexane as an internal standard. The quenched reaction solution was precipitated into methanol and isolated by centrifugation. After three times of the precipitation, the precipitate was evaporated to dryness to yield the product, which was subsequently dried

overnight in vacuo at room temperature (2.54 g, 90% yield; M_n = 189,000, M_w/M_n = 1.18).

Measurements

The ^{1}H NMR spectra were recorded on a Varian Gemini 2000 spectrometer (400 MHz). The number-average molecular weights (M_n) and molecular weight distributions (MWDs: M_w/M_n) of the polymers were measured by size exclusion chromatography (SEC) using THF at a flow rate 1.0 mL/min at 40 ˚C on two polystyrene gel columns (both Shodex KF-805L) that were connected to a JASCO PU-980 precision pump and a JASCO RI-930 detector. The molecular weight was calibrated against seven standard poly(methyl methacrylate) samples (M_n = 1990 – 6590000) or eight standard polystyrene samples (M_n = 526 – 900000). The monomer conversions were determined from the concentration of the residual monomer measured by gas chromatography using hexane or tetralin as the internal standard. The absolute weight-average molecular weight (M_w) of the polymers was determined by multiangle laser light scattering in tetrahydrofuran (THF) at 40 ˚C on a Wyatt Technology DAWN DSP photometer (λ = 633 nm). The refractive index increment (d*n*/d*c*) was measured in THF at 25 ˚C on a Wyatt Optilab rEX refractmeter (λ = 633 nm); the d*n*/d*c* values were 0.072 – 0.127 mL/g for the A_xBA_x block–graft copolymers. Sample films for dynamic tensile viscoelasticity and transmission electron microscopy (TEM) were prepared by hot-press molding of the copolymers at 230 °C. Dynamic tensile storage (*E'*) and loss (*E"*) moduli and tan δ (= *E"*/*E'*) were measured on a UBM Rheogel-E4000 spectrometer, operating at 11 Hz frequency (heating rate: 10 °C/min). For TEM, the ultrathin sections of the sample were cut on a Leica Ultracut FCS microtome at –100 °C (ca. 70 nm) and collected on mesh copper grids. The thin sections were stained with an aqueous solution of PTA [12-tungsto(VI)phosphoric acid, *n*-hydrate] containing small amounts of benzyl alcohol, washed with water, and then vacuum-dried at room temperature. Micrographs were obtained by a transmission electron microscope H-7100 FA (Hitachi, Ltd.) equipped with a CCD digital camera (AMT, Ltd.) operated at an acceleration voltage of 100 kV. Atomic force microscopy (AFM) observations were performed on a Nanoscope IIIa microscope (Digital Instruments, Santa Barbara, CA) in air using standard silicon tips (NCH-10V) in the tapping mode. All the images were collected with the maximum available number of pixels (512) in each direction (2 μm or 500 nm).

REFERENCES AND NOTES

(1) (a) Morton, M. *Anionic Polymerization: Principles and Practice;* Academic Press: New York, 1983; pp 221–232. (b) Kennedy, J. P.; Ivan, B.; *Designed Polymers by Carbocationic Macromolecular Engineering: Theory and Practice;* Hanser Publishers: Munich, 1992; p 96. (c) Sawamoto, M.; Kamigaito, M. In *New Methods of Polymer Synthesis;* Ebdon, J. R., Eastmond, G. C., Eds.; Blackie: Glasgow, U.K., 1995; Vol. 2, pp 37–68.

(2) (a) Georges, M. K.; Veregin, R. P. N.; Kazmaier, P. M.; Hamer, G. K. *Macromolecules* **1993**, *26*, 2987–2988. (b) Georges, M. K.; Veregin, R. P. N.; Kazmaier, P. M.; Hamer, G. K. *Trends*. *Polym*. *Sci*. **1994**, *2*, 66–72.

(3) (a) Hawker, C. J. *J*. *Am*. *Chem*. *Soc*. **1994**, *116*, 11185–11186. (b) Hawker, C. J.; Bosman, A. W.; Harth, E. *Chem*. *Rev*. **2001**, *101*, 3661–3688.

(4) (a) Kato, M.; Kamigaito, M.; Sawamoto, M.; Higashimura, T. *Macromolecules* **1995**, *28*, 1721–1723. (b) Kamigaito, M.; Ando, T.; Sawamoto, M. *Chem*. *Rev*. **2001**, *101*, 3689–3745.

(5) Kamigaito, M.; Ando, T.; Sawamoto, M. *Chem*. *Rec*. **2004**, *4*, 159–175.

(6) (a) Wang, J.-S.; Matyjaszewski, K. *J*. *Am*. *Chem*. *Soc*. **1995**, *117*, 5614–5615. (b) Matyjaszewski, K.; Xia, J. *Chem*. *Rev*. **2001**, *101*, 2921–2990.

(7) Percec, V.; Barboiu, B. *Macromolecules* **1995**, *28*, 7970–7972.

(8) Granel, C.; Dubois, P.; Jérôme, R.; Teyssié, P. *Macromolecules* **1996**, *29*, 8576–8582.

(9) Haddleton, D. M.; Jasieczek, C. B.; Hannon, M. J.; Shooter, A. J. *Macromolecules* **1997**, *30*, 2190–2193.

(10) (a) Chiefari, J.; Chong, Y. K.; Ercole, F.; Krstina, J. Jeffery, K.; Tam, P. T. Le.; Mayadunne, R. T. A.; Meijs, G. F.; Moad, C. L.; Moad, G.; Rizzardo, E.; Thang, S. H. *Macromolecules* **1998**, *31*, 5559–5562. (b) Chong, Y. K.; Kristina, J.; Tam, P. T. Le.; Moad, G.; Postma, A.; Rizzardo, E.; Thang, S. H. *Macromolecules* **2003**, *36*, 2256–2272. (c) Chiefari, J.; Mayadunne, R. T. A.; Moad, C. L.; Moad, G.; Rizzardo, E.; Postma, A.; Skidmoe, M. A.; Thang, S. H. *Macromolecules* **2003**, *36*, 2273–2283.

(11) Destarac, M.; Bzducha, W.; Taton, D.; Gauthier-Gillaizeau, I.; Zard, S. Z. *Macromol. Rapid Commun*. **2002**, *23*, 1049–1054.

(12) (a) Yamago, S.; Iida, K.; Yoshida, J. *J*. *Am*. *Chem*. *Soc*. **2002**, *124*, 2874–2875. (b) Yamago, S.; Ray, B.; Iida, K.; Yoshida, J.; Tada, T.; Yoshizawa, K.; Kwak, Y.; Goto, A.;

Fukuda, T. *J. Am. Chem. Soc.* **2004**, *126*, 13908–13909.

(13) Wayland, B. B.; Poszmik, G.; Mukerjee, S. L.; Fryd, M. *J. Am. Chem. Soc.* **1994**, *116*, 7943–7944.

(14) Debuigne, A.; Caille, J.-R.; Jérôme, R. *Angew. Chem., Int. Ed.* **2005**, *44*, 1101–1104.

(15) Kotani, Y.; Kato, M.; Kamigaito, M.; Sawamoto, M. *Macromolecules* **1996**, *29*, 6979–6982.

(16) Chapter 2 of this thesis; *Polym. J.* **2006**, *38*, 930–939.

(17) (a) Ueda, J.; Matsuyama, M.; Kamigaito, M.; Sawamoto, M. *Macromolecules* **1998**, *31*, 557–562. (b) Ueda, J.; Kamigaito, M.; Sawamoto, M. *Macromolecules* **1998**, *31*, 6762–6768. (c) Baek, K.-Y.; Kamigaito, M.; Sawamoto, M. *Macromolecules* **2001**, *34*, 215–221.

(18) Holden, G.; Kricheldorf, H. R.; Quirk, R. P. *Thermoplastic Elastomers,* 3rd ed.; Hanser Publishers: Munich, 2004.

(19) (a) Moineau, G.; Minet, M.; Teyssié, Ph.; Jérôme, R. *Macromolecules* **1999**, *32*, 8277–8282. (b) Tong, J. D.; Moineau, G.; Leclère, Ph.; Bredas, J. L.; Lazzaroni, R.; Jérôme, R. *Macromolecules* **2000**, *33*, 470–479.

(20) Matyjaszewski, K.; Shipp, D. A.; McMurtry, G. P.; Gaynor, S. G.; Pakula, T. *J. Polym. Sci., Part A: Polym. Chem.* **2000**, *38*, 2023–2031.

(21) For reviews, see: (a) Davis, K. A.; Matyjaszewski, K. *Adv. Polym. Sci.* **2002**, *159*, 107–152. (b) Börner, H.; Matyjaszewski, K. *Macromol. Symp.* **2002**, *177*, 1–15. (c) Bhattacharya, A.; Misra, B. N. *Prog. Polym. Sci.* **2004**, *29*, 767–814.

(22) (a) Beers, K. L.; Gaynor, S. G.; Matyjaszewski, K.; Sheiko, S. S.; Möller, M. *Macromolecules* **1998**, *31*, 9413–9415. (b) Börner, H. G.; Beers, K. L.; Matyjaszewski, K.; Sheiko, S. S.; Möller, M. *Macromolecules* **2001**, *34*, 4375–4383. (c) Börner, H. G.; Duran, D.; Matyjaszewski, K.; da Silva, M.; Sheiko, S. S. *Macromolecules* **2002**, *35*, 3387–3394. (d) Qin, S.; Matyjaszewski, K.; Xu, H.; Sheiko, S. S. *Macromolecules* **2003**, *36*, 605–612. (e) Lord, S. J.; Sheiko, S. S.; LaRue, I.; Lee, H.-I.; Matyjaszewski, K. *Macromolecules* **2004**, *37*, 4235–4240. (f) Lee, H.; Matyjaszewski, K.; Yu, S.; Sheiko, S. S. *Macromolecules* **2005**, *38*, 8264–8271.

(23) Sumerlin, B. S.; Neugebauer, D.; Matyjaszewski, K. *Macromolecules* **2005**, *38*, 702–708.

(24) (a) Cheng, G.; Böker, A.; Zhang, M.; Krausch, G.; Müller, A. H. E. *Macromolecules*

(25) Ma, Y. H.; Cao, T.; Webber, S. E. *Macromolecules* **1998**, *31*, 1773–1778.

(26) Chen, G.; Hoffman, A. S. *Nature (London)* **1995**, *373*, 49–52.

(27) Shibanuma, T.; Aoki, T.; Sanui, K.; Ogata, N.; Kikuchi, A.; Sakurai, Y.; Okano, T. *Macromolecules* **2000**, *33*, 444–450.

(28) Li, C.; Gunari, N.; Fischer, K.; Janshoff, A; Schmidt, M. *Angew. Chem., Int. Ed.* **2004**, *43*, 1101–1104.

(29) Janata, M.; Lochmann, L.; Brus, J.; Holler, P.; Tuzar, Z.; Kratochvíl, P.; Schmitt, B.; Radke, W.; Müller, A. H. E. *Macromolecules* **1997**, *30*, 7370–7374.

(30) (a) Floudas, G.; Hadjichristidis, N.; Iatrou, H.; Avgeropoulos, A.; Pakula, T.; *Macromolecules* **1998**, *31*, 6943–6950.

(31) Houli, S.; Iatrou, H.; Hadjichristidis, N.; Vlassopoulos, D. *Macromolecules* **2002**, *35*, 6592–6597.

(32) Knauss, D. M.; Huang, T. *Macromolecules* **2002**, *35*, 2055–2062.

(33) (a) Huang, T.; Knauss, D. M. *Polym. Bull. (Berlin)* **2002**, *49*, 143–150. (b) Huang, T.; Knauss, D. M. *Macromol. Symp.* **2004**, *215*, 81–93.

(34) Knauss, D. M.; Huang, T. *Macromolecules* **2003**, *36*, 6036–6042.

(35) (a) Ruckenstein, E.; Zhang, H. *Macromolecules* **1998**, *31*, 2977–2982. (b) Zhang, H.; Ruckenstein, E. *Macromolecules* **1998**, *31*, 4753–4759.

(36) Lai, M.-K.; Wang, J.-Y.; Tsiang, R. C.-C. *Polymer* **2005**, *46*, 2558–2566.

(37) Pan, Q.; Liu, S.; Xie, J.; Jiang, M. *J. Polym. Sci., Part A: Polym. Chem.* **1999**, *37*, 2699–2702.

(38) Ning, F.; Jiang, M.; Mu, M.; Duan, H.; Xie, J. *J. Polym. Sci., Part A: Polym. Chem.* **2002**, *40*, 1253–1266.

(39) Truelsen, J. H.; Kops, J.; Batsberg, W. *Macromol. Rapid Commun.* **2000**, *21*, 98–102.

(40) (a) Truelsen, J. H.; Kops, J.; Batsberg, W.; Armes, S. P. *Macromol. Chem. Phys.* **2002**, *203*, 2124–2131. (b) Truelsen, J. H.; Kops, J.; Batsberg, W.; Armes, S. P. *Polym. Bull. (Berlin)* **2002**, *49*, 235–242.

(41) Lecolley, F.; Waterson, C.; Carmichael, A. J.; Mantovani, G.; Harrisson, S.; Chappell, H.; Limer, A.; Williams, P.; Ohno, K.; Haddleton, D. M. *J. Mater. Chem.*, **2003**, *13*,

2689–2695.

(42) Ohno, S.; Matyjaszewski, K. *J. Polym. Sci., Part A: Polym. Chem.* **2006**, *44*, 5454–5467.

(43) Fuji, Y.; Watanabe, K.; Beak, K.-Y.; Ando, T.; Kamigaito, M.; Sawamoto, M. *J. Polym. Sci., Part A: Polym. Chem.* **2002**, *40*, 2055–2065.

(44) Takahashi, H.; Ando, T.; Kamigaito, M.; Sawamoto, M. *Macromolecules* **1999**, *32*, 3820–3823.

(45) Podzimek, S.; Vlcek, T. *J. Appl. Polym. Sci.* **2001**, *82*, 454–460.

(46) Vankan, R.; Fayt, R.; Jérôme, R.; Teyssié, Ph. *Polym. Eng. Sci.* **1996**, *36*, 1675–1684.

(47) (a) Fox, T. G.; Flory, P. J. *J. Appl. Phys.* **1950**, *21*, 581–591. (b) Fox, T. G.; Flory, P. J. *J. Polym. Sci.* **1954**, *14*, 315–319.

(48) Turner, D. T. *Polymer* **1978**, *19*, 789–796.

(49) Bates, F. S.; Fredrickson, G. H. *Annu. Rev. Phys. Chem.* **1990**, *41*, 525–557.

(50) Kitayama, T.; Ogawa, M.; Kawauchi, T. *Polymer* **2003**, *44*, 5201–5207.

(51) Matyjaszewski, K.; Qin, S.; Boyce, J. R.; Shirvnyants, D.; Sheiko, S. S. *Macromolecules* **2003**, *36*, 1843–1849.

CHAPTER 4

A_xBA_x-TYPE BLOCK–GRAFT POLYMERS WITH SOFT METHACRYLATE MIDDLE SEGMENTS AND HARD STYRENE OUTER GRAFTS: MULTIPLE CONTROL FOR HIGHER ORDER STRUCTURED MATERIALS

ABSTRACT

This chapter reveals that novel controlled architectural copolymers, A_xBA_x-type block–graft copolymers prepared by living radical polymerization, can function as new building blocks for controlled nanostructures based on microphase separation, which is different from that of the conventional ABA triblock copolymers. A series of well-defined A_xBA_x-type block–graft copolymers consisting of soft middle segments [dodecyl methacrylate (DMA)] and hard outer graft chains [styrene (St)] were thus synthesized by the ruthenium-catalyzed living radical block and graft polymerizations. NMR and size exclusion chromatography equipped with multiangle laser light scattering confirmed the well-defined structure of the A_xBA_x block–graft copolymers with controlled lengths of the backbone and the graft chains. Transmission electron microscopy and transmission electron microtomography studies revealed a series of morphologies that change from PSt-"honeycomb"-cylinders, lamellae, and PDMA-cylinders with increasing PSt graft contents, while the phase diagram was significantly shifted to lower volume fractions of the larger number component, i.e., St, in comparison with those of the corresponding ABA triblock copolymers. More specifically, the PDMA-cylinders were observed even before the St content reached 50 wt %. The A_xBA_x and ABA copolymers with 17–30 wt % of St exhibited characteristics of a thermoplastic elastomer with tensile strengths of 1–6 MPa and elongations at break of 70–300%. These mechanical properties were well related to the microphase structures of the A_xBA_x and ABA copolymers.

INTRODUCTION

Well-defined block copolymers consisting of immiscible segments can form self-assembled ordered nano- or mesoscopic structures depending on the compositions, the molecular weights, and the sequence of the segments.[1] Such nano-ordered structures have been applied to the fabrication of microelectronic devices, separation devices, and optoelectronics as templates or scaffolds and have been contributing to the recent nanotechnology developments.[2] Another wide market for such block copolymers is a thermoplastic elastomer (TPE) based on the ABA triblock copolymers consisting of glassy outer chains coupled to a rubbery central chain,[3] such as poly(styrene-*b*-butadiene-*b*-styrene), in which the microphase structure functions for the mechanical properties. The construction of the molecular structures including the selection of monomers, molecular weights, compositions, and sequences of the blocks is very important for the material designs because these parameters highly affect the morphologies, the mechanical properties, and other characteristics.

The effects of their molecular parameters on the morphologies have been extensively studied for the block copolymers mainly prepared by living anionic polymerizations of hydrocarbon monomers,[4] such as styrenes and dienes, under stringent conditions, and a series of microphase-ordered structures such as spheres, cylinders, lamellae, and bicontinuous structures have been constructed. Further developments in living anionic polymerization techniques using coupling agents have enabled the synthesis of more complex copolymers possessing a combination of block and graft structures, such as A-*g*-B_x,[5,6] A_xB,[7–9] A_xBA_x.[10,11] The effects of branching on the morphologies were discussed for some polymers with A_2B-, A_3B-, A_5B-miktoarm, and A_2BA_2-H-shaped copolymers. Although these studies indicated that the morphologies and mechanical properties could be drastically changed or purposefully controlled by the molecular structures of the block or graft copolymers, the limitations of the monomers and the cumbersome synthetic procedures inherent in the living anionic polymerizations, including repetitive purifications by fractionation and/or preparative size-exclusion chromatography (SEC), restricted the variety of the accessible polymers and their practical applications.

However, recent progress in living or controlled radical polymerizations has readily expanded the accessible controlled architectural polymers, such as block, graft, and star

polymers, from a variety of monomers including non-polar, polar, and functionalized monomers.[12–17] They were further applied to the synthesis of more complex polymers with combined architectures such as A-*g*-B_x,[18–22] A_xB,[23,24] A_xAA_x,[25] A_xBA_x,[26–29] etc. Although a variety of these complex structural polymers have become readily accessible by living radical polymerizations, there have been few comprehensive and detailed studies on the relationships between their architectures and their morphologies as well as their mechanical properties,[28,29] which might greatly contribute to the developments of new polymeric materials for emerging nanotechnologies.

Quite recently, the author has succeeded relatively easily in the preparation of a series of all-methacrylic well-defined A_xBA_x-type block–graft copolymers consisting of soft middle segments [dodecyl methacrylate (DMA)] and hard outer graft chains [methyl methacrylate (MMA)] by utilizing ruthenium-catalyzed living radical polymerizations.[30] The obtained copolymers have been characterized by NMR, SEC, multiangle laser light scattering (MALLS), differential scanning calorimetry (DSC), dynamic viscoelasticity, and transmission electron microscopy (TEM) and a single molecule of the copolymer has been visualized by atomic force microscopy (AFM). These studies revealed that the synthesis proved quite successful without any cumbersome synthetic procedures and any purification by fractionation and preparative SEC and that branching affected the morphologies to provide different properties from those of the corresponding ABA triblock copolymers. However, the morphological details could not be fully understood due to the difficulty in the differentiation or the segregation of poly(DMA) segments from PMMA, in which both segments processed alkyl ester moieties.

To develop such novel A_xBA_x block–graft copolymers for the construction of ordered periodic nanoscale morphologies as well as new TPEs, the author constructed a new series of A_xBA_x with soft middle poly(DMA) and hard outer polystyrene (PSt) grafts and focused on the analysis of the morphologies by TEM and transmission electron microtomography (TEMT),[31] which enabled the direct observation of nano-scale morphologies in three-dimension (3D),[32] and the mechanical properties by comparing with those of the corresponding ABA triblocks. The synthetic method was based on the ruthenium-catalyzed living radical block copolymerization of DMA and 2-(trimethylsilyloxy)ethyl methacrylate (TMSHEMA) initiated by a bifunctional initiator followed by the direct in-situ conversion of the trimethylsilyl groups into C–Br bonds for multifunctional macroinitiator (I_xBI_x) and the

subsequent Ru-catalyzed "grafting-from" living radical polymerization of St (Scheme 1).

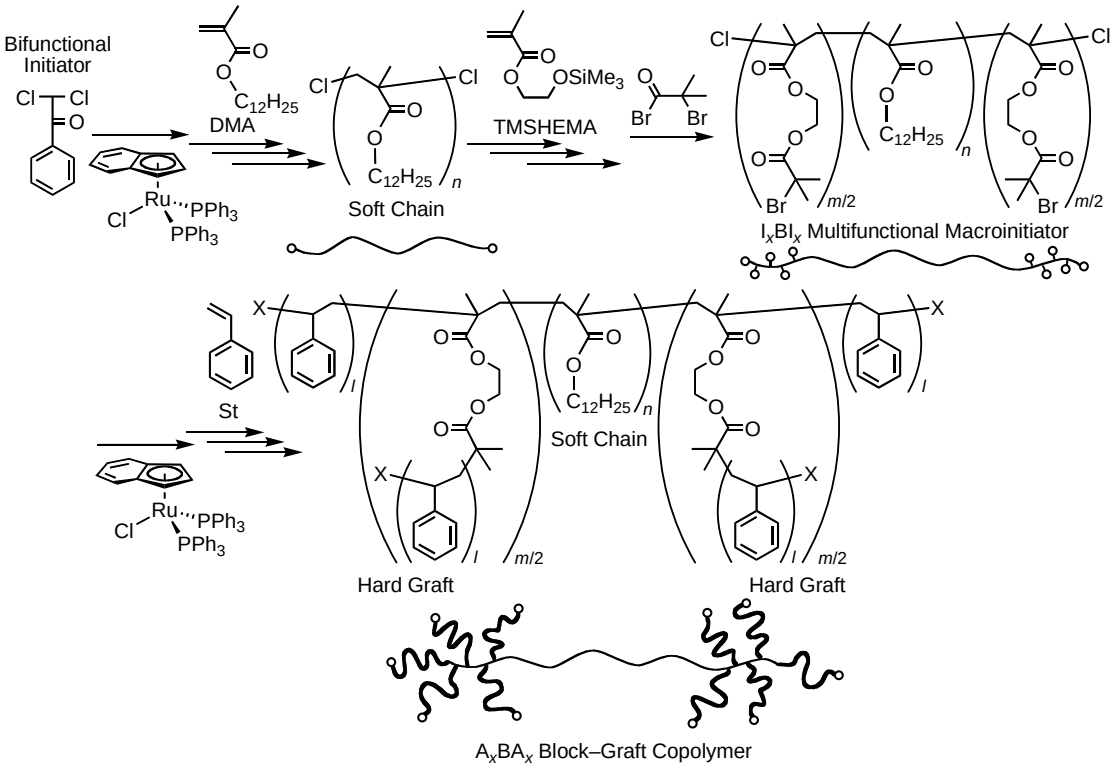

Scheme 1. Synthesis of A_xBA_x block–graft copolymers via ruthenium-catalyzed living radical polymerization.

RESULTS AND DISCUSSION

1. Synthesis of Methacrylate–Styrene-Based A_xBA_x Block–Graft Copolymers: Ruthenium-Catalyzed Living Radical Grafting-From Polymerization of Styrene.

Prior to the synthesis of the A_xBA_x block–graft copolymers, the macroinitiators (I_xBI_x) consisting of DMA (B) and multi-initiating sites (I) [the number-average molecular weights (M_n) = 132,000 by MALLS, molecular weight distributions (MWDs) (M_w/M_n = 1.17), the initiating sites (f) = 10.9] were prepared as reported previously.[30] The ruthenium-catalyzed living radical polymerization of styrene was then initiated from the macroinitiator in the presence of $Ru(Ind)Cl(PPh_3)_2$ and n-Bu_3N in toluene at 100 ˚C to form the A_xBA_x block–graft copolymers.

Figure 1 shows the SEC curves, M_n, and M_w/M_n of the copolymers obtained simply by the precipitation of the polymerization mixtures into methanol. As the graft polymerization

proceeded, the SEC curves shifted toward higher molecular weights retaining the unimodal and narrow MWDs ($M_w/M_n \leq 1.4$). The M_n obtained from the absolute molecular weights (M_w) by MALLS agreed well with the calculated values assuming that one molecule of the I_xBI_x macroinitiator generates one molecule of the A_xBA_x polymers. However, the M_n values based on a PMMA standard calibration by SEC were lower than the calculated values due to the smaller hydrodynamic volumes of the branched structures.[30] These results indicate that the methacrylate–styrene-based A_xBA_x copolymers were successfully prepared by the ruthenium-catalyzed living radical grafting-from polymerizations of styrene.

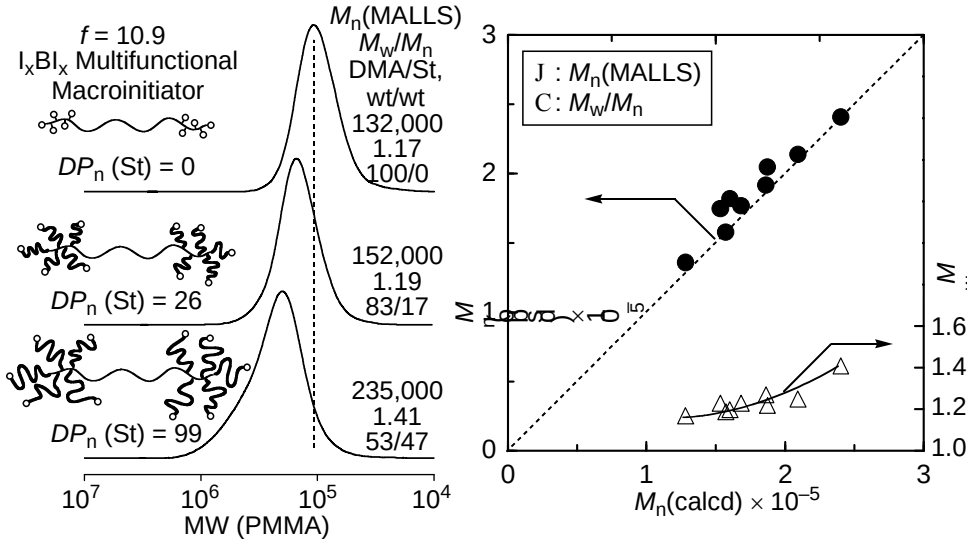

Figure 1. Graft copolymerization of styrene (St) from the I_xBI_x multifunctional macroinitiator [M_n(MALLS) = 132,000, M_w/M_n = 1.17] with Ru(Ind)Cl(PPh_3)$_2$/*n*-Bu_3N in toluene at 100 ˚C [●: M_n(MALLS); △: M_w/M_n]. $[St]_0$ = 3.0–6.0 M; [C–X bonds in the macroinitiator]$_0$ = 10 mM; [Ru(Ind)Cl(PPh_3)$_2$]$_0$ = 1.0 mM; [*n*-Bu_3N]$_0$ = 5.0 mM.

The A_xBA_x block–graft copolymers and the macroinitiators were also analyzed by ^{1}H NMR (Figure 2). The I_xBI_x macroinitiators (Figure 2A) showed the characteristic signals of DMA units, i.e., the ester methylene protons (*g*) and other alkyl protons (*h–j*), and the multifunctional initiating sites, i.e., the ester ethylene protons (*a* and *b*) with the isobutyryl groups (*d*) adjacent to the C–Br bonds, in addition to the large absorptions of the α-methyl (*f*) and main-chain methylene protons (*e*) of both units. The unit ratio of DMA to the initiating sites calculated from the peak intensity ratio (*g* vs *b*) was 491/8.7, in good agreement with the calculated value of 491/8.9 for the macroinitiator. The obtained macroinitiators thus

possessed about 11 initiating sites, including the C–Br bonds and the original C–Cl bonds at the chain ends, per molecule.

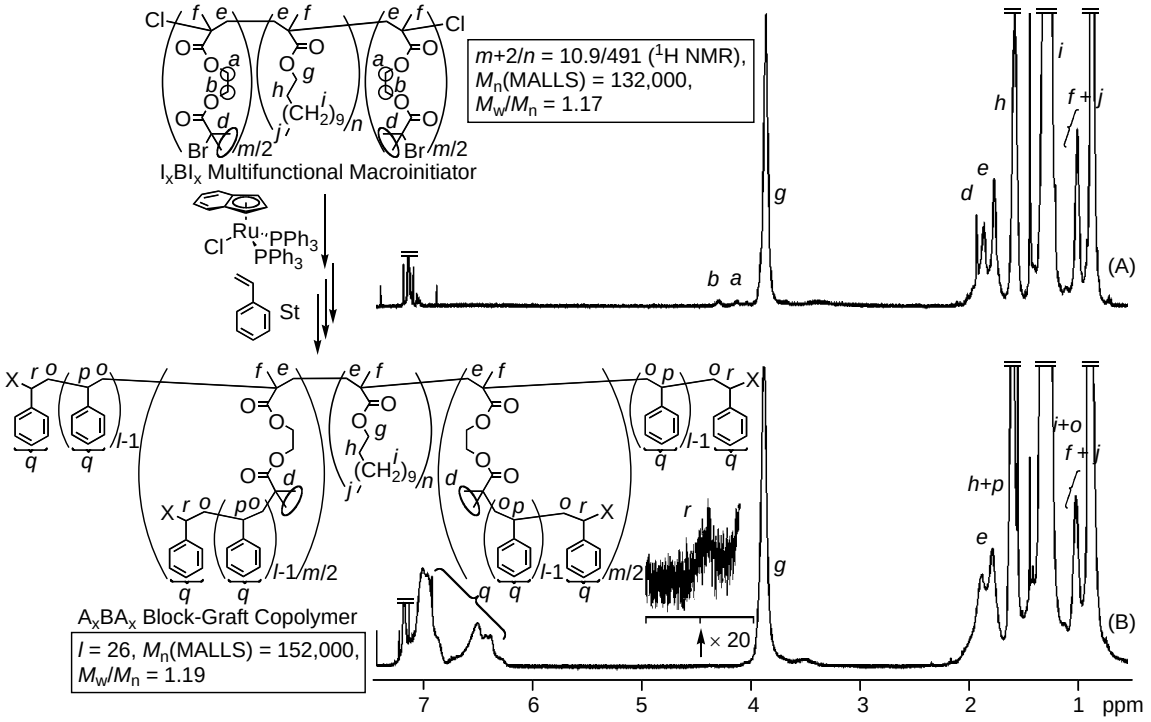

Figure 2. ^{1}H NMR spectra ($CDCl_3$, 50 ˚C) of the I_xBI_x multifunctional macroinitiator [A: M_n(MALLS) = 132,000, M_w/M_n = 1.17] and the A_xBA_x block–graft copolymer [B: M_n(MALLS) = 152,000, M_w/M_n = 1.19] obtained with $Ru(Ind)Cl(PPh_3)_2$/*n*-Bu_3N in toluene at 100 ˚C.

The A_xBA_x block–graft copolymers showed the characteristic signals of the aromatic protons (*q*) of the polystyrene graft chains and the methine proton (*r*) adjacent to the C–X terminals in addition to the absorptions of the prepolymer (Figure 2B). The DMA/St unit ratio (83/17 wt/wt), calculated from the peak intensity ratio (*g* vs *q*), agreed with the calculated DMA/St ratio from the monomer feed ratio and the monomer conversion (81/19 wt/wt). These results also support that the simple synthetic method, based on the ruthenium-catalyzed living radical block and graft polymerization, is quite effective in the synthesis of the methacrylate–styrene A_xBA_x block–graft copolymer with controlled molecular weights and compositions. A series of the A_xBA_x block–graft polymers with varying graft chain lengths were thus successfully synthesized simply by changing the monomer conversions and are summarized in Table 1. All these copolymers had controlled molecular weights, narrow MWDs, and variable monomer compositions ranging from

DMA/St = 85/15 to 53/47 wt/wt.

Table 1. A_xBA_x Block–Graft and ABA Triblock Copolymers Obtained via Ruthenium-Catalyzed Living Radical Polymerization.[a]

code	n[b]	f[b] (m+2)	l[b]	M_w	M_n			M_w/M_n[e]	R_z,[c]	dn/dc[g]	DMA/St, wt/wt		T_g,[i]
				MALLS[c]	calcd[d]	SEC[e]	MALLS[f]		nm		calcd[h]	obsd[b]	°C
1	491	10.9	0	154 000	128 000	97 000	132 000	1.17	22.9	0.0715	-	-	n.d.
2	491	10.9	22	198 000	153 000	115 000	161 000	1.23	25.3	0.0946	83/17	85/15	n.d.
3	491	10.9	26	181 000	157 000	114 000	152 000	1.19	26.3	0.0980	81/19	83/17	–50.8, 42.9
4	491	10.9	28	210 000	160 000	122 000	175 000	1.20	25.8	0.1036	80/20	82/18	n.d.
5	491	10.9	35	206 000	168 000	124 000	167 000	1.23	26.8	0.3080	76/24	77/23	–51.6, 54.1
6	491	10.9	51	236 000	186 000	142 000	186 000	1.27	28.8	0.1292	69/31	70/30	–51.1, 67.5
7	491	10.9	52	246 000	187 000	136 000	202 000	1.22	27.8	0.1208	68/32	70/30	n.d.
8	491	10.9	71	252 000	209 000	152 000	202 000	1.25	30.1	0.1376	60/40	62/38	–51.5, 73.2
9	491	10.9	99	332 000	240 000	197 000	235 000	1.41	33.8	0.1603	52/48	53/47	–52.2, 80.5
10	560	2	0	176 000	142 000	123 000	149 000	1.18	24.4	0.0825	-	-	n.d.
11	560	2	158	229 000	175 000	170 000	191 000	1.20	27.3	0.1120	81/19	81/19	–51.4, 86.1
12	560	2	298	273 000	204 000	214 000	228 000	1.20	30.5	0.1276	70/30	70/30	–51.0, 92.5

[a]Polymerization conditions: $[St]_0/[C–X$ bonds in the macroinitiator$]_0/[Ru(Ind)Cl(PPh_3)_2]_0/[n\text{-}Bu_3N]_0$ = 3000–6000/10/1.0/5.0 mM in toluene at 80–100 °C (codes 1–9). $[St]_0/[C–X$ bonds in the macroinitiator$]_0/[Ru(Cp^*)Cl(PPh_3)_2]_0/[n\text{-}Bu_3N]_0$ = 2000/2.5/4.0/40 mM in toluene at 80 °C (codes 10–12). [b]Determined by ^1H NMR. [c]Measured on SEC by multiangle laser light scattering (MALLS) detector (λ = 633 nm). [d]M_n(calcd) = M_n(macroinitiator, calcd)+$([M]_0/[C–X]_0) \times$ conv $\times f \times$ MW(St). [e]The number-average molecular weight (M_n), the weight-average molecular weight (M_w), and polydispersity index (M_w/M_n) were determined on size exclusion chromatography (SEC) by refractive index (RI) detector (PMMA standard). [f]M_n(MALLS) = M_w(MALLS)/[M_w/M_n(SEC)]. [g]Measured by refractometer (λ = 633 nm). [h]Calculated from feed ratio and monomer conversion. [i]Determined by differential scanning calorimetry (DSC).

The PSt graft chains in the A_xBA_x block–graft copolymers thus prepared are connected to the backbone chain via the ester linkages, which can be hydrolyzed into the backbone and the graft chains. To confirm the molecular weights and the uniformity of the PSt graft chain lengths, hydrolysis of the copolymers was carried out using potassium hydroxide in a mixture of methanol and *N*,*N*-dimethylformamide (1/3 v/v) at 80 ˚C (Scheme 2).[22]

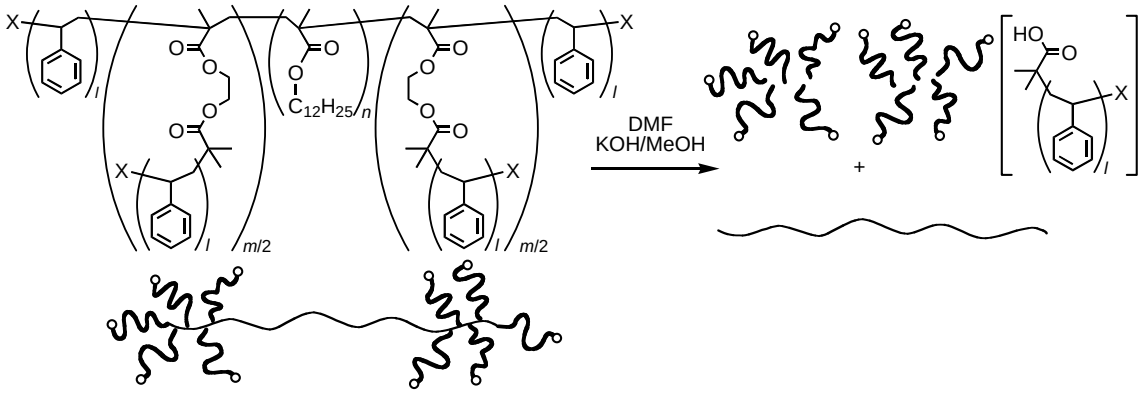

Scheme 2. Detachment of PSt graft chains from the backbone chain.

Figure 3 shows a series of SEC curves of the hydrolyzed products (dashed and dotted lines) from the A_xBA_x block–graft copolymers obtained at different monomer conversions as well as that of the I_xBI_x macroinitiator (solid line). After the hydrolysis, each SEC curve showed two peaks. The higher molecular weight peak was attributed to the original

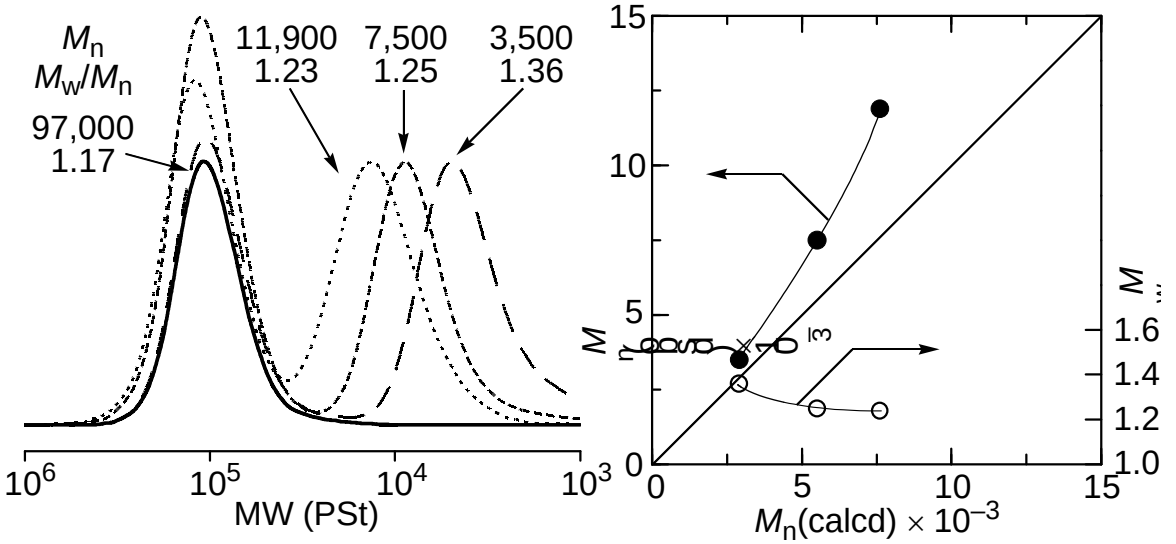

Figure 3. SEC curves of the original I_xBI_x multifunctional macroinitiator (solid line) and the hydrolyzed products from the A_xBA_x block–graft copolymers (codes 3, 6, and 8 in Table 1) (dashed or dotted lines) and M_n (●) and M_w/M_n (○) of the detached PSt graft chains.

backbone chain from which the PSt grafts were removed, while the lower one was ascribed to the detached PSt graft chains. The lower molecular weight peaks shifted with the styrene conversion and showed narrow MWDs (M_w/M_n <1.4). The M_n of the detached PSt graft chains increased in direct proportion to the monomer conversion and agreed with the calculated values assuming that each initiating site in the macroinitiator generates one PSt graft chain. These results indicate that each initiating site initiates the graft polymerization of styrene to form the PSt graft chains with controlled molecular weights and gives the well-defined methacrylate–styrene-based A_xBA_x block–graft copolymers.

2. Morphology of A_xBA_x Block–Graft Copolymers: TEM and TEMT Analysis.

The author thus analyzed the bulk morphology of a series of the methacrylate–styrene-based A_xBA_x block–graft copolymers, for which the PSt graft chain lengths were systematically changed while keeping the same molecular weight for the mid-poly(DMA) to result in varying DMA/St contents (85/15–53/47 wt/wt) by TEM (Figure 4). In these TEM micrographs, the PSt domains were stained dark with RuO_4. In contrast to the TEM micrographs of the all-methacrylate A_xBA_x block–graft copolymers, which exhibited a complex microphase-separated structure probably due to the similarity in the structures of PMMA and poly(DMA) segments,[30] the methacrylate–styrene-based counterparts showed clearer nano-ordered microphase-separated structures. Similar to the linear block polymers, the morphologies can be systematically changed by the composition. As the fraction of PSt (ϕ_{PSt}) increased, the morphology changed in the following order; sphere or cylinder of PSt [ϕ_{PSt} = 0.15 (a) – 0.17 (b)], coexistence of PSt cylinder and lamella [ϕ_{PSt} = 0.23 (c)], lamella [ϕ_{PSt} = 0.30 (d) – 0.38 (e)], and coexistence of poly(DMA) cylinder and lamella or two cylindrical phases [ϕ_{PSt} = 0.47 (f)]. Especially in the micrograph of the specimen with the 17 wt % PSt fraction (Figure 4b), the morphology of highly-ordered and long-range hexagonally packed PSt domains in a poly(DMA) matrix was observed. More interestingly, the PSt cylinders seem to be hexagonally-shaped to form a “honeycomb” morphology, as described later.

According to Milner’s theory, introduction of a branching architecture into block copolymers results in asymmetry in copolymer microphases, in which the larger excluded volume of the graft chains, anchored around the domain boundary, compared to that of a single block chain causes an interfacial curvature.[33] The volume fraction windows for our

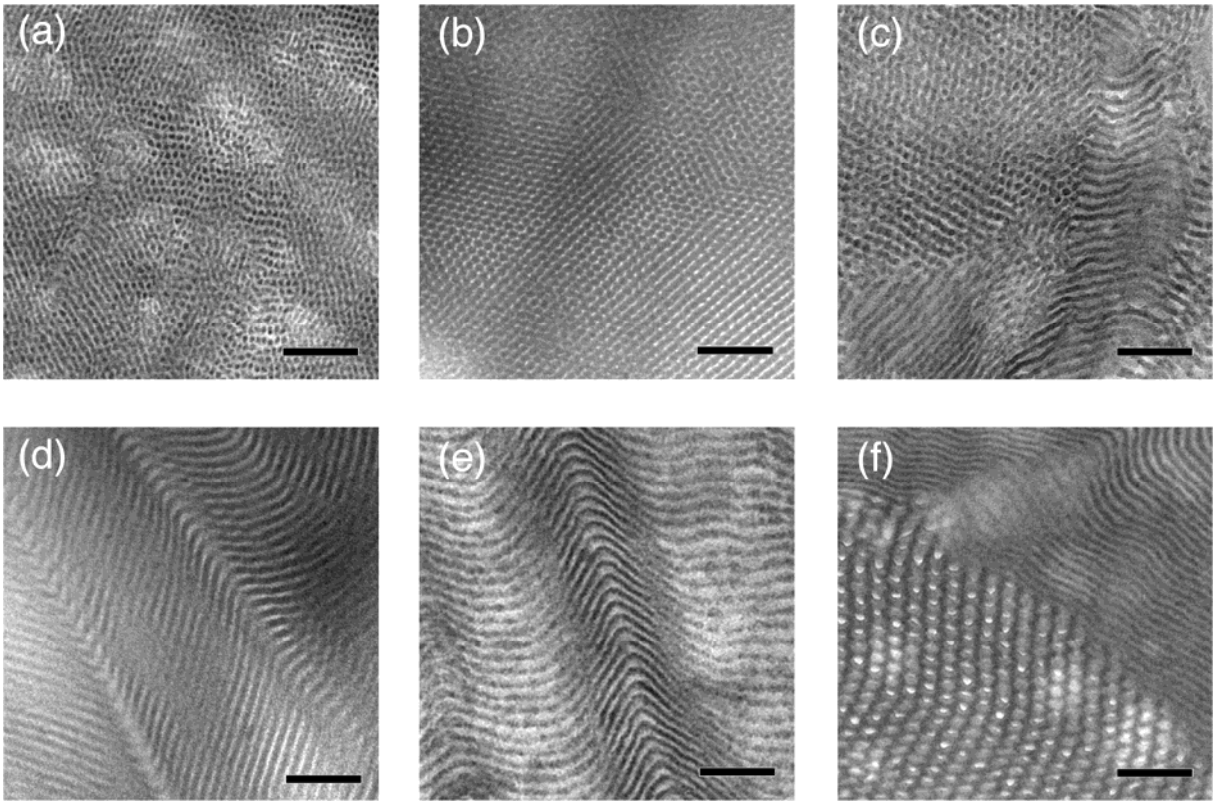

Figure 4. Transmission electron microscopy (TEM) images of the A_xBA_x block–graft copolymers (f = 10.9) [a: M_n(MALLS) = 161,000, M_w/M_n = 1.23, B/A = 85/15; b: M_n(MALLS) = 152,000, M_w/M_n = 1.19, B/A = 83/17; c: M_n(MALLS) = 167,000, M_w/M_n = 1.23, B/A = 77/23; d: M_n(MALLS) = 186,000, M_w/M_n = 1.27, B/A = 70/30; e: M_n(MALLS) = 202,000, M_w/M_n = 1.25, B/A = 62/38; f: M_n(MALLS) = 235,000, M_w/M_n = 1.41, B/A = 53/47]. Bars indicate 200 nm. Stained by RuO_4.

A_xBA_x block–graft copolymers were thus shifted to lower volume fractions of the larger number component, i.e., PSt in this case, than in the corresponding linear block copolymers. These phenomena were also observed for A_2B-, A_3B-, and A_5B-miktoarm, and A_2BA_2-H-shaped copolymers of isoprene and styrene prepared by living anionic polymerizations, although some deviations from the theory were suggested.[7–10] The A_xBA_x block–graft copolymers prepared by such simple living radical polymerizations also showed a similar asymmetry as predicted by Milner's theory and similar deviations. It is worth noting that the coexistence of poly(DMA) cylinder and lamella or two cylindrical phases vertical and parallel to the cross-sectional direction were observed even at a 47 wt % PSt fraction (Figure 4f). The microstructure was further clarified by TEMT as below. This would be beneficial for material designs because the morphology can be controlled by the branching number

without changing the volume fraction or the hardness of the materials. While the precedent results for the miktoarm and H-shaped polymers, prepared by living anionic polymerizations, have already shown that the morphological design can be attained not only by the volume fraction but also by the molecular architectural change, this study further widens this scope to living radical polymerizations, which would be more practical for making materials.

To clarify the morphologies of the A_xBA_x block–graft copolymers in more detail, TEMT observations were carried out for two samples; one for the hexagonal-cylinder-like morphology (ϕ_{PSt} = 0.17) and the other for the mixtures of cylinders and lamellae or two lamellar phases (ϕ_{PSt} = 0.47). Figure 5 shows two-dimensional planar (x,y) and

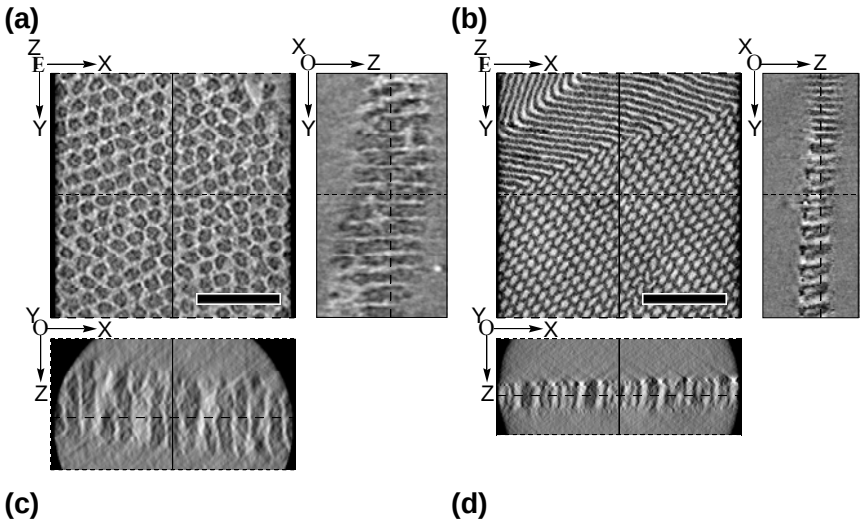

Figure 5. Two-dimensional planar (x,y) and cross-sectional (x,z; y,z) slices of the morphologies generated from 3D TEMT (a and b) and the 3D solid renditions of the poly(DMA) microdomains within a transparent PSt matrix (c and d: 400 × 400 × 50 nm). Z axis is parallel to the depth direction of the ultrathin section. Dashed and solid lines in each cross section represent position of two other orthogonal cross sections.

cross-sectional (*x*,*z*; *y*,*z*) slices of the morphologies generated from 3D TEMT and the 3D solid-rendered images of the poly(DMA) microdomains within a transparent PSt matrix. As shown in Figures 5c and 5d, the 3D reconstructed images of the morphologies proved the orthogonally aligned "honeycomb" cylinder (ϕ_{PSt} = 0.17) and the coexistence of lamellar/cylindrical morphologies (ϕ_{PSt} = 0.47) both in alignment with the *Z* axis, respectively. Thus, TEMT was quite effective in determining the microstructure. Although the "honeycomb" morphology has been reported in multiple component copolymers such as ABC triblock, ABC heteroarm star, ABCD tetrablock copolymers, and their blends, this is the first time that the "honeycomb" morphology was observed in the two-component A_xBA_x block–graft copolymers.[34-36]

To further characterize the morphologies built by the A_xBA_x block–graft copolymers in comparison to the ABA triblock copolymers, a series of poly(St-*b*-DMA-*b*-St) with a similar composition was thus synthesized by the ruthenium-catalyzed living radical polymerizations according to Scheme 3. As summarized in Table 1, the obtained triblock copolymers also showed the controlled molecular weights, narrow MWDs, and the desired compositions of DMA and St, in which codes 11 and 12 of the ABA triblocks have values similar to codes 3 or 4 and 6 or 7 of the A_xBA_x block–grafts, respectively.

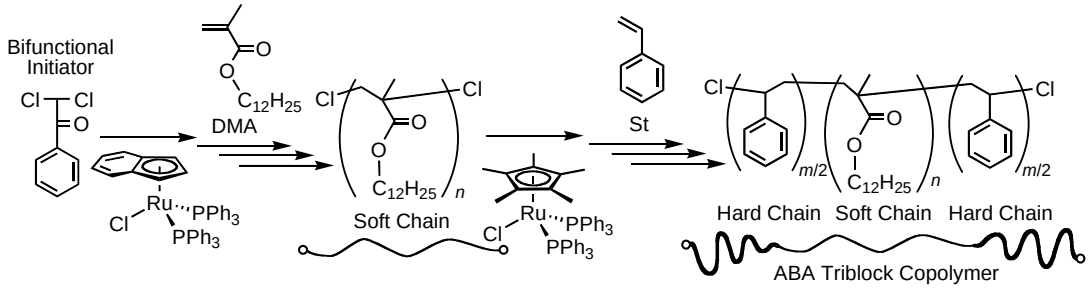

Scheme 3. Synthesis of ABA triblock copolymers via ruthenium-catalyzed living radical polymerization.

The ABA samples with DMA/St = 81/19 (Figure 6a) and 70/30 (Figure 6b) exhibited spherical and cylindrical morphologies, respectively, as expected from the comonomer compositions for the conventional block copolymers. As mentioned above, the A_xBA_x samples that have similar PSt compositions showed cylinders (Figure 6c; DMA/St = 83/17) and lamellae (Figure 6d; DMA/St = 70/30), respectively, which were apparently shifted to lower volume fractions of the larger number component. As stated below, these

morphologies were crucial for some of the mechanical properties, in which the A_xBA_x block–grafts showed similar mechanical properties to the ABA triblocks with different compositions but with similar morphologies.

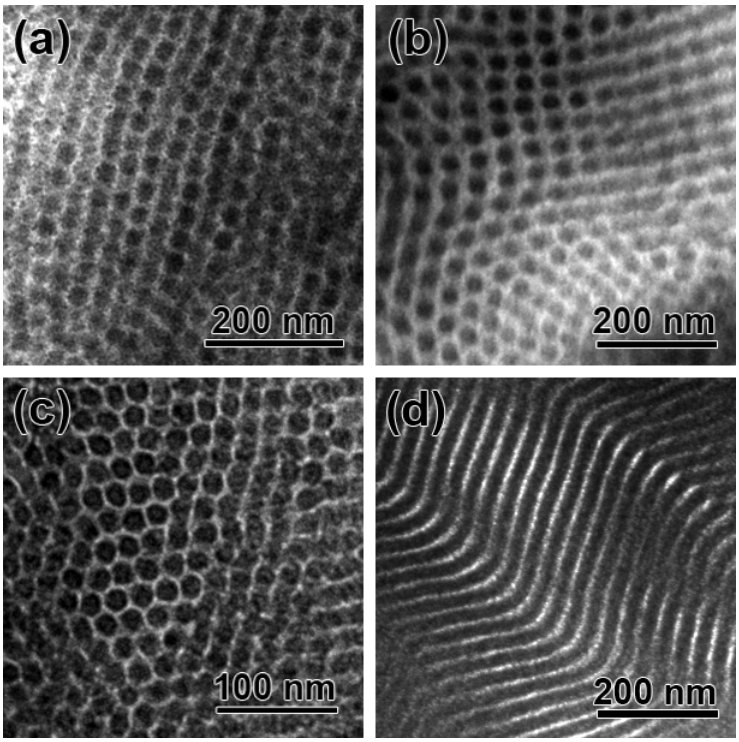

Figure 6. TEM images of the ABA triblock copolymers [a: M_n(MALLS) = 191,000, M_w/M_n = 1.20, B/A = 81/19; b: M_n(MALLS) = 228,000, M_w/M_n = 1.20, B/A = 70/30] and the A_xBA_x block–graft copolymers (f = 10.9) [c: M_n(MALLS) = 152,000, M_w/M_n = 1.19, B/A = 83/17; d: M_n(SEC) = 186,000, M_w/M_n = 1.27, B/A = 70/30]. Stained by RuO_4.

3. Mechanical Properties of A_xBA_x Block–Graft Copolymers: Comparison with ABA Triblock Copolymers.

The mechanical characteristics of the A_xBA_x copolymers were then evaluated by the dynamic viscoelasticity and tensile stress-strain property along with the ABA triblock copolymers. Figure 7 shows the dynamic tensile storage modulus (E') and tan δ ($= E''/E'$) as a function of temperature. In all the spectra, the storage moduli showed the two loss peaks, associated with the glass transitions of the poly(DMA) and PSt domains in the microphase-separated structure, and the rubbery plateau between the two transition

temperatures. These indicate that the A_xBA_x block-graft copolymers (blue and green lines) also behave as thermoplastic elastomers between the two transitions, where the PSt domains serve as anchor phases, similar to the ABA triblock copolymers (red and black lines). The storage moduli of the plateau in the A_xBA_x block–graft copolymers were higher than those in the corresponding ABA triblocks and became lower as the PSt contents increased. More interestingly, at a lower temperature, the tensile moduli of A_xBA_x (green line; code 4; DMA/St = 82/18) and ABA (red line; code 12; DMA/St = 70/30) were the same, though they had different A/B compositions, and became different at a higher temperature due to the difference in the T_g of the PSt segments. These results most probably resulted from the differences in the morphologies as mentioned above.

Figure 8 shows the stress-strain curves of the A_xBA_x block–graft and the ABA triblock copolymers. As also summarized in Table 2, the mechanical strength and strain at break of all the copolymers were relatively low (1–6 MPa) compared to the commercially available styrene–diene block copolymers,[3] most probably due to the central poly(DMA) blocks which had a high molecular weight between chain entanglements (M_e) [M_e(DMA) = 115,000].[37,38] The stresses at the early stage of the tensile test (Young's modulus) of the A_xBA_x block–graft copolymers (blue and green lines) were apparently dependent on the PSt content and were much higher than those of the corresponding ABA copolymers (red and black lines), which were also ascribed to the differences in the morphologies. The tensile strength and strain at break of the A_xBA_x block–graft copolymers were comparable to those of the corresponding ABA samples. This is contrary to the result for the multigraft copolymers with equally spaced grafting chains prepared by living anionic polymerization, in which the mechanical values increased in proportion to the number of the junction points.[6] Thus, the mechanical properties at break for these DMA/St copolymers are dependent on the comonomer compositions but not on the microphase structures, whereas the dynamic viscoelastic property and Young's modulus were determined by the morphology, as mentioned above. These results suggest that the A_xBA_x block–graft copolymers have specific mechanical properties, which are clearly different from those of the ABA triblocks and equally-spaced graft copolymers. The rheological properties of the A_xBA_x block–graft copolymers are now under investigation.

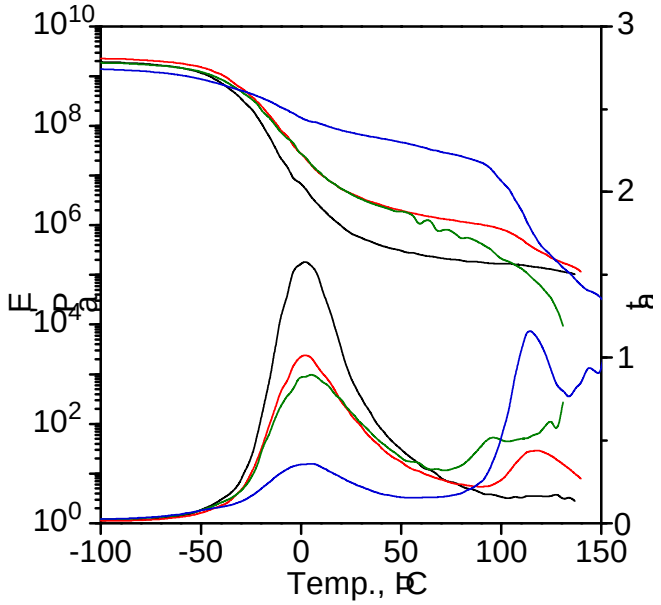

Figure 7. Dynamic tensile storage moduli (E') and tan δ as a function of temperature for the A_xBA_x block–graft copolymers (f = 10.9) [green: M_n(MALLS) = 175,000, M_w/M_n = 1.20, B/A = 82/18; blue: M_n(MALLS) = 202,000, M_w/M_n = 1.22, B/A = 70/30] and the ABA triblock copolymers [black: M_n(MALLS) = 191,000, M_w/M_n = 1.20, B/A = 81/19; red: M_n(MALLS) = 228,000, M_w/M_n = 1.20, B/A = 70/30]. Heating rate: 10 ˚C/min.; frequency: 11 Hz.

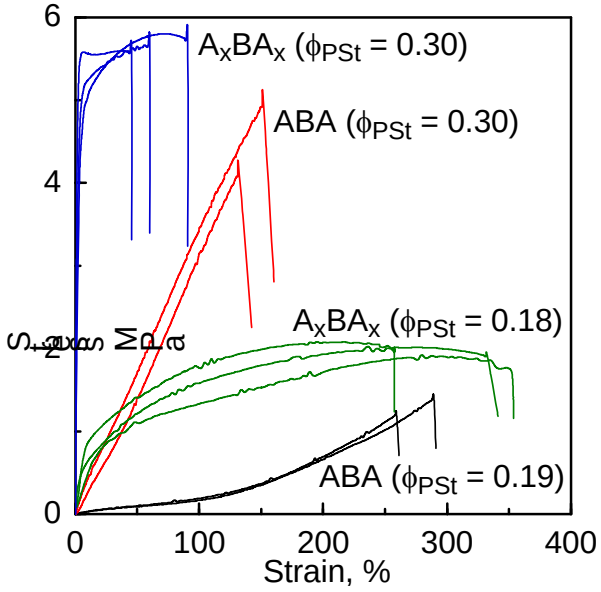

Figure 8. Stress-strain curves of the A_xBA_x block–graft copolymers (f = 10.9) [green: M_n(MALLS) = 175,000, M_w/M_n = 1.20, B/A = 82/18; blue: M_n(MALLS) = 202,000, M_w/M_n = 1.22, B/A = 70/30] and the ABA triblock copolymers [black: M_n(MALLS) = 191,000, M_w/M_n = 1.20, B/A = 81/19; red: M_n(MALLS) = 228,000, M_w/M_n = 1.20, B/A = 70/30].

Table 2. Tensile Properties of A_xBA_x Block–Graft and ABA Triblock Copolymers.

Code[a]	f^b (m+2)	DMA/St, wt/wt[b]	Young's modulus, MPa	100% modulus, MPa	Tensile strength at break, MPa	Elongation at break, %	Morphology[c]
4	10.9	82/18	8.4	1.6	1.8	310	cylinder
7	10.9	70/30	210	-	5.6	66	lamella
11	2	81/19	0.33	0.18	1.3	280	sphere
12	2	70/30	3.5	3.3	4.6	140	cylinder

[a]Code numbers as in Table 1. [b]Determined by ^{1}H NMR. [c]Observed by transmission electron microscopy (TEM).

CONCLUSIONS

Novel well-defined A_xBA_x-type block–graft copolymers were readily prepared by ruthenium-catalyzed living radical block and graft copolymerizations and induced the characteristic nano-ordered microphase separation, which is different from that of the conventional ABA triblock copolymers, to result in different types of TPEs. This study can thus widen the scope of material design based on the well-defined copolymer structures because the morphologies can be controlled by the molecular architecture, i.e, branching numbers, without changing the comonomer compositions, which may affect other properties of the materials.

EXPERIMENTAL SECTION

Materials

Styrene (Wako Chemicals, >98%), DMA (Tokyo Kasei, >99%), and TMSHEMA (Aldrich, >96%) were distilled from calcium hydride under reduced pressure before use. $Ru(Ind)Cl(PPh_3)_2$ and $Ru(Cp^*)Cl(PPh_3)_2$ (both provided from Wako Chemicals) were used as received. All metal compounds were handled in a glove box (VAC Nexus) under a moisture- and oxygen-free argon atmosphere (O_2, <1 ppm). Toluene was distilled over sodium benzophenone ketyl and bubbled with dry nitrogen over 15 minutes just before use. n-Bu_3N (as an additive) and tetralin (as an internal standards for NMR or gas

chromatographic analysis of the monomers) were distilled from calcium hydride before use. 2-Bromoisobutyryl bromide (Aldrich, >98%) and 2,2-dichloroacetophenone (Aldrich, >97%) were distilled before use.

Synthesis of Multifunctional Macroinitiator: Ruthenium-Catalyzed Sequential Living Radical Block Copolymerization of DMA and TMSHEMA and One-Pot Transformation to Macroinitiator

All polymerizations were carried out by syringe technique under dry nitrogen in glass tubes equipped with a three-way stopcock. A typical example for the polymerization of DMA with $CHCl_2(COPh)$/$Ru(Ind)Cl(PPh_3)_2$/*n*-Bu_3N is given below. In a 100 mL round-bottomed flask was placed $Ru(Ind)Cl(PPh_3)_2$ (25.4 mg, 0.032 mmol), toluene (14.3 mL), tetralin (0.5 mL), DMA (46.8 mL, 160 mmol), $CHCl_2(COPh)$ (0.8 mL of 400 mM solution in toluene, 0.320 mmol) and *n*-Bu_3N (1.6 mL of 400 mM solution in toluene, 0.640 mmol) at room temperature. The total volume of reaction mixture was 64.0 mL. The flask was placed in an oil bath kept at 80 ˚C under vigorous stirring. After the monomer conversion reached 91%, the reaction solution was added TMSHEMA (3.2 mL of 1.0 M solution in toluene, 3.20 mmol). In predetermined intervals, the polymerization was terminated by cooling the reaction mixtures to –78 ˚C. Monomer conversion was determined by ^{1}H NMR with tetralin as an internal standard. The quenched reaction solution was then added toluene (20 mL) and 2-bromoisobutyryl bromide (0.8 mL, 6.4 mmol, 2.0 equiv to the trimethylsilyoxyl unit) at room temperature under stirring for 24 h. The reaction mixture was precipitated into acetone and isolated by centrifugation. After three times of the precipitation, the precipitate was diluted with toluene and precipitated into methanol. The procedure was repeated three times. The precipitate was then evaporated to dryness to yield the product, which was subsequently dried overnight in vacuo at room temperature (38.0 g, 93% yield; M_n = 99,000, M_w/M_n = 1.21). The polymer was diluted with distilled toluene and 2.0 M solution was prepared for the following graft copolymerization.

Synthesis of A_xBA_x Block–Graft Copolymers: Ruthenium-Catalyzed Grafting-from Polymerization of St

Graft copolymerizations were also carried out by syringe technique under dry nitrogen in glass tubes equipped with a three-way stopcock. A typical example for the graft

copolymerization of St with the multifunctional macroinitiator I_xBI_x with Ru(Ind)Cl(PPh_3)$_2$/*n*-Bu_3N is given below. In a 50 mL round-bottomed flask was placed macroinitiator I_xBI_x (17.7 mL, 0.381 mmol C-Br bonds), toluene (5.0 mL), tetralin (1.7 mL), St (13.5 mL, 117 mmol), Ru(Ind)Cl(PPh_3)$_2$ (30 mg, 0.038 mmol), and *n*-Bu_3N (0.48 mL of 400 mM solution in toluene, 0.192 mmol) at room temperature. The total volume of reaction mixture was 38.4 mL. The flask was placed in an oil bath kept at 100 ˚C under vigorous stirring. In predetermined intervals, the polymerization was terminated by cooling the reaction mixtures to –78 ˚C. Monomer conversion was determined by gas chromatography with hexane as an internal standard. The quenched reaction solution was precipitated into methanol and isolated by centrifugation. After three times of the precipitation, the precipitate was evaporated to dryness to yield the product, which was subsequently dried overnight in vacuo at room temperature (6.36 g, 94% yield; M_n = 136,000, M_w/M_n = 1.22).

Synthesis of ABA Triblock Copolymers by Ruthenium-Catalyzed Block Copolymerization of St

Block copolymerizations were carried out from the poly(DMA) bifunctional initiator. A typical example for the synthesis of poly(DMA) bifunctional macroinitiator with $CHCl_2$(COPh)/Ru(Ind)Cl(PPh_3)$_2$/*n*-Bu_3N is given below. In a 50 mL round-bottomed flask was placed Ru(Ind)Cl(PPh_3)$_2$ (12.7 mg, 0.017 mmol), toluene (7.0 mL), tetralin (0.6 mL), DMA (23.4 mL, 79.8 mmol), $CHCl_2$(COPh) (0.1 mL of 800 mM solution in toluene, 0.080 mmol) and *n*-Bu_3N (0.80 mL of 400 mM solution in toluene, 0.320 mmol) at room temperature. The total volume of reaction mixture was 32.0 mL. The flask was placed in an oil bath kept at 80 ˚C under vigorous stirring. In predetermined intervals, the polymerization was terminated at ~50% conversion by cooling the reaction mixtures to –78 ˚C. Monomer conversion was determined by ^{1}H NMR with tetralin as an internal standard. The reaction mixture was precipitated into acetone and isolated by centrifugation. After three times of the precipitation, the precipitate was diluted with toluene and precipitated into methanol. The procedure was repeated three times. The precipitate was then evaporated to dryness to yield the product, which was subsequently dried overnight in vacuo at room temperature (12.5 g, 94% yield; M_n = 116,000, M_w/M_n = 1.21). The polymer was diluted with distilled toluene and 2.0 M solution was prepared for the following block

copolymerization. A typical example for the block copolymerization of St on the poly(DMA) bifunctional macroinitiator with $Ru(Cp^*)Cl(PPh_3)_2$/*n*-Bu_3N is given below. In a 50 mL round-bottomed flask was placed poly(DMA) bifunctional macroinitiator (18.2 mL, 0.0702 mmol C-Cl bond), tetralin (0.50 mL), St (6.5 mL, 56.5 mmol), $Ru(Cp^*)Cl(PPh_3)_2$ (89.5 mg, 0.112 mmol), and *n*-Bu_3N (2.81 mL of 400 mM solution in toluene, 1.12 mmol) at room temperature. The total volume of reaction mixture was 28.1 mL. The flask was placed in an oil bath kept at 80 ˚C under vigorous stirring. In predetermined intervals, the polymerization was terminated by cooling the reaction mixtures to –78 ˚C. Monomer conversion was determined by gas chromatography with tetralin as an internal standard. The quenched reaction solution was precipitated into acetone and isolated by centrifugation. After three times of the precipitation, the precipitate was evaporated to dryness to yield the product, which was subsequently dried overnight in vacuo at room temperature (6.65 g, 93% yield; M_n = 214,000, M_w/M_n = 1.20).

Detachment of PSt Graft Chains from the Backbone

The A_xBA_x block–graft copolymers with PSt graft chains (50 mg) was placed in a 25 mL round-bottom flask and dissolved in *N*,*N*-dimethylformamide (7.5 mL). After adding KOH solution (0.3 g dissolved in 2.5 mL of methanol), the mixture was heated to 60 ˚C for 24 h. The solvent was removed by evaporation, and 10.0 mL of $CHCl_3$ was added to the remaining solid. The solution was washed with water (10.0 mL × 3). The organic layer was evaporated to dryness to yield the product, which was subsequently dried overnight in vacuo at room temperature to give 39 mg of the mixture of the backbone polymers and the detached PSt.

Measurements

The ^1H NMR spectra were recorded on a Varian Gemini 2000 spectrometer (400 MHz). The number average molecular weights (M_n) and molecular weight distributions (MWDs: M_w/M_n) of the polymers were measured by size exclusion chromatography (SEC) using THF at a flow rate 1.0 mL/min. at 40 ˚C on two polystyrene gel columns; both Shodex KF-805L, that were connected to a JASCO PU-980 precision pump and a JASCO RI-930 detector. The molecular weight was calibrated against seven standard poly(methyl methacrylate) samples (M_n = 1,990 – 6,590,000) or eight standard polystyrene samples (M_n =

526 – 900,000). The monomer conversions were determined from the concentration of the residual monomer measured by gas chromatography using tetralin as the internal standard. The absolute weight-average molecular weight (M_w) of the polymers was determined by multiangle laser light scattering in tetrahydrofuran (THF) at 40 ˚C on a Wyatt Technology DAWN DSP photometer (λ = 633 nm). The refractive index increment (d*n*/d*c*) was measured in THF at 25 ˚C on a Wyatt Optilab rEX refractmeter (λ = 633 nm), the d*n*/d*c* values were 0.072–0.160 mL/g for the A_xBA_x block-graft copolymers. Glass transition temperature (T_g) of the polymer was recorded on SSC-5200 differential scanning calorimetry (Seiko Instruments Inc.). Samples were first heated to 150 °C at 10 °C/min., equilibrated at this temperature for 5 min, and cooled to –120 °C at 5 °C/min. After being held at this temperature for 20 min, the samples were then reheated to 150 °C at 10 °C/min. All T_g values were obtained from the second scan, after removing the thermal history. Sample films for dynamic tensile viscoelasticity was prepared by hot-press molding of the copolymers at 230 °C. Dynamic tensile storage (*E'*) and loss (*E"*) moduli and tan δ (= *E"*/*E'*) were measured on a UBM Rheogel-E4000 spectrometer, operating at 11 Hz frequency (heating rate: 10 °C/min). For transmission electron microscopy (TEM), a film specimen was prepared by casting from 5 wt% toluene solution for 2 weeks. The cast film was annealed at 140 ˚C for 24 h under vacuum, which was subsequently stained by exposing the film to ruthenium tetraoxide (RuO_4) vapor for 2 min. The stained film thus obtained was cryomicrotomed with a diamond knife at –120 ˚C using a Lica Ultracut UCT. The ultrathin section of ca. 100 nm was transferred onto a Cu mesh grid with a polyvinylformal substrate. TEM and transmission electron microtomography (TEMT) experiments were performed using an energy-filtering transmission electron microscope with a field-emission gun operated at 200 kV (JEM-2200FS JEOL Co., Ltd., Japan).[31a] The tensile properties (Young's modulus, tensile strength at break, and elongation at break) were measured on compression-molded dogbone specimens (width: ca. 4.0 mm, thickness: ca. 0.6–0.7 mm) using an Instron Universal Testing Machine 5566 at a crosshead speed of 200 mm/min at 23 °C. At least two specimens per sample were tested.

REFERENCES

(1) (a) Riess, G.; Hurtrez, G.; Bahadur, P.; In *Block copolymers*, *2nd ed*.: *Encyclopedia of*

polymer science and engineering; New York, Wiley; 1985; vol. 2, pp 324–434. (b) Bates, F. S.; Fredrickson, G. H. *Annu. Rev. Phys. Chem.* **1990**, *41*, 525–557. (c) Bates, F. S.; Fredrickson, G. H. *Phys. Today* **1999**, *52*, 32–38. (d) Avetz, V.; Simon, P. F. W. *Adv. Polym. Sci.* **2005**, *189*, 125–212.

(2) (a) *Block Copolymers in Nanoscience*, Lazzari, M.; Liu, G.; Lecommandoux, S. Eds.; Wiley-VCH, Weinheim, Germany, 2006. (b) Hawker, C. J.; Wooley, K. *Science* **2005**, *309*, 1200–1205. (c) Hawker, C. J.; Russell, T. P.; *MRS Bulletin* **2005**, *30*, 952–967. (d) Naito, K.; Hieda, H.; Sakurai, M.; Kamata, Y.; Asakawa, K. *IEEE Trans. Magn.* **2002**, *38*, 1949–1951.

(3) Holden, G.; Kricheldorf, H. R.; Quirk, R. P.; *Thermoplastic Elastomers*, 3rd ed.; Hanser Publishers: Munich, 2004.

(4) (a) Morton, M. *Anionic Polymerization*: *Principles and Practice*; Academic Press: New York, 1983; pp 221–232. (b) Kennedy, J. P.; Ivan, B.; *Designed Polymers by Carbocationic Macromolecular Engineering*: *Theory and Practice*; Hanser Publishers: Munich, 1992; p 96. (c) M. Sawamoto, M.; Kamigaito, In *New Methods of Polymer Synthesis*; Ebdon, J. R.; Eastmond, G. C. Eds.; Blackie: Glasgow, U.K., 1995; Vol. 2, pp 37–68.

(5) (a) Xenidou, M.; Beyer, F. L.; Hadjichristidis, N.; Gido, S. P.; Tan, N. B. *Macromolecules* **1998**, *31*, 7959–7667. (b) Beyer, F. L.; Gido, S. P.; Büschl, C.; Iatrou, H.; Uhrig, D.; Mays, J. W.; Chang, M. Y.; Garetz, B. A.; Balsara, N. P.; Tan, N. B.; Hadjichristidis, N. *Macromolecules* **2000**, *33*, 2039–2048.

(6) (a) Weidisch, R.; Gido, S. P.; Uhrig, D.; Iatrou, H.; Mays, J. W.; Hadjichristidis, N. *Macromolecules* **2001**, *34*, 6333–6337. (b) Zhu, Y.; Weidisch, R.; Gido, S. P.; Veils, G.; Hadjichristidis, N. *Macromolecules* **2002**, *35*, 5903–5909. (c) Uhrig, D.; Mays, J. W. *Macromolecules* **2002**, *35*, 7182–7190. (d) Zhu, Y.; Burgaz, E.; Gido, S. P.; Staudinger, U.; Weidisch, R.; Uhrig, D.; Mays, J. *Macromolecules* **2006**, *39*, 4428–4436.

(7) (a) Pochan, D. J.; Gido, S. P.; Pispas, S.; Mays, J. W.; Ryan, A. J.; Fairclough, J. P. A.; Hamley, I. W.; Terrill, N. J. *Macromolecules* **1996**, *29*, 5091–5098. (b) Tselikas, Y.; Iatrou, H.; Hadjichristidis, N.; Liang, K. S.; Mohanty, K.; Lohse, D. J. *J. Chem. Phys.* **1996**, *105*, 2456–2462. (c) Beyer, F. L.; Gido, S. P.; Veils, G.; Hadjichristidis, N.; Tan, N. B. *Macromolecules* **1999**, *32*, 6604–6607. (d) Yang, L.; Hong, S.; Gido, S. P.; Veils, G.; Hadjichristidis, N. *Macromolecules* **2001**, *34*, 9069–9073.

(8) (a) Mavroudis, A.; Avgeropoulos, A.; Hadjichristidis, N.; Thomas, E. L.; Lohse, D. J. *Chem*. *Mater*. **2003**, *15*, 1976–1983. (b) Mavroudis, A.; Avgeropoulos, A.; Hadjichristidis, N.; Thomas, E. L.; Lohse, D. J. **2006**, *18*, 2164–2168.

(9) (a) Matsushita, Y.; Watanabe, J.; Katano, F.; Yoshida, Y.; Noda, I. *Polymer*, **1996**, *2*, 321–325. (b) Matsushita, Y. *J*. *Polym*. *Sci*., *Part B*: *Polym*. *Phys*. **2000**, *38*, 1645–1655.

(10) (a) Gido, S. P.; Lee, C.; Pochan, D. J.; Pispas, S.; Mays, J. W.; Hadjichristidis, N. *Macromolecules* **1996**, *29*, 7022–7028. (b) Lee, C.; Gido, S. P.; Poulos, Y.; Hadjichristidis, N.; Tan, N. B.; Trevino, S. F.; Mays, J. W. *J*. *Chem*. *Phys*. **1997**, *107*, 6460–6469.

(11) For synthesis, see: (a) Houli, S.; Iatrou, H.; Hadjichristidis, N.; Vlassopoulos, D. *Macromolecules* **2002**, *35*, 6592–6597. (b) Knauss, D. M.; Huang, T. *Macromolecules* **2002**, *35*, 2055–2062. (c) Huang, T.; Knauss, D. M. *Polym*. *Bull*. **2002**, *49*, 143–150. (d) Huang, T.; Knauss, D. M. *Macromol*. *Symp*. **2004**, *215*, 81–93. (e) Lai, M.-K.; Wang, J.-Y.; Tsiang, R. C.-C. *Polymer* **2005**, *46*, 2558–2566.

(12) (a) Georges, M. K.; Veregin, R. P. N.; Kazmaier, P. M.; Hamer, G. K. *Macromolecules* **1993**, *26*, 2987–2988. (b) Georges, M. K.; Veregin, R. P. N.; Kazmaier, P. M.; Hamer, G. K. *Trends*. *Polym*. *Sci*. **1994**, *2*, 66–72.

(13) (a) Hawker, C. J. *J*. *Am*. *Chem*. *Soc*. **1994**, *116*, 11185–11186. (b) Hawker, C. J.; Bosman, A. W.; Harth, E. *Chem*. *Rev*. **2001**, *101*, 3661–3688.

(14) (a) Kato, M.; Kamigaito, M.; Sawamoto, M.; Higashimura, T. *Macromolecules* **1995**, *28*, 1721–1723. (b) Kamigaito, M.; Ando, T.; Sawamoto, M. *Chem*. *Rev*. **2001**, *101*, 3689–3745. (c) Kamigaito, M.; Ando, T.; Sawamoto, M. *Chem*. *Rec*. **2004**, *4*, 159–175.

(15) (a) Wang, J.-S.; Matyjaszewski, K. *J*. *Am*. *Chem*. *Soc*. **1995**, *117*, 5614–5615. (b) Matyjaszewski, K.; Xia, J. *Chem*. *Rev*. **2001**, *101*, 2921–2990.

(16) (a) Chiefari, J.; Chong, Y. K.; Ercole, F.; Krstina, J. Jeffery, K.; Tam, P. T. Le.; Mayadunne, R. T. A.; Meijs, G. F.; Moad, C. L.; Moad, G.; Rizzardo, E.; Thang, S. H. *Macromolecules* **1998**, *31*, 5559–5562. (b) Moad, G.; Rizzardo, E.; Thang, S. H. *Aust*. *J*. *Chem*. **2005**, *58*, 379–410.

(17) Destarac, M.; Bzducha, W.; Taton, D.; Gauthier-Gillaizeau, I.; Zard, S. Z. *Macromol*. *Rapid Commun*. **2002**, *23*, 1049–1054.

(18) For reviews, see: (a) Davis, K. A.; Matyjaszewski, K. *Adv*. *Polym*. *Sci*. **2002**, *159*, 107–152. (b) Börner, H.; Matyjaszewski, K. *Macromol*. *Symp*. **2002**, *177*, 1–15. (c)

Bhattacharya, A.; Misra, B. N. *Prog*. *Polym*. *Sci*. **2004**, *29*, 767–814.

(19) (a) Beers, K. L.; Gaynor, S. G.; Matyjaszewski, K.; Sheiko, S. S.; Möller, M. *Macromolecules* **1998**, *31*, 9413–9415. (b) Börner, H. G.; Beers, K. L.; Matyjaszewski, K.; Sheiko, S. S.; Möller, M. *Macromolecules* **2001**, *34*, 4375–4383. (c) Börner, H. G.; Duran, D.; Matyjaszewski, K.; da Silva, M.; Sheiko, S. S. *Macromolecules* **2002**, *35*, 3387–3394. (d) Qin, S.; Matyjaszewski, K.; Xu, H.; Sheiko, S. S. *Macromolecules* **2003**, *36*, 605–612. (e) Lord, S. J.; Sheiko, S. S.; LaRue, I.; Lee, H.-I.; Matyjaszewski, K. *Macromolecules* **2004**, *37*, 4235–4240. (f) Lee, H.; Matyjaszewski, K.; Yu, S.; Sheiko, S. S. *Macromolecules* **2005**, *38*, 8264–8271.

(20) (a) Cheng, G.; Böker, A.; Zhang, M.; Krausch, G.; Müller, A. H. E. *Macromolecules* **2001**, *34*, 6883–6888. (b) Mori, H.; Müller, A. H. E. Müller, *Prog*. *Polym*. *Sci*. **2003**, *28*, 1403–1439. (c) Cai, Y.; Hartenstein, M.; Müller, A. H. E. *Macromolecules* **2004**, *37*, 7484–7490.

(21) Chapter 2 of this thesis, *Polym*. *J*. **2006**, *38*, 930–939.

(22) For synthesis of macrocyclic graft copolymer, see: Jia, Z.; Fu, Q.; Huang, J. *Macromolecules* **2006**, *39*, 5190–5193.

(23) (a) Ruckenstein, E.; Zhang, H. *Macromolecules* **1998**, *31*, 2977–2982. (b) Zhang, H.; Ruckenstein, E. **1998**, *31*, 4753–4759.

(24) Lecolley, F.; Waterson, C.; Carmichael, A. J.; Mantovani, G.; Harrisson, S.; Chappell, H.; Limer, A.; Williams, P.; Ohno, K.; Haddleton, D. M. *J*. *Mater*. *Chem*., **2003**, *13*, 2689–2695.

(25) Ohno, S.; Matyjaszewski, K. *J*. *Polym*. *Sci*., *Part A*: *Polym*. *Chem*. **2006**, *44*, 5454–5467.

(26) (a) Pan, Q.; Liu, S.; Xie, J.; Jiang, M. *Polym*. *Sci*., *Part A*: *Polym*. *Chem*. **1999**, *37*, 2699–2702. (b) Ning, F.; Jiang, M.; Mu, M.; Duan, H.; Xie, J. *J*. *Polym*. *Sci*., *Part A*: *Polym*. *Chem*. **2002**, *40*, 1253–1266.

(27) (a) Truelsen, J. H.; Kops, J.; Batsberg, W. *Macromol*. *Rapid Commun*. **2000**, *21*, 98–102. (b) Truelsen, J. H.; Kops, J.; Batsberg, W.; Armes, S. P. *Macromol*. *Chem*. *Phys*. **2002**, *203*, 2124–2131. (c) Truelsen, J. H.; Kops, J.; Batsberg, W.; Armes, S. P. *Polym*. *Bull*. **2002**, *49*, 235–242.

(28) (a) Li, Y. G.; Shi, P. J.; Pan, C. Y. *Macromolecules* **2004**, *37*, 5190–5195. (b) Cong, Y.; Li, B. Y.; Han, Y. C.; Li, Y. G.; Pan, C. Y. *Macromolecules* **2005**, *38*, 9836–9846.

(29) Pakula, T.; Zhang, Y.; Matyjaszewski, K.; Lee, H.; Börner, H.; Qin, S.; Berry, G. C.

Polymer **2006**, *47*, 7198–7206.

(30) Chapter 3 of this thesis, *Macromolecules*, *in press*.

(31) (a) Jinnai, H.; Nishikawa, Y.; Ikehara, T.; Nishi, T. *Adv*. *Polym*. *Sci*. **2004**, *170*, 115–167. (b) Kawase, N.; Kato, M.; Nishioka, H.; Jinnai, H. *Ultramicroscopy* **2007**, *107*, 8–15. (c) Nishioka, H.; Niihara, K.; Kaneko, T.; Yamanaka, J.; Nishikawa, Y.; Inoue, T.; Nishi, T.; Jinnai, H. *Compos*. *Interfac*. **2006**, *13*, 589–603. (d) Sugimori, H.; Nishi, T.; Jinnai, H. *Macromolecules* **2005**, *38*, 10226–10233. (e) Kaneko, T.; Nishioka, H.; Nishikawa, Y.; Nishi, T.; Jinnai, H. *J*. *Electron*. *Micros*. **2005**, 54, 437–444.

(32) (a) Kaneko, T.; Suda, K.; Satoh, K.; Kamigaito, M.; Kato, T.; Ono, T.; Nakamura, E.; Nishi, T.; Jinnai, H. *Macromol*. *Symp*. **2006**, *242*, 80–86. (b) Jinnai, H.; Kaneko, T.; Nishioka, H.; Hasegawa, H.; Nishi, T. *Chem*. *Rec*., **2006** *6*, 267–274. (c) Jinnai, H.; Hasegawa, H.; Nishikawa, Y.; Sevink, G. J. A.; Braunfeld, M. B.; Agard, D. A.; Spontak, R. J. *Macromol*. *Rapid Commun*., **2006** *27*, 1424–1429. (d) Jinnai, H.; Sawa, K.; Nishi, T. *Macromolecules*, **2006** *39*, 5815–5819.

(33) Milner, S. T. *Macromolecules* **1994**, *27*, 2333–2335.

(34) Gido, S. P.; Schwark, D. W.; Thomas, E. L.; Gonçalves, M. C. *Macromolecules* **1993**, *26*, 2636–2640.

(35) Hückstädt, H.; Göpfert, A.; Abetz, V. *Macromol*. *Chem*. *Phys*. **2000**, *201*, 296–307.

(36) Takahashi, K.; Hasegawa, H.; Hashimoto, T.; Bellas, V.; Iatrou, H.; Hadjichristidis, N. *Macromolecules* **2002**, *35*, 4859–4861.

(37) Fetters, L. J.; Lohse, D. J.; Grassley, W. W. *J*. *Polym*. *Sci*., *Part B*: *Polym*. *Phys*. **1999**, *37*, 1023–1033.

(38) Tong, J.-D.; Jérôme, R. *Macromolecules* **2000**, 33, 1479–1481.

CHAPTER 5

STEREPGRADIENT POLYMERS BY RUTHENIUM-CATALYZED STEREOSPECIFIC LIVING RADICAL COPOLYMERIZATION OF TWO MONOMERS WITH DIFFERENT STEREOSPECIFITIES AND REACTIVITIES: MULTIPLE CONTROL OF CHAIN LENGTH AND STEREOCHEMISTRY

ABSTRACT

Stereogradient polymers, a fundamentally new type of polymers, were prepared by the stereospecific living radical copolymerization of two monomers that have different stereospecificities and reactivities. The ruthenium-catalyzed living radical copolymerization of 2-hydroxyethyl methacrylate (HEMA) and the silyl-capped HEMA [(*tert*-butyldimethylsilyl)-HEMA] (SiHEMA) in $(CF_3)_2C(Ph)OH$ afforded stereogradient poly(HEMA), in which the *rr* content gradually increased from 62 to 77% at 0 °C, due to the lower reactivity and the higher syndiospecificity of SiHEMA.

INTRODUCTION

Recently, the development of various living polymerizations has enabled the synthesis of a wide variety of well-defined polymers, including not only end-functionalized, block, graft, and star polymers but also more complex polymers built up by a combination of these architectures.[1] Living radical polymerization is one of the most suitable methods for this purpose in terms of the vast availability of monomers, tolerance to polar functional groups, and easy access to complex architectures.[2] Another recent significant development in precision polymer synthesis has been observed in stereospecific polymerizations, which can drastically alter the thermal and mechanical properties of the resulting polymers depending on the microstructure.[3] Although most of the stereospecific polymerizations were reported for the coordination polymerizations of olefins such as propylene, the stereocontrol during radical polymerizations has recently become possible.[4] Furthermore, a combination of living and stereospecific radical polymerizations permitted not only the simultaneous control of the molecular weight and the tacticity but also the synthesis of stereoblock polymers, in which segments with different tacticities are connected together.[5]

Gradient copolymers are a new class of polymers, in which the instantaneous composition continuously varies along each chain, and were recently prepared by living radical copolymerization.[6] This copolymer has a unique feature different from traditional block and random copolymers due to the continuous change in the composition from one end of the chain to the other and is expected as a new type of functional copolymer, in which the properties gradually change along the main chain.[6,7]

This study is directed toward the synthesis of stereogradient polymers by the stereospecific living radical copolymerization of two monomers that have different stereospecificities and reactivities. Stereogradient polymers can be defined as the polymers in which the tacticity continuously varies along the chain and have never been synthesized except for a few examples.[8,9] Although a quite recent study of the living degenerative-transfer Ziegler–Natta polymerizations revealed the first example of stereogradient poly(propylene),[9] the synthetic methods for stereogradient polymers have not been well established. The author now reports the first synthesis of stereogradient polymers of 2-hydroxyethyl methacrylate (HEMA), the polymers of which are utilized as

functional biocompatible materials,[10] via the ruthenium-catalyzed stereospecific living radical copolymerizations of HEMA[11] and the silyl-capped HEMA

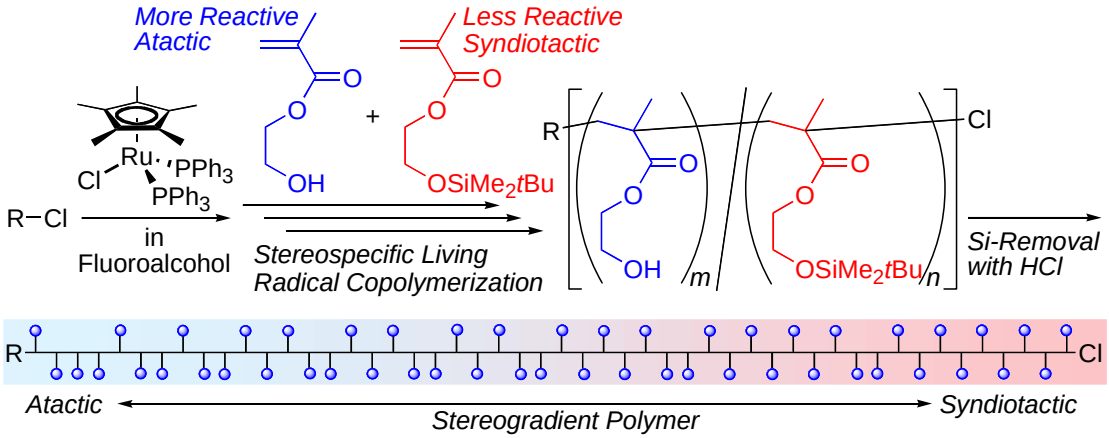

Scheme 1. Stereogradient Polymers by Ru-Catalyzed Living Radical Copolymerization of HEMA and SiHEMA.

[(*tert*-butyldimethylsilyl)-HEMA (SiHEMA)] in a fluoroalcohol (Scheme 1).

RESULTS AND DISCUSSION

Prior to the copolymerizations, preliminary experiments involving the

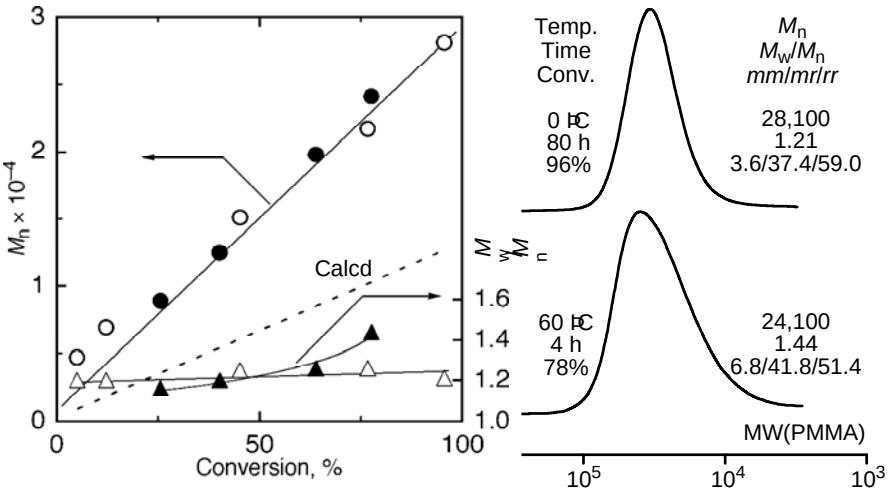

Figure 1. M_n, M_w/M_n, and size-exclusion chromatograms of poly(HEMA) obtained with H–(MMA)$_2$–Cl/Ru(Cp*)Cl(PPh$_3$)$_2$/*n*-Bu$_3$N in (CF$_3$)$_2$C(Ph)OH at 0 ˚C (○, △) and 60 ˚C (●, ▲). [HEMA]$_0$ = 1.0 M; [H–(MMA)$_2$–Cl]$_0$ = 10 mM; [Ru(Cp*)Cl(PPh$_3$)$_2$]$_0$ = 4.0 mM; [*n*-Bu$_3$N]$_0$ = 40 mM. The diagonal dotted line represents the calculated M_n values, assuming each H–(MMA)$_2$–Cl molecule generates one living polymer.

homopolymerizations of each monomer by the ruthenium-based systems [H–$(MMA)_2$–Cl/Ru Cp*$Cl(PPh_3)_2$/*n*-Bu_3N] gave the living polymers with controlled molecular weights and narrow molecular weight distributions (MWDs) even in $(CF_3)_2C(Ph)OH$ at 0 and 60 °C (Figures 1 and 2). However, the tacticity depended on the two monomers; HEMA was polymerized to give less syndiotactic or more or less atactic polymers [*rr* = 59.0% (0 °C) and 51.4% (60 °C)],[12] while SiHEMA resulted in syndiotactic-rich polymer [*rr* = 77.2%

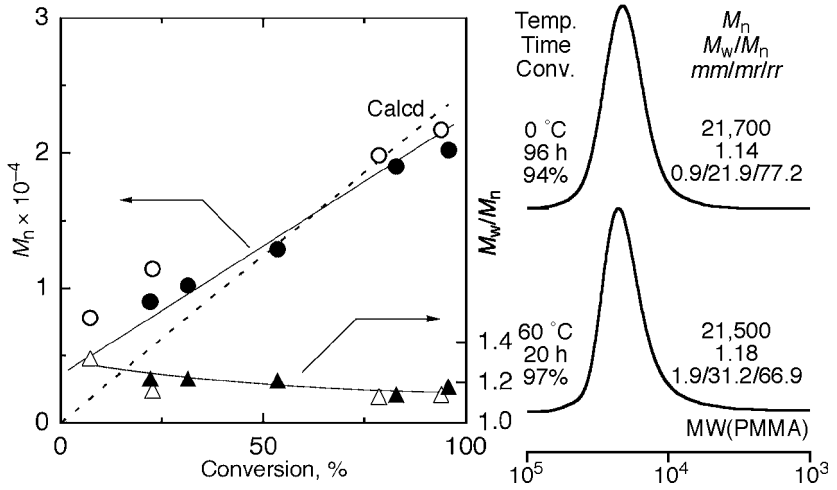

Figure 2. M_n, M_w/M_n, and size-exclusion chromatograms of poly(SiHEMA) obtained with H–$(MMA)_2$–Cl/Ru$(Cp^*)Cl(PPh_3)_2$/*n*-Bu_3N in $(CF_3)_2C(Ph)OH$ at 0 ˚C (○, △) and 60 ˚C (●, ▲). $[SiHEMA]_0$ = 1.0 M; $[H–(MMA)_2–Cl]_0$ = 10 mM; $[Ru(Cp^*)Cl(PPh_3)_2]_0$ = 4.0 mM; $[n\text{-}Bu_3N]_0$ = 40 mM. The diagonal dotted line represents the calculated M_n values, assuming each H–$(MMA)_2$–Cl molecule generates one living polymer.

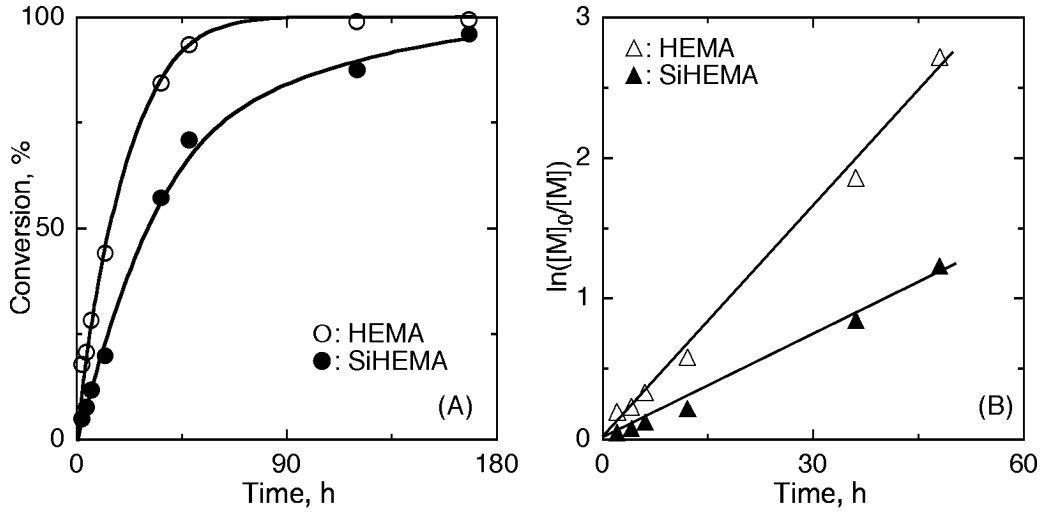

Figure 3. Kinetic plots for the ruthenium-catalyzed copolymerization of HEMA and SiHEMA (0.50/0.50 M) with H–$(MMA)_2$–Cl/RuCp*$Cl(PPh_3)_2$/*n*-Bu_3N (10/4.0/40 mM) in $(CF_3)_2C(Ph)OH$ at 0 ˚C.

(0 °C) and 66.9% (60 °C)]. This is due to the remarkable solvent effects of such a bulky fluoroalcohol on the radical polymerizations of alkyl methacrylates and HEMA.

The two monomers were then copolymerized with the ruthenium-based systems in the fluoroalcohol at 0 and 60 °C. The two monomers were consumed at different rates, but simultaneously, in which HEMA was polymerized faster than SiHEMA (Figure 3A). The reactivities obtained from the initial slopes of the first-order plots were about 2.2 times greater for HEMA than for SiHEMA at 0 °C (Figure 3B).

Figure 4 shows the number-average molecular weights (M_n), MWDs, and size-exclusion chromatograms (SEC) of the obtained copolymers. In both cases, the M_n increased in direct proportion to the monomer conversion and agreed well with the calculated values assuming that one molecule of the initiator generates one living polymer chain though the M_n values were based on the PMMA calibration. The SEC curves shifted to high molecular weights with conversion while maintaining narrow MWDs during the polymerizations. Thus, the ruthenium-based system gave the living copolymers from

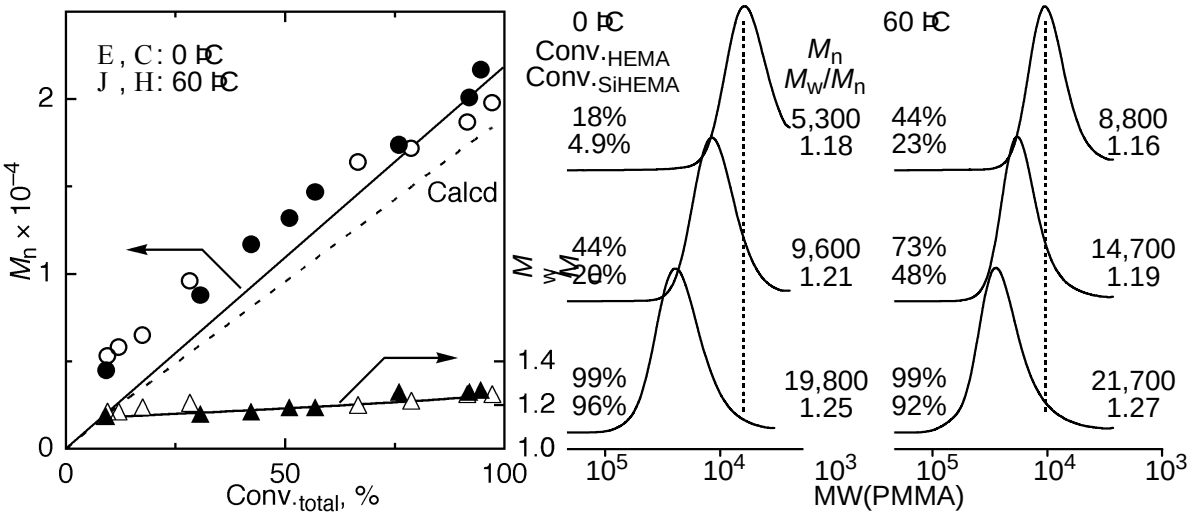

Figure 4. Ruthenium-catalyzed living radical copolymerization of HEMA and SiHEMA (0.50/0.50 M) with H–(MMA)$_2$–Cl/RuCp*Cl(PPh$_3$)$_2$/*n*-Bu$_3$N (10/4.0/40 mM) in (CF$_3$)$_2$C(Ph)OH at 0 and 60 ˚C.

the two monomers in (CF$_3$)$_2$C(Ph)OH.

The copolymers were then converted into poly(HEMA) by the acid hydrolysis of the silyl groups. The quantitative transformation of the silyl groups into hydroxyl groups was confirmed by ^{1}H NMR spectroscopy (Figure 5). The poly(HEMA)s thus obtained were analyzed by ^{13}C NMR spectroscopy to determine the tacticity of poly(HEMA) (Figure

6 and Table 1).

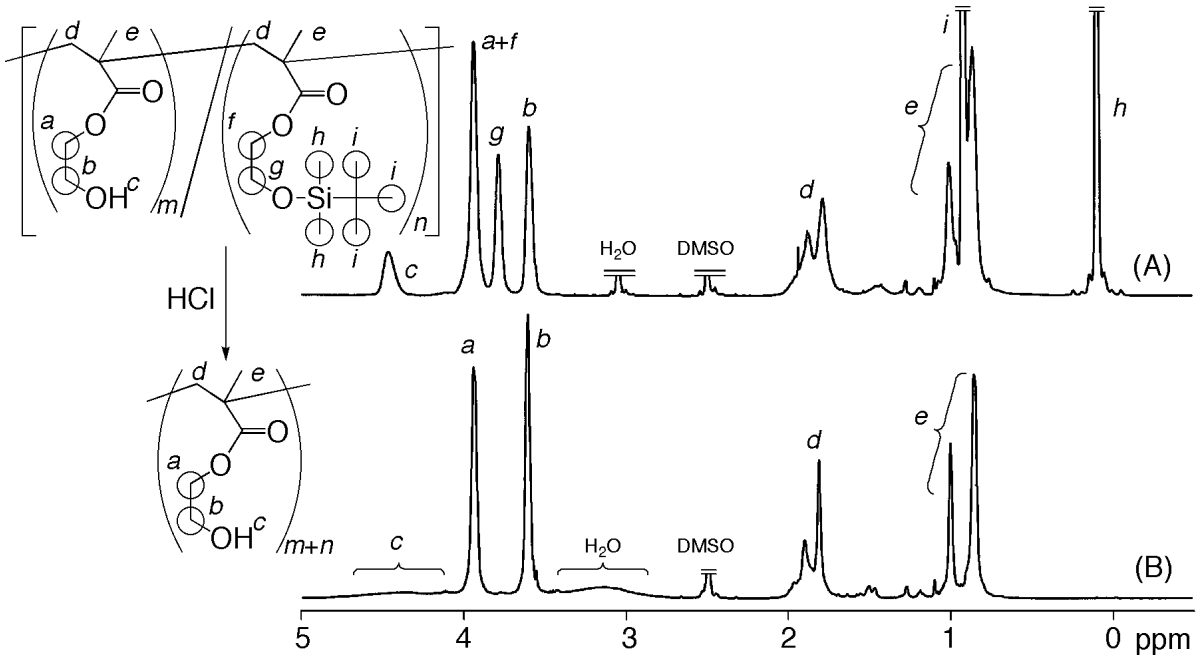

Figure 5. ^{1}H NMR Spectra (400 MHz, DMSO–d_6, 80 °C) of copoly(HEMA-*grad*-SiHEMA) (A; code 5 in Table 1) and the stereogradient poly(HEMA) after the hydrolysis of *tert*-butyldimethylsilyl group (B).

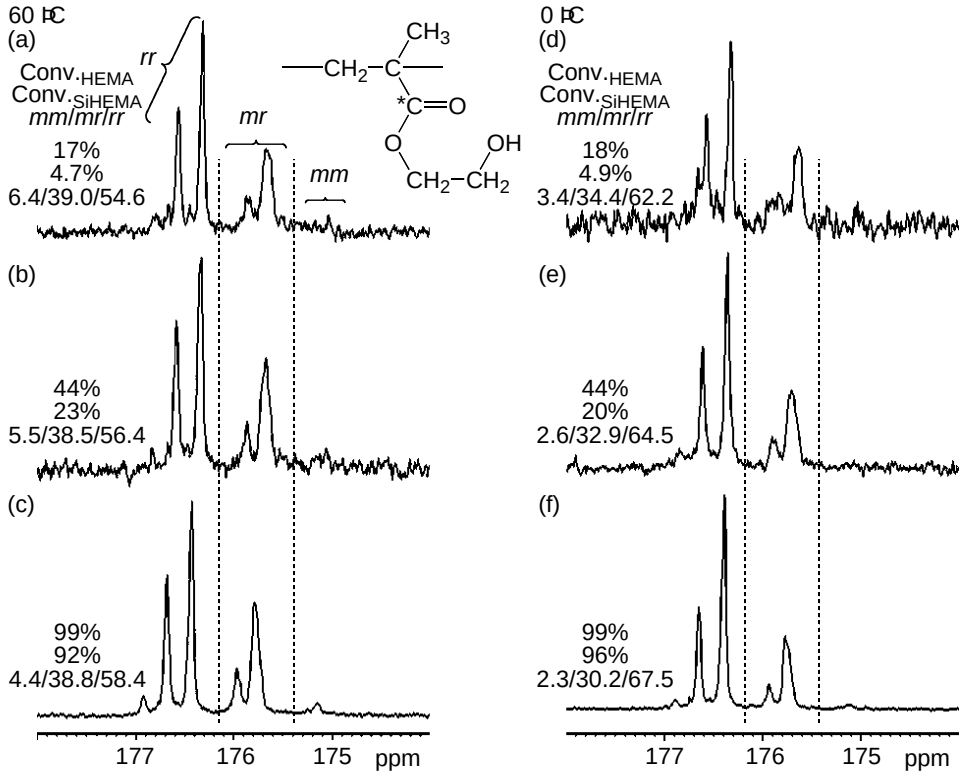

Figure 6. ^{13}C NMR spectra (100 MHz, DMSO–d_6, 80 °C) of the stereogradient poly(HEMA) obtained after the hydrolysis of copoly(HEMA-*grad*-SiHEMA) with H–(MMA)$_2$–Cl/Ru(Cp*)Cl(PPh$_3$)$_2$/*n*-Bu$_3$N in (CF$_3$)$_2$C(Ph)OH at 60 ˚C [(a)–(c)] or 0 ˚C [(d)–(f)].

Table 1. Ru-catayzed Stereospecific Living Radical Copolymerization of HEMA and SiHEMA in $(CF_3)_2C(Ph)OH$ at 0 and 60 °C

Code, *i*	Temp. (˚C)	Time (h)	$Conv._{b\text{-HEMA}}$ (%)	$Conv._{b\text{-SiEMA}}$ (%)	$Conv._{c\text{-total}}$ (%)	M_n [d]	M_w/M_n [d]	$F_{cum,\ SiHEMA}$ [e] (%)	rr_{cum} [f] (%)
1	0	2	18	4.9	12	5,300	1.17	21	62.2
2	0	12	44	20	32	9,600	1.21	31	64.5
3	0	36	84	57	71	16,400	1.20	40	66.0
4	0	120	99	88	94	18,700	1.25	47	67.4
5	0	168	99	96	98	19,800	1.25	48	67.5
1’	60	0.1	17	4.7	11	4,500	1.15	22	54.6
2’	60	0.25	44	23	34	8,800	1.16	34	56.4
3’	60	1	73	48	61	14,700	1.19	40	57.4
4’	60	12	99	88	94	20,100	1.26	47	58.3
5’	60	20	99	92	96	21,700	1.27	48	58.4

[a]Polymerization conditions: $[HEMA]_0/[SiHEMA]_0/[H–(MMA)_2–Cl]_0/[Ru(Cp^*)Cl(PPh_3)_2]_0/[n\text{-}Bu_3N]_0$ = 500/500/10/4.0/40 mM in $(CF_3)_2C(Ph)OH$. [b]Determined by ^1H NMR with tetralin as an internal standard in $CDCl_3$ at r.t. [c]$Conv._{\text{-total}} = (Conv._{\text{-HEMA}} + Conv._{\text{-SiHEMA}})/2$. [d]Determined by size-exclusion chromatography in DMF containing 100 mM LiCl at 40 °C. [e]$F_{cum,\ SiHEMA} = Conv._{\text{-SiHEMA}}/(Conv._{\text{-HEMA}} + Conv._{\text{-SiHEMA}})$. [f]Determined by ^{13}C NMR in DMSO–d_6 at 80 ˚C after the hydrolysis of the silyl groups in the SiHEMA units.

Figure 7A is a plot of the original SiHEMA ($F_{cum,\ SiHEMA}$) contents[6] and the *rr* (rr_{cum}) of the resulting poly(HEMA) versus the total conversion of the two monomers. These contents are for the cumulative values of the whole chains obtained at each conversion. As the conversions increased, the syndiotacticity was enhanced at both temperatures along with

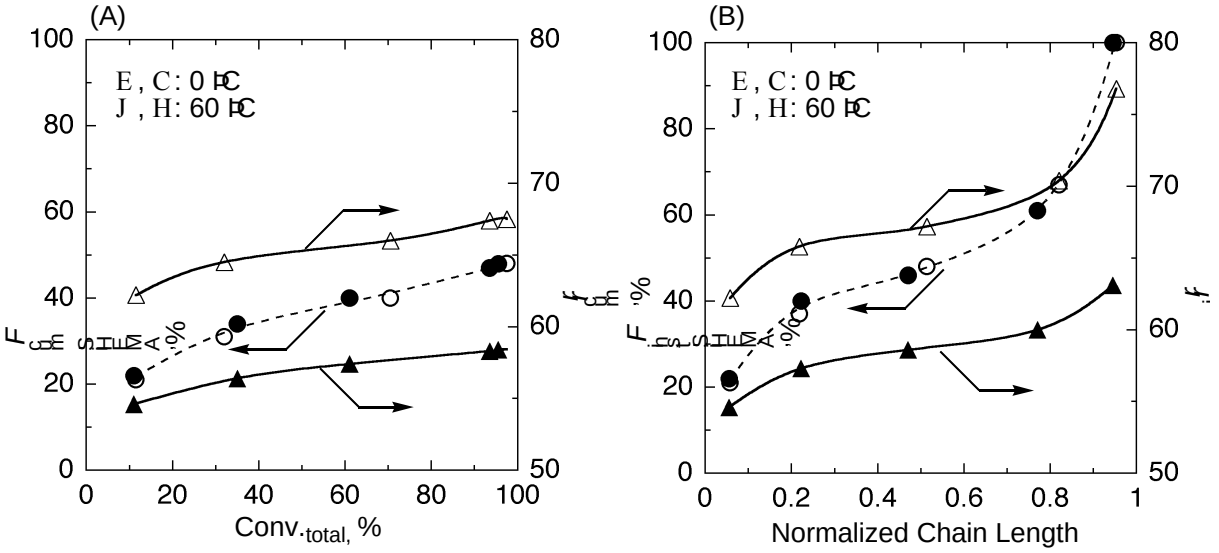

Figure 7. Dependences of SiHEMA and *rr* contents on the total conversion of monomers (A) and the normalized chain length (B) in the ruthenium-catalyzed living radical copolymerization of HEMA and SiHEMA in $(CF_3)_2C(Ph)OH$ at 0 and 60 ˚C.

an increase in the original SiHEMA content. This is due to the fact that SiHEMA, which has a lower reactivity than HEMA, shows a higher syndiospecificity at both temperatures. Therefore, a gradual increase in the syndiotacticity was observed with the increasing conversions.

Figure 7B shows the instantaneous composition of SiHEMA ($F_{inst,\ SiHEMA}$)[6] and *rr* content (rr_{inst}) plotted versus the normalized chain length of the polymers. Herein, $F_{inst,\ SiHEMA}$ and rr_{inst} are for each part that propagates during each sampling interval. The normalized chain length can then be obtained by the total conversion of the monomers, assuming the full chain length as that obtained at the complete conversions. Table 2 summarizes these data for the polymers with different conversions. The $F_{inst,\ SiHEMA}$ and rr_{inst} were plotted versus the intermediate conversions for each sampling. The rr_{inst} values gradually increased along the normalized chain length similar to $F_{inst,\ SiHEMA}$. These sigmoid curves clearly indicate the gradient nature of the two parameters. Especially for the syndiotacticity, the *rr* content gradually increased from 62.2 to 76.8% at 0 °C and from 54.6 to 63.1% at 60 °C. These results indicate the spontaneous formation of the stereogradient polymers by the stereospecific living radical copolymerizations of the two monomers without using a gradual monomer-addition technique. Furthermore, linear relationships were observed between rr_{inst} and $F_{inst,\ SiHEMA}$, in which the linear plots passed through the *rr* values for the homopolymers

Table 2. Normalized Chain Length, $F_{inst,\ SiHEMA}$, and rr_{inst} for Ru-catalyzed Stereospecific Living Radical Copolymerization of HEMA and SiHEMA in $(CF_3)_2C(Ph)OH$[a]

Code, (*i*–1)–*i*	Temp. (˚C)	Normalized Chain Length[b]	$F_{inst,\ SiHEMA}$ (%)[c]	rr_{inst} (%)[d]
0–1	0	0.058	21	62.2
1–2	0	0.22	37	65.8
2–3	0	0.51	48	67.2
3–4	0	0.82	67	70.4
4–5	0	0.95	100	76.8
0'–1'	60	0.056	22	54.6
1'–2'	60	0.22	40	57.3
2'–3'	60	0.47	46	58.6
3'–4'	60	0.77	61	60.0
4'–5'	60	0.95	100	63.1

[a]Polymerization conditions: $[HEMA]_0/[SiHEMA]_0/[H–(MMA)_2–Cl]_0/[Ru(Cp^*)Cl(PPh_3)_2]_0/[n\text{-}Bu_3N]_0$ = 500/500/10/4.0/40 mM in $(CF_3)_2C(Ph)OH$. [b]Normalized Chain Length ((i–1)– i) = (Conv.$_{total}$ (i) + Conv.$_{total}$ (i–1))/2. [c]$F_{inst,\ SiHEMA}$ ((i–1)– i) = (Conv.$_{SiHEMA}$ (i) – Conv.$_{SiHEMA}$ (i–1))/[(Conv.$_{HEMA}$ (i) – Conv.$_{HEMA}$ (i–1)) + (Conv.$_{SiHEMA}$ (i) – Conv.$_{SiHEMA}$ (i–1))]. [d]rr_{inst} ((i–1)– i) = (rr_{cum} (i) × Conv.$_{total}$ (i) – rr_{cum} (i–1) × Conv.$_{total}$ (i–1))/(Conv.$_{total}$ (i) – Conv.$_{total}$ (i–1)).

(Figure 8), though the mechanism for the chain growth should be further clarified by investigating the reactivity ratios[6] and cotactic parameters.[13] These stereogradient

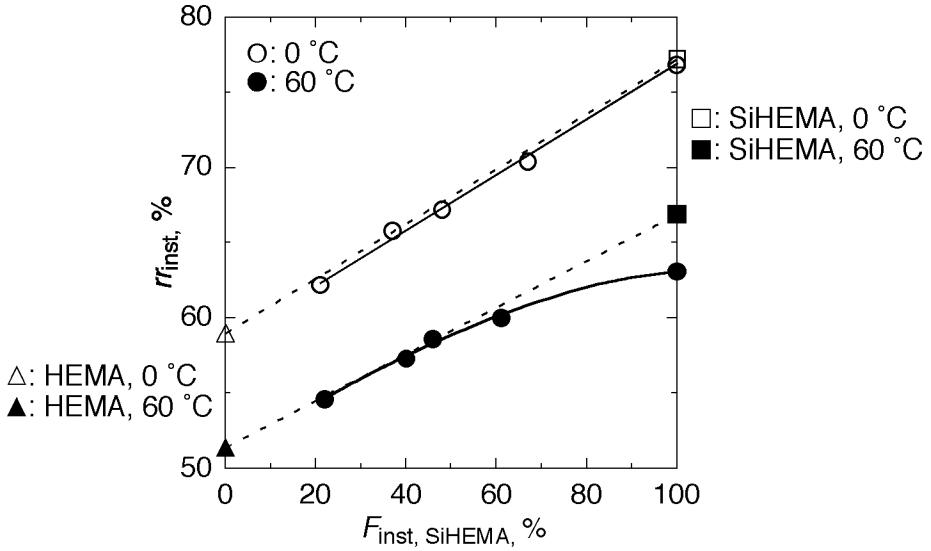

Figure 8. Dependence of rr_{inst} on $F_{inst,\ SiHEMA}$ in the ruthenium-catalyzed stereospecific living radical copolymerizations of HEMA and SiHEMA and *rr* on F_{SiHEMA} in the ruthenium-catalyzed homopolymerizations of SiHEMA and HEMA in $(CF_3)_2C(Ph)OH$ at 0 and 60 °C.

poly(HEMA) showed the intermediate glass transition temperatures (T_g) for the two homopolymers obtained at the same conditions (Table 3). Other properties of the polymers are now under investigation.

Table 3. Glass Transition Temperature (T_g) of Poly(HEMA) Obtained in the Homopolymerization of HEMA or after the Hydrolysis of Copoly(HEMA-*grad*-SiHEMA) and Poly(SiHEMA) in the Ruthenium-Catalyzed Living Radical Polymerizations in $(CF_3)_2C(Ph)OH$[a]

Monomer	Polymn Temp. (˚C)	M_n[b]	M_w/M_n[b]	M_n[c]	M_w/M_n[c]	*mm/mr/rr*[d] (%)	T_g (˚C)
HEMA	60	24,100	1,44	–	–	6.4/41.8/51.4	94.4
HEMA+SiHEMA	60	21,700	1,27	28,000	1.35	4.4/37.2/58.4	99.9
SiHEMA	60	21,500	1.18	32,800	1.23	1.9/31.2/66.9	104.7
HEMA	0	28,100	1.21	–	–	3.6/37.4/59.0	100.8
HEMA+SiHEMA	0	19,800	1.25	24,800	1.43	2.3/30.2/67.5	105.1
SiHEMA	0	21,700	1.14	33,600	1.17	0.9/21.9/77.2	107.6

[a]Polymerization conditions: $[HEMA+SiHEMA]_0/[H–(MMA)_2–Cl]_0/[Ru(Cp^*)Cl(PPh_3)_2]_0/[n\text{-}Bu_3N]_0$ = 1000/10/4.0/40 mM in $(CF_3)_2C(Ph)OH$. [b]Before hydrolysis; by size-exclusion chromatography in DMF containing 100 mM LiCl at 40 °C [poly(HEMA) and copoly(HEMA-*grad*-SiHEMA)] or in THF at 40 °C [poly(SiHEMA)]. [c]After hydrolysis; by size-exclusion chromatography in DMF containing 100 mM LiCl at 40 °C. [d]Determined by ^{13}C NMR in DMSO–d_6 at 80 ˚C after the hydrolysis of the silyl groups in the SiHEMA units.

CONCLUSIONS

In conclusion, this communication revealed a new synthetic method of stereogradient polymers, a new class of polymers, based on the stereospecific living radical copolymerizations of two monomers with different reactivities and stereospecificities. Further expansion of the stereogradient polymers can be expected in terms of the synthetic methods as well as the properties of the new polymers.

EXPERIMENTAL

Materials.

2-Hydroxyethyl methacrylate (HEMA, Tokyo Kasei, >99%) and $(CF_3)_2C(Ph)OH$ (Wako, >99%) were distilled from calcium hydride under reduced pressure before use. $Ru(Cp^*)Cl(PPh_3)_2$ (provided from Wako Chemicals) was used as received and handled in a glove box (VAC Nexus) under a moisture- and oxygen-free argon atmosphere (O_2, <1 ppm). $Me_2C(CO_2Me)CH_2C(CO_2Me)(Me)Cl$ [H–(MMA)$_2$–Cl] was prepared according to the literature.[1] (2-*tert*-Butyldimethylsilyloxy)ethyl methacrylate (SiHEMA) was synthesized according to the literature[14] as follows. HEMA (10 mL, 76 mmol) was dissolved in diethyl ether (200 mL) and cooled to 0 ˚C. Triethylamine (10.6 mL, 76 mmol) and a solution of *t*-butyldimethylsilyl chloride (11.46 g, 76 mmol) in diethyl ether (30 mL) were added to the HEMA-solution under nitrogen, and the mixture was kept at r.t. overnight. The reaction mixture was washed with aqueous 5% NaOH aqueous solution (50 mL) and water (50 mL × 3). The organic layer was dried with sodium sulfate and evaporated to dryness. The crude product was purified by distillation at 80 ˚C/2 mmHg. All other reagents were purified by the usual methods.

Ruthenium-Catalyzed Living Radical Copolymerization.

All polymerizations were carried out by syringe technique under dry nitrogen in glass tubes equipped with a three-way stopcock or in baked and sealed glass vials. A typical

example for copolymerization of HEMA and SiHEMA with H–(MMA)$_2$–Cl/ Ru(Cp*)Cl(PPh$_3$)$_2$/*n*-Bu$_3$N is given below. In a 50 mL round-bottomed flask was placed Ru(Cp*)Cl(PPh$_3$)$_2$ (47.8 mg, 0.060 mmol), (CF$_3$)$_2$C(Ph)OH (11.2 mL), tetralin (0.41 mL), HEMA (0.91 mL, 7.50 mmol), SiHEMA (2.00 mL, 7.50 mmol), H–(MMA)$_2$–Cl (0.25 mL of 602 mM solution in toluene, 0.150 mmol) and *n*-Bu$_3$N (0.14 mL, 0.600 mmol) at room temperature. The total volume of reaction mixture was 15.0 mL. Immediately after mixing, eighteen aliquots (0.80 mL each) of the solutions were injected into backed glass tubes. The reaction vials were sealed and placed in an oil bath kept at 60 ˚C or methanol bath kept at 0 ˚C. In predetermined intervals, the polymerization was terminated by cooling the reaction mixtures to –78 ˚C. Monomer conversion was determined by ^{1}H NMR in CDCl$_3$ with tetralin as an internal standard. The quenched reaction solutions were diluted with methanol (ca. 0.8 mL) and vigorously shaken with an absorbent [Kyowaad-2000G-7 ($Mg_{0.7}Al_{0.3}O_{1.15}$); Kyowa Chemical] (ca. 0.5 g) to remove the metal-containing residues. After the absorbent was separated by filtration (Advantec No.2), the filtrate was evaporated to dryness and diluted with 1,4-dioxane (5 mL) to prepare for the following hydrolysis reaction.

Hydrolysis of Silyl-Groups in SiHEMA Units.

The hydrolysis was done according to the literature[15] as follows. Conc. HCl (11 M; 1 mL) was added dropwise to a 1,4-dioxane solution of the polymer (150 mg in 5.8 mL) at 0 °C. After 24 h, the reaction mixture was concentrated to ca. 1.0 mL by evaporation, precipitated into a large amount of hexane/ethanol (3/1 v/v, 7.0 mL), collected by centrifugation, and evaporated to dryness. The hydrolysis was confirmed by ^{1}H NMR analysis of the obtained polymer in DMSO-d_6.

Measurements.

The ^{1}H and ^{13}C NMR spectra were recorded on a Varian Gemini 2000 spectrometer (400 MHz and 100 MHz), respectively. The triad tacticity of the polymer was determined by the area of the methyl carbon protons of the backbone, and the measurement was carried out at 80 °C in DMSO-d$_6$. The number-average molecular weight (M_n) and polydispersity index (M_w/M_n) were determined by size-exclusion chromatography (SEC) in DMF containing 100 mM LiCl [for poly(HEMA) and copolymers of HEMA and SiHEMA] or THF [for poly(SiHEMA)] at 40 °C on two polystyrene gel columns [Shodex K-805L (pore size:

20–1000 Å; 8.0 mm i.d. × 30 cm) × 2; flow rate 1.0 mL/min] connected to Jasco PU-980 precision pump and a Jasco 930-RI detector. The columns were calibrated against 7 standard poly(MMA) samples (Shodex; M_p = 1,990–1,950,000; M_w/M_n = 1.02–1.09). Glass transition temperature (T_g) of the polymer was recorded on SSC-5200 differential scanning calorimetry (Seiko Instruments Inc.). Samples were first heated to 150 °C at 10 °C/min, equilibrated at this temperature for 5 min, and cooled to 30 °C at 2 °C/min. After being held at this temperature for 20 min, the samples were then reheated to 150 °C at 10 °C/min. All T_g values were obtained from the second scan, after removing the thermal history.

REFERENCES

(1) Percec, V. *Chem. Rev.* **2001**, *101*, 3579–3580 and the succeeding papers in this issue of the journal.

(2) (a) Kamigaito, M.; Ando, T.; Sawamoto, M. *Chem. Rev.* **2001**, *101*, 3689–3745. (b) Kamigaito, M.; Acndo, T.; Sawamoto, M. *Chem. Rec.* **2004**, *4*, 159–175. (c) Matyjaszewski, K.; Xia, J. *Chem. Rev.* **2001**, *101*, 2921–2990. (d) Hawker, C. J.; Bosman, A. W.; Harth, E. *Chem. Rev.* **2001**, *101*, 3661–3688.

(3) Gladysz, J. A. *Chem. Rev.* **2000**, *100*, 1167–1168 and the succeeding papers in this issue of the journal.

(4) Habaue, S.; Okamoto, Y. *Chem. Rec.* **2001**, *1*, 46–52.

(5) (a) Ray, B.; Isobe, Y.; Morioka, K.; Habaue, S.; Okamoto, Y.; Kamigaito, M.; Sawamoto, M. *Macromolecules* **2003**, *36*, 543–545. (b) Ray, B.; Isobe, Y.; Matsumoto, K.; Habaue, S.; Okamoto, Y.; Kamigaito, M.; Sawamoto, M. *Macromolecules* **2004**, *37*, 1702–1710. (c) Lutz, J.-F.; Neugebauer, D.; Matyjaszewski, K. *J. Am. Chem. Soc.* **2003**, *125*, 6986–6993. (d) Kamigaito, M.; Satoh, K. *J. Polym. Sci., Part A: Polym. Chem.* **2006**, *44*, 6147–6158.

(6) (a) Matyjaszewski, K.; Ziegler, M. J.; Arehart, S. A.; Greszta, D.; Pakula, T. *J. Phys. Org. Chem.* **2000**, *13*, 775–786. (b) Min, K.; Li. M. Matyjaszewski, K. *J. Polym. Sci., Part A: Polym. Chem.* **2005**, *43*, 3616–3622.

(7) (a) Lee, S. B.; Russel, A. J.; Matyjaszewski, K. *Biomacromolecules* **2003**, *4*, 1386–1393. (b) Yoshida, T.; Kanaoka, S.; Watanabe, H.; Aoshima, S. *J. Polym. Sci., Part A: Polym.*

Chem. **2005**, *43*, 2712–2722. (c) Karaky, K.; Péré, E.; Pouchan, C.; Desbrières, J.; Dérail, C.; Billon, L. *Soft Matter* **2006**, *2*, 770–778.

(8) Buese, M. A.; Zhang, Y. *Macromol*. *Symp*. **1995**, *95*, 287–292.

(9) Harney, M. B.; Zhang, Y.; Sita, L. R. *Angew*. *Chem*., *Int*. *Ed*. **2006**, *45*, 6140–6144.

(10) Hsieh, K.-H.; Young, T.-H. Hydrogel Materials (HEMA-Based). In *Polymeric Materials Encyclopedia*; Salamone, J. C., Ed.; CRC Press: Boca Raton, FL, 1996; Vol. 5, pp 3087–3092.

(11) Shibata, T.; Satoh, K.; Kamigaito, M.; Okamoto, Y. *J*. *Polym*. *Sci*., *Part A: Polym*. *Chem*. **2006**, *44*, 3609–3615.

(12) (a) Isobe, Y.; Yamada, K.; Nakano, T.; Okamoto, Y. *Macromolecules* **1999**, *32*, 5979–5981. (b) Isobe, Y.; Yamada, K.; Nakano, T.; Okamoto, Y. *J*. *Polym*. *Sci*., *Part A: Polym*. *Chem*. **2000**, *38*, 4693–4703.

(13) (a) Yuki, H.; Okamoto, Y.; Shimada, Y.; Ohta, Y.; Hatada, K. *J*. *Polym*. *Sci*., *Polym. Chem*. *Ed*. **1979**, *17*, 1215–1225. (b) Hatada, K.; Kitayama, T.; Ochi, T.; Yuki, H. *Polym*. *J*. **1987**, *19*, 1105–1113.

(14) Ando, T.; Kamigaito, M.; Sawamoto, M. *Macromolecules* **2000**, *33*, 2819–2824.

(15) Mori, H.; Wakisada, O.; Hirao, A.; Nakahama, S. *Macromol*. *Chem*. *Phys*. **1994**, *195*, 3213–3224.

LIST OF PUBLICATIONS

PAPERS

CHAPTER 1

"Graft Polymerization of Styrene and Acrylates on the Prepolymer Having TEMPOL Residues"

Yu Miura, Yutaka Isobe, Tetsuya Nakamura, Motoyuki Sugiura, and Yoshio Okamoto

Polym. J. **2005**, *37*, 617–624.

CHAPTER 2

"Well-Defined Graft Copolymers of Methacrylate, Acrylate, and Styrene *via* Ruthenium-Catalyzed Living Radical Polymerization"

Yu Miura, Kotaro Satoh, Masami Kamigaito, and Yoshio Okamoto

Polym. J. **2006**, *38*, 930–939.

CHAPTER 3

"A_xBA_x-Type Block–Graft Polymers with Middle Soft Segments and Outer Hard Graft Chains by Ruthenium-Catalyzed Living Radical Polymerization: Synthesis and Characterization"

Yu Miura, Kotaro Satoh, Masami Kamigaito, Yoshio Okamoto, Takeshi Kaneko, Hiroshi Jinnai, and Syuji Kobukata

Macromolecules **2007**, *40*, 465–473.

CHAPTER 4

"A_xBA_x-Type Block–Graft Polymers with Soft Methacrylate Middle Segments and Hard Styrene Outer Grafts: Synthesis, Morphology, and Mechanical Properties"

Yu Miura, Takeshi Kaneko, Kotaro Satoh, Masami Kamigaito, Hiroshi Jinnai, and Yoshio Okamoto

Chem. Asian J. **2007**, *in press*.

CHAPTER 5

"Stereogradient Polymers by Ruthenium-Catalyzed Stereospecific Living Radical Copolymerization of Two Monomers with Different Stereospecificities and Reactivities"

Yu Miura, Takuya Shibata, Kotaro Satoh, Masami Kamigaito, and Yoshio Okamoto

J. Am. Chem. Soc., **2006**, *128*, 16026–16027.

ACKNOWLEDGEMENT

This thesis presents the studies which the author carried out from 2001 to 2007 at the Department of Applied Chemistry of Nagoya University under the direction of Professors Yoshio Okamoto (2001–2003) and Masami Kamigaito (2003–2007).

The author would like to express his deep gratitude to Professors Yoshio Okamoto and Masami Kamigaito for their continuous guidance and encouragement throughout the course of his work. He is also grateful to Dr. Kotaro Satoh for his helpful and convincing suggestions, stimulating discussions, and his kind guidance in experimental techniques. Very sincere thanks to Drs. Chiyo Yamamoto and Shigeki Habaue for their help and advice. It is pleasure to express his appreciation to Drs. Yutaka Isobe, Hiroharu Ajiro, Kohei Morioka, Messrs. A. K. M. Fakhrul Azam, Tomoyuki Ikai, Kazuhiko Koumura, Takuya Shibata, Fumitaka Sugiyama, Tatsuya Kojima, Satoshi Yamashita, and all colleagues for useful suggestion and sharing his pleasant student life.

He also acknowledges the guidance of Messrs. Tetsuya Nakamura and Motoyuki Sugiura (NOF Corporation) for technical supports and useful suggestions for the work in Chapter 1, Dr. Jiro Kumaki (Yashima Super-structured Helix Project, Exploratory Research for Advanced Technology: ERATO), Mr. Sousuke Ohsawa, and Professor Eiji Yashima (Nagoya University and Yashima Super-structured Helix Project, Exploratory Research for Advanced Technology: ERATO) for technical support and useful suggestions on atomic force microscopy, Messrs. Takeshi Kaneko, Kazuya Suda, and Associate Professor Hiroshi Jinnai (Kyoto Institute of Technology) for the measurements of transmission electron microscopy and transmission electron microtomography, and Messrs. Shuji Kobukata, Atsuhiro Nakahara, Katsuei Takahashi, and Isamu Okamoto (Kuraray Co. Ltd., Tsukuba Research Laboratories) for the measurements of transmission electron microscopy, tensile viscoelasticity experiments, and tensile tests.

He is very grateful to the Fellowship of the 21st Century COE Program “Creation of Nature-Guided Materials Processing” during 2004–2007.

Finally, he would like to give his special thanks to Professors Yushu Matsushita and Shinobu Koda for serving on his dissertation committee.

January, 2007

三浦 悠

Yu MIURA